On control approaches for estimation purposes : application to tunneling current and magnetic levitation processes

Andrei Popescu

▶ **To cite this version:**

Andrei Popescu. On control approaches for estimation purposes : application to tunneling current and magnetic levitation processes. Automatic. Université Grenoble Alpes, 2019. English. NNT : 2019GREAT062 . tel-02527247

HAL Id: tel-02527247
https://theses.hal.science/tel-02527247v1

Submitted on 1 Apr 2020

HAL is a multi-disciplinary open access archive for the deposit and dissemination of scientific research documents, whether they are published or not. The documents may come from teaching and research institutions in France or abroad, or from public or private research centers.

L'archive ouverte pluridisciplinaire **HAL**, est destinée au dépôt et à la diffusion de documents scientifiques de niveau recherche, publiés ou non, émanant des établissements d'enseignement et de recherche français ou étrangers, des laboratoires publics ou privés.

THÈSE

Pour obtenir le grade de

DOCTEUR DE L'UNIVERSITÉ GRENOBLE ALPES

Spécialité : AUTOMATIQUE - PRODUCTIQUE

Arrêté ministériel : 25 mai 2016

Présentée par

Andrei POPESCU

Thèse dirigée par **Gildas BESANCON** , Professeur, Université Grenoble Alpes
et codirigée par **Skandar BASROUR** , UGA
et **Alina VODA**, UJF Grenoble I

préparée au sein du **Laboratoire Grenoble Images Parole Signal Automatique**
dans **l'École Doctorale Electronique, Electrotechnique, Automatique, Traitement du Signal (EEATS)**

Approches de commande pour des objectifs d'estimation - Application au courant tunnel et aux processus de lévitation magnétique

On control approaches for estimation purposes - Application to tunneling current and magnetic levitation processes

Thèse soutenue publiquement le **25 novembre 2019**,
devant le jury composé de :

Monsieur Gildas BESANCON
Professeur des Universités, Grenoble INP, Directeur de thèse
Madame Gabriela Iuliana BARA
MAITRE DE CONFERENCES HDR, Université de Strasbourg , Rapporteur
Monsieur Micky RAKOTONDRABE
Professeur des Universités, ENIT Toulouse INP, Rapporteur
Monsieur Philippe LUTZ
Professeur des Universités, UNIVERSITE DE FRANCHE-COMTE, Président
Monsieur Dan STEFANOIU
Professeur, UNIV. POLYTECHNIQUE BUCAREST - ROUMANIE, Examinateur
Madame Alina VODA
Maître de Conférences, Université Grenoble Alpes , Examinateur
Monsieur Skandar BASROUR
Professeur des Universités, Université Grenoble Alpes, Co-directeur de thèse

On control approaches for estimation purposes - Applications to tunneling current and magnetic levitation processes

Thesis by
Andrei POPESCU

In Partial Fulfillment of the Requirements for the
Degree of
Doctor of Philosophy of the University Grenoble Alps

UNIVERSITY GRENOBLE ALPS
Saint-Martin-d'Hères, France
ISBN: 978-2-11-129263-5

2019
Defended 25th November

© 2019

Andrei POPESCU
ORCID: xxxxx

All rights reserved except where otherwise noted

TABLE OF CONTENTS

LIST OF ILLUSTRATIONS

Number *Page*

LIST OF TABLES

Number *Page*

Acknowledgments

... I will start this short thank you letter with a quote by Richard Feynman, who said: *nobody ever figures out what this life is all about, and it doesn't matter. Explore the world. Nearly everything is really interesting if you go into it deeply enough*... This is one of the reasons why I fell in love with research and why I decided to begin this endeavor to become a researcher.

But, at that point, you find yourself in front of some simple questions (... with way too complicated answers – the mind of the young researcher wasn't even capable to grasp the complexity of the answers, not to mention the ability to actually find an accurate answer): What does it mean to be a researcher? ... and since we are part of a super egocentric species – Will I be a good researcher? In the following moments I will try to scratch the surface of the answer for the former question, as for the latter only time can tell.

So, what does it mean to be a researcher? The first lesson I have learned is that you have to ask questions in order to be able to find answers. However, just asking questions is not enough, you have to ask the right questions in order to find the right answers. Another important part is that you can't choose just the answers you like and fit your theory, you have to accept all answers, and you have to learn how to deal with your fails and also with your successes. This particular aspect also helped me to grow as a person. Moreover, being a researcher/explorer is more than just a job that you will do during working hours, it's a state of mind, it's a mindset that has ripples effect through all of your way of being (at least this is my personal experience).

Another defining aspect of this endeavor is the mentorship. I would like to take advantage of this opportunity to thank to my supervisors Gildas Besancon, Alina Voda and Skandar Basrour who have led my research activity during this initial period teaching me from their own experience and passing to me a set of tools that have already been proven useful for my life as a researcher. Also I what to thank for their support for any problem that have arisen, either work related or of personal matter.

Next on the list, are my beloved office mates Sophie, Firas and Anne. There are no words to describe what you mean for me and how your presence and support helped me throughout this experience. Thus from my bottom of my heart I want or say thank you. You are like family to me. Now, I want to thank to my actual family, to my mom, dad, and brother who supported me and my decisions at every step no matter what and how hard it was. I am and I will always be deeply grateful to you! Moreover, I had the most amazing group of friends that one can ask or even dream. Without you the whole experience wouldn't have been the same. I cherish all the moments spent together, every beer we had, every hug, every kiss, every single philosophical conversation, every single thing we shouldn't supposed to do... our best and our worst... Again, the words are futile... we will always have our memories that will link throughout eternity. The only thing I want to say is that I love you sooooo much and I want to thank you for everything. You are the best! You will always be tattooed on my mind and soul via our memories together: Adela, Sophie, Firas, Matthieu, Gael, Omar, Makia, Raul, Anne, Alex, Alex H, Matheus, Pish, Caro, Olivian, Costin, Alexandra, Teo, Mihai, Irina, Adi, Cata, Vlad, Radu, Roxana, Daria, Cami, Iulia, Ovi, Radu, Marian, Gabi, Bogdan, Raul, and all the other people I interacted and left a mark on my existence.

I also want so send a special thank you to Cami, who took time from her busy schedule to proofread my thesis. Also, I want to thank to Valentine and Gaetan from CIME Nanotech who helped me during my periods spent in CIME Nanotech.

With love,

Andrei

Abstract in French:

Cette thèse de doctorat regroupe ses principales contributions dans le domaine des observateurs de systèmes dynamiques, motivés à l'origine par des applications en systèmes MEMS ou NEMS (systèmes micro ou nano électromécaniques), avec un cas plus particulier lié au courant tunnel. Il est également arrivé d'envisager des expériences avec un système de lévitation magnétique.

Les contributions de cette thèse sont de deux types, en fonction de ses deux parties principales:

1. *Partie méthodologique*: concevoir différentes stratégies de contrôle pour obtenir des observateurs en utilisant le paradigme basé sur le contrôle. En particulier, nous nous sommes concentrés sur la non-optimale approches (comme Proportionnelle et Proportionnelle- Intégrale), optimale (Linéaire Régulateur Quadratique et Linéaire Quadratique Intégrateur) et méthodes sous-optimales (Contrôleur Hinf). De plus, nous nous concentrons sur les deux principaux moyens de formuler un problème de contrôle (poursuite). C'est-à-dire Le problème de régulation du retour d'erreur et Le problème de régulation en utilisant l'information complète d'état.

2. *Partie expérimentale*: application des méthodes obtenues pour améliorer l'imagerie topographique à l'aide d'un microscope basé sur l'effet tunnel et à l'amélioration de l'estimation de perturbation sur les entres pour un processus de lévitation magnétique

Plus précisément, chaque partie prendra la forme de deux chapitres:

1. Chapitre II, consacré à une introduction formelle et à une discussion contributive sur l'approche "observateur basée sur le contrôle" que cette thèse étudie, et le chapitre III, qui porte sur l'utilisation de cette approche pour la conception d'un nouveau concept d'observateur robuste, en particulier dans un cadre Hinf

2. Chapitre IV, relatif à l'application STM, et Chapitre V, présentant l'affaire MAGLEV. Un dernier chapitre VI résume les principales conclusions de ce travail ainsi que certaines perspectives.

CHAPTER 1
INTRODUCTION

This Chapter Answers

1. What is an observer?
2. How can one use control strategies to design an observer?
3. What is the contribution of this PhD?

1.1 Preamble

The present manuscript results from a PHD study conducted with both the Control Systems Department of Gipsa-lab and TIMA laboratory, and largely supported by LabEx PERSYVAL-Lab (ANR-11-LABX-0025-01) funded by the French program Investissement d'avenir.

It gathers its main contributions in the field of *observers* for dynamical systems, originally motivated by applications in MEMS or NEMS (Micro or Nano Electromechanical Systems), with a more particular case related to *tunneling current*. It also happened to consider experiments with a *magnetic levitation* system.

1.2 Motivation

In this chapter we will present the motivation underlying our work in the field of observer design, in particular the special case of estimating both the state and the unknown inputs of a system. In addition, we will also try to highlight the reason why one can focus on control strategies for estimation purposes, bringing us to introduce the reader into the topic of what can be called *control-based observer* paradigm. Keeping also in mind the importance of observers for control applications, special cases that will be considered in this manuscript will be introduced as well.

This work is thus divided in two main parts: a methodological one and an experimental one. The first part presents the control-based observer paradigm, while the second one is focused on validating the proposed methods using real-time experiments. After this introduction to the topic, the problem formulation for such an observer is given, together with our contributions concerning this particular topic.

a. Methodology part

i. State Observers

The concept of observation is deeply embedded in our human nature and it was proved to be an important and powerful tool in our evolution. To support the idea one can mention people observing the stars and using rudimentary maps in order to find the path to their destination, so called navigators. Moreover, other people were using the stars to predict the coming season so that they could decide if they continued their journey or if it was a better idea for them to camp.

The examples can go on, for instance, people observing the clouds or the sun position to predict rain or to estimate time.

One of my favorite examples to outline the concept of observer, which for me seems quite illustrative, comes from the medical field. The doctor interacts with his patient 'measuring' some physical or mental features, known as symptoms, in order to be able to diagnose his patient's condition. Once he successfully 'estimates' it, he can prescribe a suitable treatment so that his patient's health can be improved.

Trying to find a common feature among the examples mentioned above, one can notice that the main idea is that based on some "measurable" quantities like stars position, clouds movements, sun position or the symptoms of a patient, one can reveal some hidden information about a particular behavior as the ship position, the arrival of a season, the change in weather, the passing of time or the condition of a patient.

This concept can be extrapolated to the automatic control field as well. Thus, the problem of observer design in this particular case can be formulated when searching to reveal some internal information (hidden behavior) concerning a system using its external measurements.

When dealing with systems it is usually difficult or even impossible to use sensors to measure all the signals of interest. Some common reasons are either economical ones (the sensors might be too expensive, or a huge number of them is needed), or technological ones (some signals are hardly accessible, or maybe the technology is not there yet to measure some quantities).

The motivation for obtaining the internal information characterizing a system can be multiple. For instance, one can be interested in controlling the behavior of a process and having access to the hidden information describing that system can improve the controller performances. Moreover, some applications require a modeling (identification) component, for which the design of an observer proves to be quite useful. Another direct application is for monitoring purposes, either for fault detection or unknown input reconstruction. Both of them ask for some knowledge about the internal information of a system. Therefore, it turns out that the observer design is of great interest in the automatic control field and its central role in this kind of application can be summarized in Figure 1.1

Based on the information presented so far, one can notice that an observer is basically an auxiliary system following some particular design specifications. Therefore,

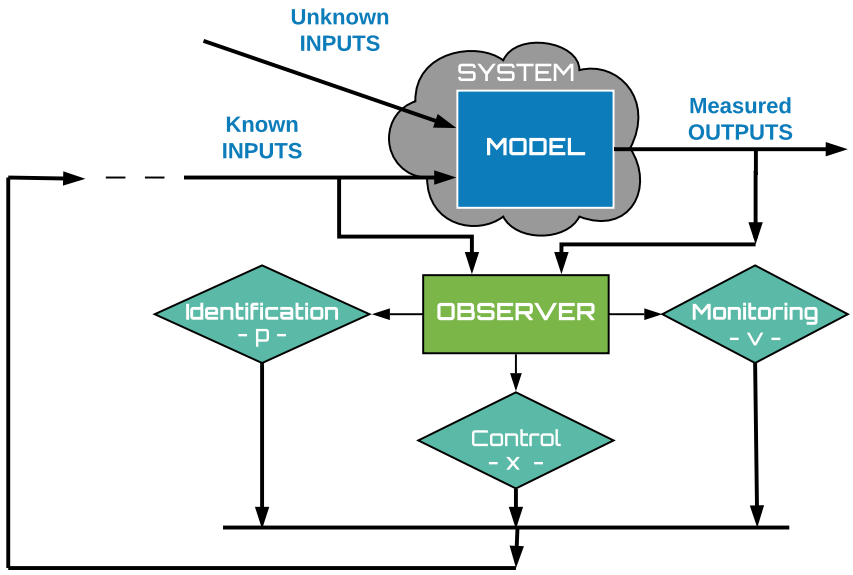

Figure 1.1: Observer general diagram

the observer problem can be briefly formulated as follows

Observer Problem:

Given a system described by a model, find an auxiliary system to estimate the system state (internal information) based on the knowledge of the external information, namely the known inputs and measured outputs.

The topic was heavily studied in the field of automatic control system. Starting with the classical solutions for continuous linear system like Luenberger observer [Lue64] or the optimal one namely Kalman filter [Kal60a], moving to robust solutions in terms of H_∞ observer [NK91].

In addition, either solutions for continuous nonlinear system have been proposed as well such as Extended Kalman filter, Unscented Kalman filter or Particle filter (for a more detailed description the interested reader can check [Sim06]). Another particular class of observers, nonlinear and discontinuous, has been intensively developed based on sliding mode techniques, namely Utkin's observer [DU95], Slotine's observer [SHM87] or more advanced ones like Super-Twisting [FB07] and Generalized Super Twisting observers [Sal+11]. Other methods worth mentioning are based on Lyapunov techniques as in high-gain observers from [GHO92] to [MMP10], on optimization techniques or on related notion of dissipativity [Mor04]. See also [Bes07].

Notice that some discrete versions of the observers mentioned before are also well

developed, but in this manuscript we are interested to design an observer for a continuous system.

Let us consider a general mathematical description in terms of nonlinear equations as

$$\begin{aligned} \dot{x}(t) &= f(x(t), u(t)) \\ y(t) &= h(x(t)) \end{aligned} \tag{1.1}$$

where $x(t)$ stands for the state vector (internal information), $u(t)$ is the known input and $y(t)$ is the measured output.

The following equation can be proposed as an observer to deliver $\hat{x}(t)$ an estimate of $x(t)$

$$\dot{\hat{x}}(t) = f(\hat{x}(t), u(t)) + \kappa(y(t) - h(\hat{x}(t), t)) \tag{1.2}$$

where the term $\kappa(\bullet)$ is called the correction term and in particular $\kappa(0, t)$ is zero.

Clearly, one can notice that equation (1.2) contains all the elements stated in the observer problem formulation, namely the model (functions f and h), the known inputs ($u(t)$) and the measured outputs ($y(t)$). The equation (1.2) is known as the most common form of an observer for a system described by equation (1.1).

Finally, we can say that equation (1.2) represents an observer for the system described by equation (1.1), as soon as the error term $x(t) - \hat{x}(t)$ converges to zero.

ii. Unknown Input Observers

Another class of observers very useful in practical applications, are the so called *unknown input observers* (UIO). These particular observers extend the class of processes for which it is aimed to design an auxiliary system for observation purposes, namely the ones affected by unknown inputs. This is definitely not an easy task, proven somehow by the hard work that has been done for decades to advance slowly in this research field.

As expected, the aim of such an observer is to provide an accurate state estimation (internal information) even if the process is affected by unknown inputs. Moreover,

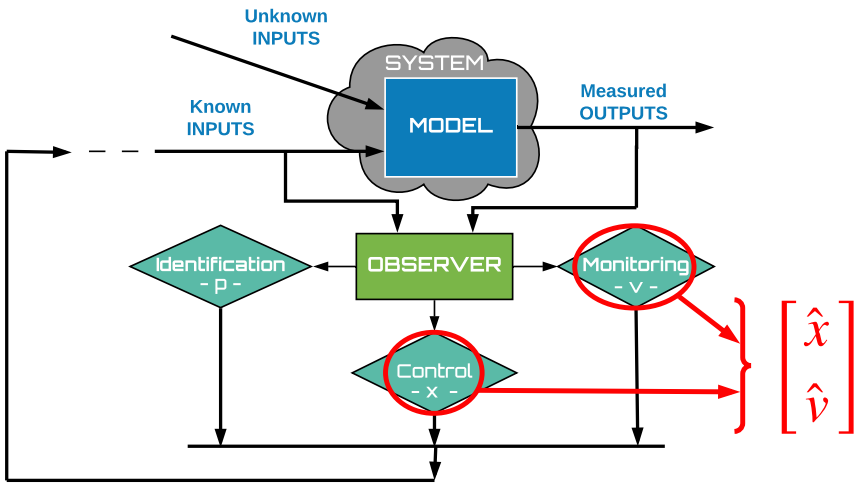

Figure 1.2: Unknown Inputs Observer general diagram

one might be interested to estimate the state of the system, as well as to reconstruct the unknown inputs, see for instance Figure 1.2.

For a better illustration of the notions which will be presented next, let us give the linear state space representation of the system in equation (1.2) with the particular remark that the process is affected by unknown inputs:

$$\begin{aligned} \dot{x}(t) &= Ax(t) + B_0u(t) + B_2v(t) \\ y(t) &= Cx(t) \end{aligned} \tag{1.3}$$

where the variables $x(t) \in \mathbb{R}^n$, $u(t) \in \mathbb{R}^m$, $v(t) \in \mathbb{R}^q$ and $y(t) \in \mathbb{R}^p$ classically stand for the state, the known inputs, the unknown inputs and the outputs of the system.

In this introduction we will focus on three main classes of unknown input observers, for which a brief historical perspective is presented.

The classes are:

1. Luenberger-like Unknown Input Observers
2. Sliding Mode Observers
3. PI-observers

1. Luenberger-like Unknown Input Observers

After Luenberger published in 1964 his first paper on observers for linear systems [Lue64], researchers have tried to extend his results for systems having unknown inputs. In the early works, they made some assumptions about the unknown inputs, such as they can be modeled by linear differential equations, see for example [BM69], [HM73], [Joh75] or [Bha78].

Other ones adapted some techniques or algorithms that already existed to solve this particular problem as in [KN82].

Assumptions about the unknown inputs could then be removed thanks to the observers designed, as in [WD78] or later in [GS91] and [HM92], also presenting a way to reconstruct the unknown inputs.

Moreover, the existence conditions for an observer as designed in [WD78] were described in [KVR80] and [Kur82]. Finally, in [Hau83] useful concepts to extend the notions of observability and detectability for systems having unknown inputs to strong observability, strong detectability, as well as, strong* detectability have been described.

Briefly speaking, the necessary and sufficient condition to design a Luenberger-like Unknown Input Observers is that the systems having unknown inputs as described in equation (1.3) should be strong* detectability. This condition is twofold:

a. Any invariant zero of the triple (A, B_2, C) must lie on the left side of the complex plane, $i.e.$

   For all $s \in C$ which satisfy $rank \begin{bmatrix} sI - A & -B_2 \\ C & 0 \end{bmatrix} < n + q$ we have $Re(s) < 0$

b. rank$\Big[CB_2\Big] = rank \Big[B_2\Big] = q$

In other words, one can state that the transfer function between the unknown inputs (v) and the system output (y) must be minimum phase (condition $a.$) and relative degree one (condition $b.$). As a remark, the relative degree refers to the concept described by Isidori [Isi96].

So far, one can easily notice that the relative degree condition is very conservative and can pose problems even for simple applications like mechanical systems when unknown forces are present and only the position is measured, see for instance [DFP06]. Basically, the information about unknown input is supposed to be fully available from the measured output.

Next, our focus is switched to sliding mode techniques which originally were best known for their capabilities on robust control. They were extensively studied in 1960 in the former Soviet Union. This approach is a member of a larger class of methods called Variable Structure Control Systems which are described by a series of feedback control laws and a decision rule.

In particular sliding mode observers have an interesting property namely to generate a sliding motion on the error between system output and the observer output leading to a set of state estimates which are precisely proportional with the measured outputs of the system.

Several design approaches have been studied in order to obtain a sliding mode observer.

The first attempt can be defined as a 'classical' sliding mode observer (or a more intuitive name can be 'first order' sliding mode observer - the reason for this naming will reveal itself when we talk about the existence conditions to obtain such an observer). The main idea of this observer strategy, as stated earlier, is that the output error is fed back with the particular objective to ensure the so called sliding patch. Depending on the form of the feedback term, 'classical' sliding mode observers can be divided into two classes: on the one hand, we have the Utkin observer [DU95], which implies that the compensation term is based only on the discontinuous injection input. On the other hand, we find the Slotine observer [SHM87] or the Wallcot and Żak observer [WZ87], for that matter, which assume that the feedback term has two components, a linear one (Luenberger-like term) and a discontinuous injection input, both of them are functions of the output error. The latter ones solve a well known problem in sliding mode called chattering. Furthermore, the existence conditions for designing such an observer are similar with the ones specified for Luenberger-like unknown input observers. In this particular framework, the condition b. is called observer matching condition. Thus the relative degree of an appropriate sliding variable with respect to the injection signal is one (hence the name suggestion earlier).

To avoid the limitation imposed by the observer matching conditions some methods have been developed such as to transform the system into a special form which exhibits some novel observability properties [FB06] or furthermore due to the deployment of higher order sliding mode differentiators some extra outputs can be reconstructed and then classical sliding modes observers can be used for state estimation

[FES07]. This last idea was also exploited in [Kal+10] where some high-gain observers were used as approximate differentiators in order to reconstruct the needed outputs.

Finally, higher order sliding mode observers were developed for state space reconstruction using the direct connection between the concept of differentiators and the observability problem [FLD07], [FDL11]. The evolution of this kind of observers started with second order sliding mode observers like super twisting observer [FB07] or generalized super twisting observer [Sal+11].

Even though some of the disadvantages of sliding mode control are not present anymore in the context of sliding mode observers, like chattering, while more advantages like finite time convergence and robustness against some model uncertainties can be found, still, this technique exhibits some downsides like nonlinearities, discontinuity, or sensitivity to measurement noise.

3. PI-observers

The last category that we are going to talk about in this introduction is PI-observers. Thus far we have seen that the control techniques have inspired the design of observers, because of the duality between controlability and observability, for instance Proportional control for Luenberger observer and sliding mode control for sliding mode observers. Thus, one might consider adding an integral term to enhance the capabilities of an observer so that now besides the current information about the estimation error, it is also used the past information via the integral action. The presence of such a term gives the name of the observer.

The PI observer was first introduced by Wojciechowski in his PhD thesis [Woj78] for single-input single-output systems. Further improvements and extensions of a multiple-inputs multiple-outputs system affected by nonlinearities can be found in [Kac79], [SC85] and [YM95]. A brief survey for this type of observers can be found in [BS88a].

The conditions for such an observer are similar with the ones presented in the case of Luenberger-like unknown input observers, but condition $b.$ is a bit different. The existence conditions are the following

a. The pair (A, C) is observable.

b. $rank \begin{bmatrix} A & B_2 \\ C & 0 \end{bmatrix} = n + q$

c. $CA^iB_2 = 0, i = 0, 1, \ldots n-2$, where n is the observability index of pair (A, C).

The main difference between these conditions and the ones described for Luenberger-like unknown input observers is that the relative degree of the system output (y) with respect to unknown input (v) is n - the dimension of the state system (instead of one, like in the previous case).

Various ways to compute the gain of PI-observer have been developed and validated in practice like non-optimal ones [BS88b], optimal and sub-optimal solution [GK08] and [Yam+15] or some advanced gain-scheduling techniques [BS88a].

iii. Towards control-based strategies for estimation purposes

Let us recall equation (1.2). As it was mentioned before, it represents the most common form of an observer.

$$\dot{\hat{x}}(t) \quad = \quad f(\hat{x}(t), u(t)) + \kappa(y(t) - h(\hat{x}(t), t)) \tag{1.4}$$

The correction term, $\kappa(y(t) - h(\hat{x}(t), t))$, can be usually chosen as a simple product between a matrix, say L (having the appropriate dimensions) and the error vector given by the difference $y(t) - h(\hat{x}(t))$.

Let us take for instance the linear case for a system defined by equation (1.1) and consider the classical solutions for observer design. For instance, the Luenberger observer provides L using a pole placement technique (ensuring the observer internal stability). Moreover, for Kalman observer, L is an optimal solution for an optimization problem which minimizes the mean-square error between the system state and the estimated one. On the other hand, in the case of an H_∞ observer, L is a suboptimal solution for a similar optimization problem obtained either solving a Riccati equation or a set of linear matrix inequalities (LMI).

In our case, as it was proposed in [BM15], the correction term, $\kappa(y(t)-h(\hat{x}(t), t))$, can be designed as a controller for equation (1.4) such that the error $y(t)-h(\hat{x}(t))$ goes to zero. Basically the observer problem is converted into a control one. In this context, taking advantage of *robust* control methods, our aim is to obtain better observers to estimate the state and eventually to reconstruct the unknown inputs.

b. Experimental part

Concerning applications of the proposed methodologies, experimental results will be presented focusing particularly on two practical examples.

The first one is a very precise microscope which allows to obtain images having nanometric resolution. The device is called Scanning-Tunneling-Microscope (STM) [BR86]. In particular, this device is based on a quantum principle called tunneling-current phenomenon, which will be detailed in Chapter 5. Briefly speaking, the governing physical law states that if two electrically conductive materials are brought close enough (at a distance less than one nanometer) and a voltage bias is applied between them, then the electrons will break the potential barrier creating a really sensitive tunneling current. If one can ensure that a certain intensity of this tunneling current is kept constant while a sample is scanned, then an image having nanometer resolution of the surface variation can be delivered. Classically, the 3D movement of this kind of device is provided by piezoelectric actuators, which have given rise to a lot of studies in control [KRL12]. Dealing with phenomena and measurements at a submicronic scale more generally means facing uncertain effects, and large levels of noise, as this is typical in nanoscience applications [EM11]. This has motivated a lot of research in the last decade, in particular regarding the STM variant known as Atomic Force Microscope (AFM) [BQG86].

Our ultimate goal in this first application is to improve the surface reconstruction by the STM device when using the proposed observer approach. Experiments are mostly based on an STM prototype developed in Gipsa-lab a few years ago [Bla10], but also partly on a standard STM from CIME Nanotech platform of Grenoble INP-UGA.

The second application to be considered in this thesis is a magnetic levitation system, back to macro scale, for which we are particularly interested in estimating some unknown inputs affecting the system (fault detection application). This device is made of a coil, which is used to generate an appropriate magnetic field, and an infra-red sensor which measures the position of an iron ball. The goal of the experiment is to maintain the iron ball at a given position by using the magnetic field variation. This has motivated various studies in control [YA18], but very few observer applications [Bob+18]. Experiments in that case are based on a Feedback Maglev system [Bib] which was made available in UGA-Polytech teaching facilities.

1.3 Contributions

The contributions of this PHD are of twofold:

1. *Methodological part:* designing different control strategies to obtain observers using the control-based paradigm. In particular, we focused on non-optimal approaches (like Proportional and Proportional-Integral), optimal ones (Linear Quadratic Regulator and Linear Quadratic Integrator) and sub-optimal methods (H_∞ controller). Moreover, we focus on the main two ways to formulate a control (tracking) problem, namely *Error feedback regulation problem* and *Full information regulation problem*.

2. *Experimental part:* Applying the obtained methods to improve the topographic reconstruction for a Scanning-Tunneling Microscope as well as to improve the disturbance estimation for a magnetic levitation process.

More precisely, each part will take the form of two chapters:

- *Chapter II* is dedicated to a formal introduction and a contributive discussion about the 'control based observer' approach this PhD investigates. In particular the initial formulation of control-based observer paradigm is given, followed by the conditions which have to be met in order to design such an observer. Next, a set of control strategies are deployed to solve the related control problem to estimate the state of a system which is not affected by unknown inputs, besides other disturbances like state and measurement noises. In addition, it is also shown how to obtain some classical observers like Luenberger, PI, Kalman and H_∞, if one carefully designs an appropriate control law.

  Chapter III is focusing on the use of such an approach for the purpose of a new *robust* observer design in particular within an H_∞ framework. Hereby, we deal with the case when the system is also affected by some unknown inputs, which leads to the situation where both the state and the unknown inputs will be estimated. Simulation results will be given to support the theoretical claims.

- *Chapter IV* is related to STM application. One first attempt is a direct application of a control-based observer designed to improve both the control of such a device and also the topological imaging of a graphite sample. A second attempt is to improve the control methodology itself for an STM by using a H_∞

controller. In both cases real time results are presented to illustrate the performances of the proposed solutions.

Chapter V is presenting the MAGLEV case. In particular, an application of a fault estimation category is illustrated, in terms of designing a control-based observer to reconstruct some unknown input disturbance which affects the magnetic levitation process. Also in this case, real time experimental results are provided to support our claims.

A final *chapter VI* summarizes the main conclusions of this work as well as some perspectives.

1.4 Publications

- Conferences:
  - **3D H_∞ controller design for an experimental Scanning-Tunneling-Microscope device**

    Andrei Popescu, Alina Voda, Gildas Besancon, Yujin Wu. *3D H_∞ controller design for an experimental Scanning-Tunneling-Microscope device.* 58th IEEE Conference on Decision and Control (CDC 2019), Dec 2019, Nice, France.
  - **Comparison between different control strategies for estimation purposes using Control-based Observer paradigm**

    Andrei Popescu, Gildas Besancon, Alina Voda. *Comparison between different control strategies for estimation purposes using Control-based Observer paradigm.* 22nd International Conference on System Theory, Control and Computing (ICSTCC 2018), Oct 2018, Sinaia, Romania.
  - **Control-observer technique for surface imaging with an experimental platform of Scanning-Tunneling-Microscope type**

    Andrei Popescu, Gildas Besancon, Alina Voda, Skandar Basrour. *Control-observer technique for surface imaging with an experimental platform of Scanning-Tunneling-Microscope type.* American Control Conference (ACC 2018), Jun 2018, Milwaukee, United States.
  - **A new robust observer approach for unknown input and state estimation**

Andrei Popescu, Gildas Besancon, Alina Voda. *A new robust observer approach for unknown input and state estimation.* 16th European Control Conference (ECC 2018), Jun 2018, Limassol, Cyprus.

- **Control-based observer for unknown input disturbance estimation in magnetic levitation process**

  Andrei Popescu, Gildas Besancon, Alina Voda. *Control-based observer for unknown input disturbance estimation in magnetic levitation process.* 21st International Conference on System Theory, Control and Computing (ICSTCC 2017), Oct 2017, Sinaia, Romania.

- **Control-based Observer design for surface reconstruction using a Scanning-Tunneling-Microscopy device**

  Andrei Popescu, Gildas Besancon, Alina Voda. *Control-based Observer design for surface reconstruction using a Scanning-Tunneling-Microscopy device.* 20th IFAC World Congress (IFAC WC 2017), Jul 2017, Toulouse, France.

• Journals:

- **Observer-based Control enhancement for surface reconstruction using a Scanning Tunneling Microscope**

  (Under review - 2^{nd} revision) Andrei Popescu, Gildas Besançon, Alina Voda and Skandar Basrour. *Observer-based Control enhancement for surface reconstruction using a Scanning Tunneling Microscope*. IEEE Transactions on Control Systems Technology.

CHAPTER 2

CONTROL-BASED OBSERVER

This Chapter Answers

1. What is the motivation for a Control-based Observer (CbO)?
2. How can an estimation problem be converted into a control one?
3. How is Control-based Observer paradigm formulated?
4. Can different objectives for CbO problem be formulated?
5. Which are the conditions to obtain a CbO?
6. How to design a CbO?
7. What are the relations between the CbO paradigm and classical observer designs?

2.1 Introduction

As an introductory part to the considered framework of 'control-based observer' for the PhD, this chapter will first recall its original statement and derive two possible approaches towards observer design, depending on the considered information availability. In particular, the first one is *Full control error feedback regulation problem* and the second one is *Full information regulation problem*.

Required conditions and possible designs related to each of them will then be presented, including some classical observers as particular cases, for instance solving the *Full control error feedback regulation problem* for the control-based observer paradigm, depending on the chosen control law, the following classical observers can be found: Luenberger observer, PI observer, Kalman observer and H_∞ observer.

2.2 Recalls on Control-based Observer

a. Separation principle in control theory

As we previously have noticed, one of the reasons to build a *state observer* is often motivated by solving a control problem. Namely, in order to design a *state feedback controller*, one has to have access to all system states. This is not always possible for multiple reasons as stated before. Thus, the concept of *state estimation* becomes essential for this kind of control strategies. Solving this particular problem leads to a special class of control methods the so-called *observer-based feedback control* or *model-based controller*.

One of the most representative example to illustrate the special class of controllers described above is the *Linear Quadratic-Gaussian control (LQG)* [Ast70], which proved to be of great interest for many applications. In particular, to solve the *LQG* problem, one has to apply a two-step approach: firstly a *Kalman Observer* [Kal60a] is designed to obtain the optimal state estimations of the system and secondly, a *Linear Quadratic Regulator* [Son98] is computed in order to obtain the *observer-based feedback controller*. This problem can be found in control theory as the separation principle, or more formally as the principle of separation between estimation and control, as defined in [Ast70].

Following the separation principle described above, one can notice that an interesting idea can be to exploit in some sense this duality between control and observer in a

converse way to design a controller for an observer purpose. This idea was recently proposed in [BM15] and represents the basis of this PhD thesis. This technique leads to a paradigm for observer design called *Control-based Observer (CbO)*.

In other words, briefly speaking, if one can choose to control a model (copy) of the real system such that the output of the system model follows the output of the real system, then an estimation of the system states can be obtained, assuming of course that some appropriate observability and controllability conditions are satisfied.

This formulation clearly converts the observer problem into a tracking control problem. Thus, if one can design a controller for the above mentioned control problem, then a solution for the estimation problem can be delivered too. The idea, then, is to take advantage of control methods to obtain possible new observer designs and eventually compute better estimations than with the classical methods.

b. Control-based Observer Paradigm

Originally, the control-based observer paradigm was formulated as follows: consider the nonlinear system described by a state space-representation as:

$$\begin{aligned} \dot{x}(t) &= f(x(t), u(t)) \\ y(t) &= h(x(t)) \end{aligned} \tag{2.1}$$

where $x(t)$ stands for the *state vector*, $u(t)$ is the *known input* and $y(t)$ is the *measured output*. It is also assumed that the system described by equation (2.1) exhibits some observability property (or at least detectability one).

The idea is that if one can drive a model of the system of the form:

$$\begin{aligned} \dot{\hat{x}}(t) &= F(\hat{x}(t), u(t), \hat{v}(t)) \\ \hat{y}(t) &= h(\hat{x}(t)) \\ \hat{v}(t) &= \kappa(\epsilon_y(t), t) \end{aligned} \tag{2.2}$$

where F has the property that $F(\hat{x}(t), u(t), 0) = f(x(t), u(t))$ and $\hat{v}(t)$ is a well designed control input such that $\hat{y}(t)$ follows $y(t)$, as soon as the error between $\hat{y}(t)$ and $y(t)$, namely $\epsilon_y(t)$, approaches zero, $\hat{x}(t)$ will be an estimate of the system state, $x(t)$. A block diagram of this problem formulation can be seen in Figure 2.1a.

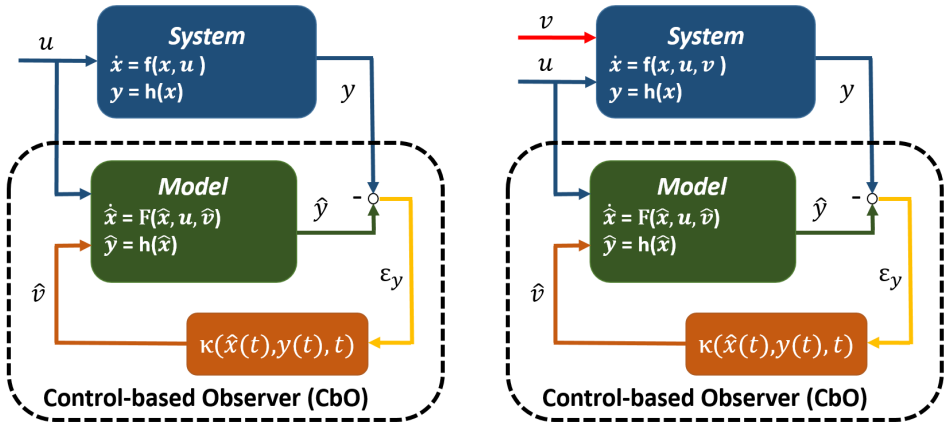

(a) No unknown inputs (b) With unknown inputs

Figure 2.1: Control-based Observer paradigm

Notice that this approach can also be used for *unknown input reconstruction*, if one also considers that system (2.1) is affected by some unknown inputs, $v(t)$ as described next:

$$\begin{aligned} \dot{x}(t) &= f(x(t), u(t), v(t)) \\ y(t) &= h(x(t)) \end{aligned} \tag{2.3}$$

Clearly now, if $\hat{v}(t)$ is designed such that $\hat{y}(t)$ follows the output of the system described by equation (2.3), besides the state estimation $\hat{x}(t)$, the method delivers also the estimation of *unknown inputs*, $v(t)$ in terms of $\hat{v}(t)$, as shown in Figure 2.1b, assuming of course that the system 2.3 exhibits 'enough observabilty' so that the state, $x(t)$, and the unknown input, $v(t)$, can be reconstructed.

One can also notice that in the original formulation the ideal case is considered, as the state and measurement noises are not taken into account. In practical applications the robustness against the noise is mandatory, thus in later formulations the noise will also be considered (apart from the 'deterministic' unknown inputs like $v(t)$ in equation (2.3)).

c. Different ways to formulate Control-based Observer problem

At this point it is worth noticing that *control-based observer* can have different structures depending on how the *estimation problem* is addressed. For instance, as specified in the previous subsection, the system might also be affected by unknown inputs, $v(t)$. In consequence, the objectives of the estimation problem are important, namely,

what we want to estimate: the state, the unknown inputs or both the state and the unknown inputs. Moreover, another way to see the problem is from the point of view of the controller, in particular, what the information available to design a control law is, $\hat{v}(t)$ and how the generated control input enters into the model. Basically, we have to specify the inputs and outputs of the controller. This will lead to two specific problem formulations as it will be seen further.

For the moment, let us consider every aspect individually and try to give a hint on how the structure of the *control-based observer* will be shaped.

The first aspect taken into account leads to the question: what if the system is affected by unknown inputs? The main point here is, if this is true, the system model is driven only via the unknown inputs. The advantage of doing this, as it will be seen later, is that an estimation of the unknown inputs can be directly obtained (as a consequence of how the problem was formulated), but in the end a trade off between the observer complexity and the quality of the estimations will take place (since the model is controlled just via the unknown inputs).

The second aspect in terms of problem formulation gives rise to a discussion about the objectives of the estimation problem. More precisely, the question asked is what will be the goal of the observer, to estimate only the state, or only the unknown inputs, or maybe the objective is to estimate both, the state and the unknown inputs.

Finally, the last aspect deals with the information availability from the point of view of the controller $\kappa(\bullet)$. To that end, two cases can be distinguished, as suggested in [Ast14] namely:

1. The *Error feedback regulator problem*, which assumes the controller is constrained to use as available information only the error between the system output $y(t)$ and model output $\hat{y}(t)$, namely $\epsilon_y(t)$. A particular case of this formulation can be also suggested, for instance, when the controller can directly act upon all states of the model. This problem is known as the full control approach and throughout this manuscript it will be called *Full control error feedback regulator problem*.

2. The *Full information regulator problem*, on the other hand, assumes that the available information for the controller is the full state of the model, $\hat{x}(t)$ and also the system output, $y(t)$.

2.3 System and model definition

Let us consider the linear case of the control-based paradigm, in particular the equations for the system and the chosen model are provided. As it was suggested above, two cases can be depicted, on the one hand the system is not affected by unknown inputs, while on the other hand (more general case) the system is influenced by unknown inputs.

In this chapter, only the first case will be taken into account, namely when the system is not affected by unknown inputs. The second one remains to be detailed in the following chapter.

a. Case study: No unknown inputs

Let us consider the equations of the *linear system not affected by unknown inputs* as follows (only noise):

System:

$$\begin{aligned} \dot{x}(t) &= Ax(t) + B_0u(t) + B_1w(t) \\ y(t) &= Cx(t) + D_0u(t) + D_1w(t) \end{aligned} \tag{2.4}$$

where classically the variables have the following meaning $x(t) \in \mathbb{R}^n$ is the state vector, $u(t) \in \mathbb{R}^m$ is the known input vector, $w(t) \in \mathbb{R}^{n+p}$ the vector of disturbances (like for instance state noise $w_x(t) \in \mathbb{R}^n$ and measurement noise $w_y(t) \in \mathbb{R}^p$), in particular $w(t) = \begin{bmatrix} w_x(t) \\ w_y(t) \end{bmatrix}$ and finally, $y(t) \in \mathbb{R}^p$ the vector of measured output.

Moreover, matrices A, B_0, B_1, C, D_0, D_1 and D_2, having appropriate dimensions, completely characterize the linear system.

One can notice that for the sake of simplicity and without loss of generality, D_0 in equation (2.4) can be considered as zero.

Next, a *model* of the system can be chosen as described bellow:

Model:

$$\begin{aligned} \dot{\hat{x}}(t) &= A\hat{x}(t) + B_0u(t) + B_v\hat{v}(t) \\ \hat{y}(t) &= C\hat{x}(t) \end{aligned} \tag{2.5}$$

It is pretty clear that the model is a copy of the dynamics of the real system, for which the information about the external influence, for instance noise, is not taken into account. The model has the additional term '$B_v\hat{v}(t)$' which represents the command for our control problem. The matrix dimension for control input is $\hat{v}(t) \in \mathbb{R}^q$

Further more, one can consider the model of the error between the system and the model, which is described as:

Model error:

$$\begin{aligned} \dot{\epsilon}_x(t) &= A\epsilon_x(t) - B_1 w(t) + B_v\hat{v}(t) \\ \epsilon_y(t) &= C\epsilon_x(t) - D_1 w(t) \end{aligned} \tag{2.6}$$

where $\epsilon_x(t) = \hat{x}(t) - x(t)$ and $\epsilon_y(t) = \hat{y}(t) - y(t)$. At first sight, this model seems to better capture the behavior of the real system since it also takes into account how the external signals affect the considered model.

2.4 Conditions to obtain control-based observer

In this section, the conditions to obtain a control-based observer are provided. In this chapter our main interest is to reconstruct the state of a system described by equation (2.4) which is affected by disturbances, $w(t)$, in terms of state and measurement noise.

Both full control and full information regulation problem will be presented because each of them leads to different constraints for the problem which has to be solved.

Intuitively, one can notice that for this paradigm the system and the model have to fulfill some observability conditions (since an observer is designed) and also some controllability ones (since a control strategy is used to ensure the convergence of the estimations).

Before moving on to the existence conditions for a control-based observer let us recall how to compute the notions of observability and controllability for a given system.

Observability

The system is observable if the state can be reconstructed using the information provided by the measured output, $y(t)$, of equation (2.4) and the chosen model (2.5).

For this linear case, the condition can be written as that the pair (A, C) is observable.

One of the checking methods for the above condition is using the observability matrix, $\mathcal{O} \in R^{(n\times p)\times n}$, defined as:

$$\mathcal{O} = \begin{bmatrix} C \\ CA \\ CA^2 \\ \vdots \\ CA^{n-1} \end{bmatrix} \tag{2.7}$$

The following theorem is well known in control theory [Kal60b]:

Theorem 1 *The pair (A, C) (or the linear system (2.4)) is observable if and only if the corresponding observability matrix described by equation (2.7) is full column rank $(rank\mathcal{O} = n)$.*

Controllability

On the other hand, a model is said to be controllable, here defined by equation (2.5), if all the possible states can be reached by computing an appropriate control law, $\hat{v}(t)$.

Again, for the linear case, the condition can be written as that the pair (A, B_v) is controllable.

One of the methods to check the above condition is using the controllability matrix, $\mathcal{R} \in R^{n\times(n\times q)}$, defined as:

$$\mathcal{R} = \begin{bmatrix} B_v & AB_v & A^2B_v & \cdots & A^{n-1}B_v \end{bmatrix} \tag{2.8}$$

Also, the following theorem is well known in control theory [Kal60b]:

Theorem 2 *The pair (A, B_v) (or the linear system (2.5)) is controllable if and only if the corresponding controllability matrix described by equation (2.8) is full row rank $(rank\mathcal{R} = n)$.*

Next, let us move on to define the existence conditions for control-based observer, depending on the control problem which has to be solved.

a. Full Control error feedback regulator problem

For this particular problem, one might search to design a controller for the *error model* described by equation (2.6). The *regulator* is based on the error between system output and model output, $\epsilon_y(t)$, and since it is a full control problem, it means that it has access to all the states of the model, in other words B_v, in equation (2.6), is chosen as the identity matrix. This leads to a *control law* which generally can be written as follows

$$\hat{v}(t) \quad = \quad \kappa(\epsilon_y(t), t) \tag{2.9}$$

Through this manuscript we will consider that $\hat{v}(t)$ can either be a static feedback or it can be generated by a linear, time-invariant, causal dynamical system described by the equation:

$$\begin{aligned} \dot{x}_K(t) &= A_K x_K(t) + B_K \epsilon_y(t) \\ \hat{v}(t) &= C_K x_K(t) + D_K \epsilon_y(t) \end{aligned} \tag{2.10}$$

where the controller matrices have the following dimensions: $A_K \in R^{n_K \times n_K}$, $B_K \in R^{n_K \times p}$, $C_K \in R^{n \times n_K}$ and $D_K \in R^{n \times p}$.

Clearly, when the controller doesn't have its own dynamical equation (2.10) becomes

$$\hat{v}(t) \quad = \quad K\epsilon_y(t) \tag{2.11}$$

where $K \in R^{n \times p}$ is a constant matrix. The dimension of K is given by the number of model states, on the one hand, and by the number of measured outputs, on the other hand.

The condition to obtain a control-based observer following the *full control error feedback regulation problem* is given in the next proposition:

Theorem 3 *A control-based observer for the system described by equation (2.4) can be obtained by solving the associate full control error feedback regulator problem if and only if the pair (A, C) is observable.*

Remarks:

1. The *full control error regulator problem* by definition, implies that the controller has access to all states, thus B_v is identity matrix ($q = n$).

2. The condition imposed by Theorem 3 ensures the asymptotic convergence of state estimation in the absence of disturbances ($w(t) = 0$).

3. An intuitive sketch for the proof of Theorem 3 can be considered as follows: given the error model in equation (2.6) for which one is interested in solving full control error feedback regulation problem i.e. computing $\hat{v}(t)$ as in equation (2.11) for equation (2.6) such that $\lim_{t\to\infty} \epsilon_x = 0$ assuming no disturbances ($w(t) = 0$) - stabilization problem. Now, if we consider the dual problem, it leads to the condition that (A^T, C^T) should be controllable, which clearly is equivalent with saying that (A, C) should be observable.

4. One can notice that the condition imposed by Theorem 3 assumes asymptotic convergence in absence of disturbances. When more complex control strategies are deployed such as H_2 or H_∞ solutions, one ought to expect additional conditions for stabizability and detectability of the error model and the system concerning the disturbances.

5. The observability condition, in Theorem 3 can be weakened to assume that the pair (A, C) is at least detectable.

   The relaxation of this condition leads to some additional constrains for the choice of control law, $\hat{v}(t)$. In particular, we have to extract the observable subsystem of the model (2.5) or yet model (2.6) (if there is one) for which the *full control error regulator problem* will be solved. In other words, we can control only the modes which are observable, while the unobservable ones will naturally go to zero, since they are described by stable dynamics (stable zero dynamics).

   The disadvantage of relaxing this assumption is that for those states that we can't control, we loose the ability of modifying the convergence speed of the observer. Thus, the observer is not *tunable* anymore for those particular states.

6. One can notice that this condition is basically the same as the one in the classical observer problem design.

b. Full information regulator problem

On the other hand, for this problem formulation, one might search to design a controller for the chosen *model* expressed by equation (2.5). The *regulator* is based on the full estimated state, $\hat{x}(t)$, as well as on the system output, $y(t)$ (seen as an external input - more precisely as a reference which has to be followed by the model output, $\hat{y}(t)$) which justifies the name of 'full information' problem.

This time the *control law* can be written as

$$\hat{v}(t) = \kappa(\hat{x}(t), y(t), t) \tag{2.12}$$

As before, $\hat{v}(t)$ can either be a static feedback or it can be generated by a linear, time-invariant, causal dynamical system defined as:

$$\begin{aligned} \dot{x}_K(t) &= A_K x_K(t) + B_K \begin{bmatrix} \hat{x}(t) \\ y(t) \end{bmatrix} \\ \hat{v}(t) &= C_K x_K(t) + D_K \begin{bmatrix} \hat{x}(t) \\ y(t) \end{bmatrix} \end{aligned} \tag{2.13}$$

where the controller matrices have the following dimensions: $A_K \in R^{n_K \times n_K}$, $B_K \in R^{n_K \times (n+p)}$, $C_K \in R^{q \times n_K}$ and $D_K \in R^{q \times (n+p)}$.

Again, when the controller doesn't have its own dynamical equation (2.13) becomes

$$\hat{v}(t) = K \begin{bmatrix} \hat{x}(t) \\ y(t) \end{bmatrix} = \begin{bmatrix} K_x & K_y \end{bmatrix} \begin{bmatrix} \hat{x}(t) \\ y(t) \end{bmatrix} \tag{2.14}$$

where $K \in R^{q \times (n+p)}$ is constant matrix (in particular $K_x \in R^{q \times n}$ and $K_y \in R^{q \times p}$).

The conditions to obtain a control-based observer following the *full information regulation problem* are given in the next theorem:

Theorem 4 *A control-based observer for the system described by equation (2.4) can be obtained by solving the associate full information regulator problem if*

a. *The system (2.4) (or the pair (A, C)) is observable.*

b. *The model (2.5) (or the pair (A, B_v)) is controllable*

c. *The matrix* $\begin{bmatrix} A & B_v \\ C & 0 \end{bmatrix}$ *is of rank n+p*

Remarks:

1. The *full information problem* cannot be formulated for the *error model* since the full state, $\epsilon_x(t)$, is not completely available.

2. It is worth noting that only multi-input multi-output square cases are considered. Thus, we assume that the matrix C is full row rank, while the matrix B_v is a full column rank and we have as many control variables, $\hat{v}(t)$, as measured outputs, $y(t)$, thus basically $q = p$.

3. The condition imposed by Theorem 4 ensures the state estimation error can be made less than some $\epsilon > 0$.

4. The proof of Theorem 4 can be found in [BM15], in particular in section: *Some constructive example and discussions*.

5. The condition c arises when we consider the extended system, i.e. the controller has embedded the information about the integral of output error.

6. The observability condition, in Theorem 4 can be weakened to assume that the pair (A, C) is at least detectable.

   The relaxation of this condition leads, as in the previous situation, to some additional constrains for the choice of control law, $\hat{v}(t)$. In particular, we have to extract the observable subsystem of the model (2.5) (if there is one) for which the *full information problem* will be solved. Thus, the relative degree between $\hat{v}(t)$ and $\hat{y}(t)$ suppose to be the same as the dimension of observable space to which the system (2.4) has been reduced.

   Again, the disadvantage of relaxing this assumption is that we lose the ability of modifying the convergence speed of the observer for the unobservable states. Thus, the observer will not be *tunable* anymore for those particular states.

2.5 Design of control-based observer

In this section some design methodologies for control-based observer are explored. In particular, a series of controllers are developed to find a solution for the state *estimation problem* in this control-based paradigm.

Several aspects for this methodology such as the performance of the observer (complexity, convergence, quality of estimation, robustness against noise and model uncertainties) and the differences compared with classical methods are followed throughout this section to illustrate the advantages, but also the limitations of this technique.

As it was mentioned before, the aim of control-based observer paradigm is to convert the observer problem into a control one. Consequently, by finding an appropriate solution for the latter problem such that the output of a chosen model follows the output of the system, the estimations of the state system can be delivered. Next, let us present how one can design such a control law in this framework of the control-based observer.

Two design techniques will be presented next to obtain a solution for the control-based observer, being intimately related with the tracking problem which has to be solved, namely *full information regulator problem* and *full control error feedback regulator problem*. The two representative control problems to design a control-based observer can be formulated as follows:

1. Compute a control law, $\hat{v}(t)$, as defined in equation (2.9) by solving the *full control error feedback regulator problem* for the chosen *model* described by equation (2.5) or for the *error model* described by equation (2.6), such that $\lim_{t\to\infty} \epsilon_y(t) = 0$
2. Compute a control law, $\hat{v}(t)$, as defined in equation (2.12) by solving the *full information regulator problem* for the *model* defined by equation (2.5), such that $\lim_{t\to\infty} (\hat{y}(t) - y(t)) = 0$.

As for control strategies we start with non-optimal control methods such as Proportional (P) and Proportional-Integral (PI). Continuing with optimal solutions such as Linear-Quadratic-Regulator (LQR), Linear-Quadratic-Integrator (LQI), basically some H_2 norm minimization control problems. Finally, a sub-optimal solution based on H_∞ norm is exploited.

In the forthcoming section, we will exploit the above mentioned solutions for control strategies in order to show how an observer can be obtained using this control-based paradigm and also to highlight how the structure of the observer changes depending on the chosen control strategy and the problem formulation. In addition, the convergence of the observer is also studied.

a. Full control error feedback regulator problem

i. Case: CbO - Error model based control strategies

Let us recall the model described by equation (2.6)

Error model:

$$\begin{aligned} \dot{\epsilon}_x(t) &= A\epsilon_x(t) - B_1 w(t) + B_v \hat{v}(t) \\ \epsilon_y(t) &= C\epsilon_x(t) - D_1 w(t) \end{aligned}$$

For which a controller as described in equation (2.9) is chosen

Control law:

$$\hat{v}(t) = \kappa(\epsilon_y(t), t)$$

Next, let us exploit the proposed control strategies for this case, namely *Proportional controller* (non-optimal and optimal solutions) and *Proportional-Integral controller* (non-optimal solution).

In addition, one can notice that since the *error model* takes into account how the state noise and measurement noise affect the chosen model, one can use this information when designing the *control law* leading to two well known standard control problems, namely H_2 full control problem and H_∞ full control problem, which are well detailed in [Doy+89].

1. Proportional controller (P and LQR controllers)

Problem definition:

Given the model as in equation (2.6) design a Proportional controller

$$\hat{v}(t) = -K_p \epsilon_y(t) \tag{2.15}$$

as a solution for full control error feedback regulator problem, such that $\lim_{t\to\infty} \epsilon_y(t) = 0$.

Combining equation (2.6) with equation (2.15) we get:

$$\dot{\epsilon}_x(t) = A\epsilon_x(t) - B_1 w(t) - B_v K_p \epsilon_y(t) \tag{2.16}$$

Which leads to the equation for state estimation as described bellow

Observer:

$$\dot{\hat{x}}(t) = (A - K_p C)\hat{x}(t) + B_0 u(t) + K_p y(t) \tag{2.17}$$

At this point, it is clear that in equation (2.17) B_v is identity and the only thing needed to be done is to find K_p such that the matrix $(A - K_p C)$ is stable. Two methods can be depicted to solve this problem, namely a non-optimal control strategy and an optimal one. Both of them are presented next.

a. Non-optimal solution for Proportional controller:

In order to compute K_p, a pole placement technique is used such that the matrix $(A - K_p C)$ is stable. Typically the technique used is Ackermann's formula. For more details concerning the algorithm one can check [Son98].

b. Optimal solution for Proportional controller:

For the optimal solution, a Linear Quadratic Regulator (LQR) is computed. In particular, the proposed solution for the controller is in terms of output error feedback (due to the equation (2.15) since the control law is based on output error, $\epsilon_y(t)$). The solution for how to compute K_p is described in detail in [LA70], and the optimization problem is described next:

Given the error model described by equation (2.16), and considering its solution in terms of transition matrix (assuming $w(t) = 0$)

$$\epsilon_x(t) = \Phi(t, 0)\epsilon_{x0} \tag{2.18}$$

where the transition matrix is

$$\Phi(t, 0) = e^{[A - B_v F C]t} \tag{2.19}$$

And choosing the performance criterion as

$$J = \frac{1}{2}\int_0^\infty tr[\Phi^T(t, 0)(Q + C^T K_p^T R K_p C)\Phi(t, 0)]dt \tag{2.20}$$

for some symmetric positive semi-definite and definite constant weighting matrices $Q \in R^{n \times n}$ and $R \in R^{m \times m}$,

Find K_p which minimizes the performance criterion J in equation (2.20) subject to the constrains imposed by the error model (2.16) when $w(t) = 0$.

Briefly speaking, the optimal K_p to solve this control problem is given by the following equation:

$$K_p = R^{-1}PLC^T[CLC^T]^{-1} \tag{2.21}$$

To simplify the notation, let us consider $\tilde{A} = A + K_pC$.

Furthermore, P is also a positive semi-definite solution of equation

$$P\tilde{A} + \tilde{A}^TP + Q + C^TK^TRKC = 0 \tag{2.22}$$

While L is a positive definite solution of

$$L\tilde{A}^T + \tilde{A}L + I = 0 \tag{2.23}$$

An iterative algorithm to obtain the optimal K_p is given also in [LA70].

Observer convergence:

Now, to illustrate the convergence of the obtained observer, let us consider the equation of the estimation error, when the disturbances are considered absent ($w(t) = 0$). In doing that, we obtain the following dynamic equation:

$$\dot{\epsilon}_x(t) = (A - K_pC)\epsilon_x(t) \tag{2.24}$$

Clearly, if K_p exists such that the spectrum of matrix $(A - K_pC)$ is on the left half plane (the eigenvalues real part are all negative), computed either using non-optimal solution or the optimal one, then $\epsilon_x(t)$ goes to zero, thus $\hat{x}(t)$ is an estimation of $x(t)$.

Remarks:

1. One can notice that equation (2.17) describes the Luenberger observer (in particular when K_p is computed as the non-optimal solution of the control problem). It is interesting to see that from the point of view of the control problem, Luenberger observer can be seen as a set of Proportional controllers which correct each state such that the output error, $\hat{y}(t) - y(t)$ goes to zero.

2. Also one can notice that, if we consider the optimal solution of the control problem defined above, we basically obtain an optimal way to compute a Luenberger observer.

2. Proportional-Integral controller (PI controller)

For the next method, we also consider the integral component of a controller, thus the controller has its own dynamics.

Problem definition:

Given the model described by equation (2.6) design a Proportional-Integral controller:

$$\hat{v}(t) = -K_p\epsilon_y(t) - K_i\int_0^t \epsilon_y(\tau)d\tau \tag{2.25}$$

as a solution for full control error feedback regulator problem, such that $\lim_{t\to\infty}\epsilon_y(t) = 0$.

Combining equation (2.6) with equation (2.25) to get:

$$\dot{\epsilon}_x(t) = A\epsilon_x(t) - B_1 w(t) - B_v\left[K_p\epsilon_y(t) - K_i\int_0^t \epsilon_y(\tau)d\tau\right] \tag{2.26}$$

Which leads to an extended model for state estimation, due to the integral part (the controller has his own dynamics) and also, since we are in the full control framework, B_v is identity matrix.

Observer:

$$\begin{bmatrix}\dot{x}_i(t)\\ \dot{\hat{x}}(t)\end{bmatrix} = \begin{bmatrix}0 & C\\ -K_i & A-K_pC\end{bmatrix}\begin{bmatrix}x_i(t)\\ \hat{x}(t)\end{bmatrix} + \begin{bmatrix}0\\ B_0\end{bmatrix}u(t) + \begin{bmatrix}-I\\ K_p\end{bmatrix}y(t) \tag{2.27}$$

In order to compute K_p and K_i, again a pole placement technique is used such that the matrix $\begin{bmatrix}0 & C\\ -K_i & A-K_pC\end{bmatrix}$ is stable. To find the appropriate K_p and K_i using the pole placement approach is a more difficult task than the similar one for Proportional controller. The interested reader is kindly advised to check [YW72] for a detailed algorithm to find the controller gains.

Moreover, it is worth noting that because of the additional dynamics introduced by the controller (which is also the source of difficulty for the pole placement technique), some controllability conditions for the extended system are required, as mentioned

in [YW72]. However, since we are in full control case and B_v is identity matrix, those conditions are always satisfied.

Observer convergence:

Next, let us consider the equation of the estimation error defined as $\epsilon_x(t) = \hat{x}(t) - x(t)$:

$$\begin{bmatrix} \dot{x}_i(t) \\ \dot{\epsilon}_x(t) \end{bmatrix} = \begin{bmatrix} 0 & C \\ -K_i & A - K_p C \end{bmatrix} \begin{bmatrix} x_i(t) \\ \epsilon_x(t) \end{bmatrix} \tag{2.28}$$

Since K_p and K_i are chosen such that the eigenvalues of matrix $\begin{bmatrix} 0 & C \\ -K_i & A - K_p C \end{bmatrix}$ are all negative. Thus, as a direct consequence $\epsilon_x(t)$ goes to zero which means that $\hat{x}(t)$ is an estimation of $x(t)$.

Remarks:

1. It is worth noticing that, the proposed controller has its own dynamics given by the integral component. This will increase the dimension (complexity) of the observer.
2. One can notice that the observers obtained here are full-order PI-observer.
3. Every estimated state is individually corrected by a PI controller.

3. Standard H_2/H_∞ full control problems

Problem definition:

Given the error model as in equation (2.6) design a H_2/H_∞ optimal controller

$$\hat{v}(t) = -K_p \epsilon_y(t) \tag{2.29}$$

as a solution for full control error feedback regulator problem, such that $\lim_{t\to\infty} \epsilon_y(t) = 0$.

Combining equation (2.6) with equation (2.29) we get:

$$\begin{aligned} \dot{\epsilon}_x(t) &= A\epsilon_x(t) - B_1 w(t) + B_v \hat{v}(t) \\ \epsilon_y(t) &= C\epsilon_y(t) - D_1 w(t) \\ \hat{v}(t) &= -K_p \epsilon_y(t) \end{aligned} \tag{2.30}$$

For which we can associate the cost function in terms of controlled variable, $z(t)$, as in standard formulation in terms of generalized plant, as bellow:

$$z(t) = C_z\epsilon_x(t) + D_z\hat{v}(t) \tag{2.31}$$

Following the last two equation we get the standard *full control* problem formulation:

$$\begin{aligned} \dot{\epsilon}_x(t) &= A\epsilon_x(t) - B_1 w(t) + B_v\hat{v}(t) \\ z(t) &= C_z\epsilon_x(t) + D_z\hat{v}(t) \\ \epsilon_y(t) &= C\epsilon_y(t) - D_1 w(t) \end{aligned} \tag{2.32}$$

For which a controller in terms of equation (2.29) is computed by solving the following optimization problems concerning the full control problem formulation expressed in equation (2.32):

$$\min_{\hat{v}(t)} ||T_{zw}(s)||_2 \text{ - for } H_2 \text{ case} \tag{2.33}$$

and

$$\min_{\hat{v}(t)} ||T_{zw}(s)||_\infty < \gamma^2 \text{ - for } H_\infty \text{ case} \tag{2.34}$$

where $T_{zw}(s)$ is the transfer function between external signal $w(t)$ and controlled variables $z(t)$ in equation (2.32) and $\gamma > 0$ is given attenuation level.

This control problem imposes some additional constrains in order to solve the control problem namely:

1. The pair (A, B_1) is stabilizable and the pair (A, C_z) is detectable
2. $\begin{bmatrix} B_1 \\ D_1 \end{bmatrix} D_1^T = \begin{bmatrix} 0 \\ I \end{bmatrix}$

a. Standard H_2 full control solution

To solve the up mentioned control problem in terms of H_2 norm we have to solve the following Algebraic Riccati Equation:

$$AY_2 + Y_2A^T + Y_2CRC^TY_2 + B_1B_1^T = 0 \tag{2.35}$$

Finally, the proportional gain for control law, $\hat{v}(t)$ is

$$K_p = Y_2 C^T R^{-1} \tag{2.36}$$

where Y_2 is the solution of Algebraic Riccati Equation (2.35).

b. Standard H_∞ full control solution

To solve the above mentioned control problem in terms of H_∞ norm we have to solve the following Algebraic Riccati Equation:

$$AY_\infty + Y_\infty A^T + Y_\infty(\gamma^{-2} C_z C_z^T - CC^T)Y_\infty + B_1 B_1^T = 0 \tag{2.37}$$

Finally, the proportional gain for control law, $\hat{v}(t)$ is

$$K_p = Y_\infty C^T \tag{2.38}$$

where Y_∞ is the solution of Algebraic Riccati Equation (2.37).

Which leads to the equation for state estimation as described bellow

Observer:

$$\dot{\hat{x}}(t) = (A - K_p C)\hat{x}(t) + B_0 u(t) + K_p y(t) \tag{2.39}$$

Observer convergence:

We have the error equation again:

$$\dot{\epsilon}_x(t) = (A - K_p C)\epsilon_x(t) \tag{2.40}$$

Where K_p was computed, either using equation (2.36) or equation (2.38), such that $A - KpC$ is stable, thus ϵ_x goes to 0, which means the obtained $\hat{x}(t)$ is an estimate of $x(t)$.

Remarks:

1. On the one hand, one can notice that if in the case of H_2 full control problem, the matrices $B_1 B_1^T$ respectively R are chosen as the covariance matrices for

state noise respectively measurement noise, and assuming those noises are zero-mean white-noise processes the equation (2.39) where $K_p = Y_2 C^T R^{-1}$ is in fact Kalman Filter (the steady-state version).

2. On the other hand, the observer described by equation (2.39) for which we have $K_p = Y_\infty C^T$, represents nothing but the H_∞ observer.

b. Full information regulator problem

i. Case: CbO - Model based control strategies

Let us recall the model described by equation (2.5)

Model:

$$\begin{aligned} \dot{\hat{x}}(t) &= A\hat{x}(t) + B_0 u(t) + B_v \hat{v}(t) \\ \hat{y}(t) &= C\hat{x}(t) \end{aligned}$$

For which a controller as described in equation (2.12) is chosen

Control law:

$$\hat{v}(t) = \kappa(\hat{x}(t), y(t)t)$$

Next, let us exploit the proposed control strategies for this case, namely *Proportional controller* (non-optimal and optimal solutions) and *Proportional-Integral controller* (non-optimal and optimal solution).

1. Proportional controller (P and LQR controllers)

Problem definition:

Given the model as in equation (2.5) design a Proportional controller

$$\hat{v}(t) = K \begin{bmatrix} \hat{x}(t) \\ y(t) \end{bmatrix} = \begin{bmatrix} -K_x & K_y \end{bmatrix} \begin{bmatrix} \hat{x}(t) \\ y(t) \end{bmatrix} \tag{2.41}$$

as a solution for full information regulator problem, such that $\lim_{t\to\infty} \hat{y}(t) - y(t) = 0$.

It can be noticed that the control input $\hat{v}(t)$ can be divided in two parts

$$\hat{v}(t) = \hat{v}_x(t) + \hat{v}_y(t) = -K_x \hat{x}(t) + K_y y(t) \tag{2.42}$$

Combining equation (2.5) with equation (2.41) we get:

$$\dot{\hat{x}}(t) \quad = \quad A\hat{x}(t) + B_0 u(t) - B_v K_x \hat{x}(t) + B_v K_y y(t)) \tag{2.43}$$

Which leads to the equation for state estimation as described bellow

Observer:

$$\dot{\hat{x}}(t) \quad = \quad (A - B_v K_x)\hat{x}(t) + B_0 u(t) + B_v K_y y(t) \tag{2.44}$$

At this point, we have to find K_x such that the matrix $(A - B_v K_x)$ is stable and K_y is computed so as to reduce low frequency error between $\hat{y}(t)$ and $y(t)$. Two methods can be depicted to solve this problem, namely a non-optimal control strategy and an optimal one. Both of them are presented next.

a. Non-optimal solution for Proportional controller:

On one hand, in order to compute K_x, a pole placement technique is used such that the matrix $(A - B_v K_x)$ is stable. Typically the technique used is Ackermann's formula. For more details concerning the algorithm one can check [Son98].

On the other hand, for the feedforward part of the controller, namely the gain K_y, a suitable choice can be

$$K_y \quad = \quad -[C(A - B_v K_x)^{-1} B_v]^{-1} \tag{2.45}$$

b. Optimal solution for Proportional controller:

For the optimal solution, a Linear Quadratic Regulator (LQR) is computed to find K_x. The solution for how to compute K_x can be also found in [Son98].

Briefly speaking, the stabilizing part of $\hat{v}(t)$, namely $\hat{v}_x(t) = -K_x \hat{x}(t)$ can be computed by minimizing the cost function of the form:

$$J(\hat{v}_x(t)) \quad = \quad \int_0^\infty [\hat{x}^T(t) Q \hat{x}(t) + \hat{v}_x^T R \hat{v}_x(t)] dt \tag{2.46}$$

where $Q \in R^{n \times n}$ and $R \in q \times q$ are positive semi-definite and definite matrices.

Finally, the optimal gain, K_x is given by the equation:

$$K_x \quad = \quad R^{-1} B_v X \tag{2.47}$$

where $X \in R^{n \times n}$ is the solution of Algebraic Riccati Equation:

$$A^T X + XA + K_x R K_x + Q = 0 \tag{2.48}$$

As for the computation of K_y the same equation is used, namely

$$K_y = -[C(A - B_v K_x)^{-1} B_v]^{-1} \tag{2.49}$$

Observer convergence:

To illustrate the convergence of the obtained observer, let us consider again the equation of the estimation error defined as $\epsilon_x(t) = \hat{x}(t) - x(t)$ and investigate its dynamics evolution. In doing that, we obtain the following dynamic equation:

$$\dot{\epsilon}_x(t) = (A - B_v K_p)\epsilon_x(t) \tag{2.50}$$

Clearly, if K_p exists such that the spectrum of matrix $(A - B_v K_p)$ is on the left half plane (the eigenvalues real part are all negative), computed either using non-optimal solution or the optimal one, then $\epsilon_x(t)$ goes to zero, thus $\hat{x}(t)$ is an estimation of $x(t)$.

Remark:

1. It is worth noticing that this solution (optimal) state feedback together with a feedforward correction has poor results for solving the proposed tracking problem. In particular, the reference, in this case, is the system output $y(t)$ which is usually not constant. Moreover, when the MIMO case is considered the complexity of the tracking problem increases and the estimations results decrease in quality.

2. To deal with the downsides of the proposed solution, it is recommended to consider also the integral output error as part of the control law, as it will be presented next.

2. Proportional-Integral controller (PI and LQI controllers)

Problem definition:

Given the model as in equation (2.5) design a Proportional-Integral controller

$$\hat{v}(t) = -K_x\hat{x}(t) - K_i\int_0^t \epsilon_y(\tau)d\tau \tag{2.51}$$

as a solution for full information regulator problem, such that $\lim_{t\to\infty}\hat{y}(t) - y(t) = 0.$

It can be noticed that the control input $\hat{v}(t)$ has its own dynamics. To illustrate that we write the state space representation of the equation (2.51) as suggested in (2.13), thus we get

$$\begin{aligned}\dot{x}_i(t) &= \begin{bmatrix} C & -I \end{bmatrix}\begin{bmatrix}\hat{x}(t)\\ y(t)\end{bmatrix}\\ \hat{v}(t) &= -K_i x_i(t) - \begin{bmatrix} K_x & 0\end{bmatrix}\begin{bmatrix}\hat{x}(t)\\ y(t)\end{bmatrix}\end{aligned} \tag{2.52}$$

where $x_i(t)$ is the controller state and basically represents the integration of the output error, $\epsilon_y(t)$, while I is the identity matrix having the appropriate dimension.

Combining equation (2.5) with equation (2.51) we get:

$$\dot{\hat{x}}(t) = A\hat{x}(t) + B_0u(t) + B_v[-K_x\hat{x}(t) - K_i\int_0^t (C\hat{x}(\tau) - y(\tau))d\tau] \tag{2.53}$$

Which leads to the equation for state estimation as described below

Observer:

$$\begin{bmatrix}\dot{x}_i(t)\\ \dot{\hat{x}}(t)\end{bmatrix} = \begin{bmatrix} 0 & C\\ -B_vK_i & A - B_vK_x\end{bmatrix}\begin{bmatrix}x_i(t)\\ \hat{x}(t)\end{bmatrix} + \begin{bmatrix}0\\ B_0\end{bmatrix}u(t) + \begin{bmatrix}-I\\ 0\end{bmatrix}y(t) \tag{2.54}$$

Next, we have to find K_x and K_i such that the matrix $\begin{bmatrix} 0 & C\\ -B_vK_i & A - B_vK_x\end{bmatrix}$ is stable.

It can be noticed that the state transition matrix of the observer described by equation (2.54) allows the following factorization

$$\begin{bmatrix} 0 & C\\ -B_vK_i & A - B_vK_x\end{bmatrix} = \begin{bmatrix}0 & C\\ 0 & A\end{bmatrix} - \begin{bmatrix}0\\ B_v\end{bmatrix}\begin{bmatrix} K_i & K_x\end{bmatrix} \tag{2.55}$$

In other words, we search to compute a state feedback, $K_e = \begin{bmatrix} K_i & K_x \end{bmatrix}$ for the extended model $x_e(t) = \begin{bmatrix} x_i(t) \\ \hat{x}(t) \end{bmatrix}$ obtained by augmenting the model described by (2.5) with the equation

$$x_i(t) = \int_0^\infty \epsilon_y(\tau) d\tau \quad \rightarrow \quad \dot{x}_i(t) = \epsilon_y(t) \tag{2.56}$$

which leads to the following matrices for the extended model

$$A_e = \begin{bmatrix} 0 & C \\ 0 & A \end{bmatrix} \qquad B_e = \begin{bmatrix} 0 \\ B_v \end{bmatrix} \tag{2.57}$$

Again, the same two methods presented above to solve this problem can be used, namely a non-optimal control strategy and an optimal one. In particular, we search just for the state feedback gain, while the feedforward one being the identity matrix.

a. Non-optimal solution for Proportional-Integral controller:

In order to compute K_e, a pole placement technique is used such that the matrix $(A_e - B_e K_e)$ is stable. For more details concerning the algorithm one can check [YW72]. One might notice that some controllability condition for the extended model has to be satisfied. Which is always the case, because of the conditions set by Theorem 4.

b. Optimal solution for Proportional-Integrator controller:

For the optimal solution, we compute K_e. The solution can also be found in [YW72].

We search for

$$\hat{v}(t) = -K_e x_e(t) \tag{2.58}$$

by minimizing the cost function of the form

$$J(\hat{v}(t)) = \int_0^\infty [x_e^T(t) Q x_e(t) + \hat{v}^T(t) R \hat{v}(t)] dt \tag{2.59}$$

where $Q \in R^{(n+p)\times(n+p)}$ and $R \in q \times q$ are positive semi-definite and definite matrices.

Finally, the optimal gain, K_e is given by the equation:

$$K_e = R^{-1} B_e X_e \tag{2.60}$$

where $X_e \in R^{(n+p)\times(n+p)}$ is the solution of Algebraic Riccati Equation:

$$A_e^T X_e + X_e A_e + K_e R K_e + Q = 0 \tag{2.61}$$

Observer convergence:

To illustrate the convergence of the obtained observer, let us consider again the equation of the estimation error defined as $\epsilon_x(t) = \hat{x}(t) - x(t)$ and investigate its dynamics evolution. In doing that, we obtain the following dynamic equation:

$$\begin{bmatrix} x_i(t) \\ \epsilon_x(t) \end{bmatrix} = \begin{bmatrix} 0 & C \\ -B_v K_i & A - B_v K_p \end{bmatrix} \begin{bmatrix} x_i(t) \\ \epsilon_x(t) \end{bmatrix} \tag{2.62}$$

Clearly, if K_e exist such that the spectrum of matrix $(A_e - B_e K_e)$ is on the left half plane (the eigenvalues real part are all negative), computed either using non-optimal solution or the optimal one, then $\epsilon_x(t)$ goes to zero, thus $\hat{x}(t)$ is an estimation of $x(t)$.

Remarks:

1. The first remark is about the convergence of the observer when a *full information regulator problem* is solved. Theorem 4 gives the conditions for which a control-based observer solving this particular control problem can be obtained. One can notice that besides the observability-controllability conditions, an invariant zero property is assumed. In other words, the transfer function between $\hat{v}(t)$ and $\hat{y}(t)$ is assumed to have no any zeros. Indeed, any zero of the mentioned transfer function increases the error for our estimations. This fact is highlighted in the original article introducing the control-based observer [BM15] (*Proposition 3.1*).

2. One can notice that this design method for the control-based observer offers a way to estimate also some eventual unknown inputs. Let us assume that the system (2.4) has some states which are affected by some unknown inputs. Now, if we constrain that the chosen model (2.5) is controlled only via the unknown inputs and evidently the assumptions set by Theorem 4 hold, we

find out that, besides the state estimation $\hat{x}(t)$, the control input $\hat{v}(t)$ will be an estimate of unknown inputs $v(t)$. This case will be studied in the next chapter.

2.6 Conclusions

In this section the control-based observer paradigm for systems not affected by unknown inputs apart from the noise has been presented. The main idea is to convert the observer problem into a control one, and consequently to take advantage of well known control methods to improve the quality of the estimations. In particular, some non-optimal solution like P and PI controllers, together with some optimal ones like LQR and LQI controllers and finally the sub-optimal solution in terms of H_∞ problem have been emphasized.

It has also been underlined that, based on the information available to design the control law, two control problems can be formulated to substitute the related observer one, namely the *error feedback regulation problem* (in particular, *full control error feedback regulation problem*) and *full information regulation problem*. Combining the chosen model (2.5) or the error model (2.6) with different control strategies (as specified above) to solve the proposed regulation problems, lead to a set of observers in the control-based observer paradigm.

The conditions for existence of a control-based observer has also been summarized in terms of Theorem 3 and Theorem 4. In particular, to solve the *full control error feedback regulation problem*, the system (2.4) has to be observable, while to find a solution for the *full information regulation problem* the model (2.5) has to be what is called strongly observable [Hau83].

It is worth noticing that using this paradigm, some classical observers can be obtained if one carefully chooses the appropriate control strategy for either the chosen model or the error model. For instance, Luenberger and PI observers can be found by solving *full control error feedback regulator problem* for the chosen model (2.5) (or the error model (2.6)). The Kalman observer equations can be found when solving *full control error feedback regulator problem* for the error model (2.6) in terms of minimizing the H_2 norm, while if the same problem is solved in terms of minimizing the H_∞ norm, the well known H_∞ observer is found.

Another aspect worth mentioning is that depending on the complexity of the chosen control law (when the controller has its own dynamics) the quality of the estimations increases, but also the complexity of the observer increases. Thus, there is a trade-

off between the quality of the estimation and the complexity of the observer which has to be taken into account.

For a thorough analysis of the observer performance one has to look no further than at a comparison of the proposed control methods (bandwidth, transitory regime, robustness to noise and parameter uncertainties, delay, etc). For instance, the convergence of the observer is strongly related with the bandwidth of the controller, while the robustness against noise depends on how the controller attenuates the high frequencies. It is clear that a trade-off between these characteristics arises.

The solution for obtaining a control-based observer using *full information regulation problem* for the chosen model, was presented as an alternative to classical methods such as Luenberger observer, PI-observer, Kalman observer and H_∞ observer. The solution does not intend to outperform classical observer, the main idea was to take a step towards designing observers for unknown input systems, in particular to estimate the state as well as the unknown inputs.

CHAPTER 3

UNKNOWN INPUT OBSERVER - ROBUST APPROACH

This Chapter Answers

1. What are the H_∞ tools used to design a controller to meet some desired performance specifications?
2. How to formulate the observer problem using the control-based paradigm applying H_∞ framework?
3. How to obtain the control-based observer using H_∞ framework?

3.1 Introduction

In this chapter we will talk about the particular case of Unknown Input Observer (UIO) which can be obtained using control-based paradigm. We have already seen in the previous chapter that we can choose to solve the *full information regulator problem* for the model (2.5), if Theorem 4 holds.

One can notice that the choice of B_v is not actually made just to satisfy the conditions required by Theorem 4, but it can also be related with the presence of some possible unknown inputs which affect the system. In other words, assuming that system (2.4) is affected by some unknown inputs, and the chosen model is controlled via those inputs, under certain conditions similar with Theorem 4, an observer using control-based paradigm can be designed for which, both the state and the unknown inputs can be estimated.

In previous the chapter, we have seen that to design an observer using control-based paradigm, two control (tracking) problems can be solved, namely the *error feedback regulation problem* for error model and the *full information regulation problem* for the chosen model. In consequence, when dealing with systems having unknown inputs, the same two solutions can be applied in order to get the estimation of both the state and unknown inputs of the system.

Our goal is to design a robust control-based observer, thus to that end we chose as control technique the one relying on H_∞ tools, mainly motivated by the well known robustness properties of the method. In particular, to solve *error feedback regulation problem* an Output Feedback H_∞ controller is design, while handle the *full information regulation problem* the corresponding Full Information H_∞ controller is used. The main difference between them is that the output feedback solution is more complex (it requires to solve two Riccati equations), but it leads to better results in terms of state and unknown inputs estimation, on the other hand, the full information solution is less complex (just one Riccati equation is solved), but it doesn't consider all the information available about the external signals, such as the state noise and unknown inputs, which clearly leads to results less accurate than the first proposed solution.

Next, a recall on H_∞ tools is given, in particular for the completeness of the chapter. The readers who are familiar with those tools or if they are not interested in the theoretical aspects of H_∞ method can skip the section 3.2 and continue directly with the section 3.3.

3.2 Recalls on H_∞

In this section some useful information regarding H_∞ tools are recalled in order to prepare the ground for designing a robust control-based observer using H_∞ techniques. Concepts like H_∞ norm definition and how to compute it, H_∞ framework description, problem statement and solution for computing an robust controller are expected to be mentioned next.

Many control objectives can be stated in terms of the size of some particular signals (the error, the control input, the output, etc). Therefore a quantitative technique to measure the performance of a control system is required. To that end, the concept of norms have been introduced to characterize the size of a signal. One of the most known and used ones are $p - norms$. In particular we have L_1 norm, L_2 norm (measures the energy of a signal) and L_∞ norm (measures the maximum value of a signal).

Naturally, the concept of norm has also been extended to measure 'the size' of a system. Traditionally, two system norms have been defined for this purpose.

On the one hand, we have H_2 norm which is used to design controllers based on quadratic cost minimization, like Linear-Quadratic Regulator. In control theory this problem can be found under the name of H_2 *Optimal Control*.

On the other hand, we have H_∞ norm which gave rise to a new class of controllers in the 1980's well known for their robustness against noise and model uncertainties. The problem dealing with the design of such controllers is called H_∞ *Optimal Control*. Recalls presented here after are taken mainly from [Zho99].

a. H_∞ system norm

Let us consider a transfer matrix $G(s) \in RH_\infty$, where RH_∞ is the subspace of all proper and real rational stable transfer matrices. The H_∞ norm is defined as:

$$||G(s)||_\infty = \max_\omega \bar{\sigma}[G(j\omega)] \tag{3.1}$$

where $\bar{\sigma}[\bullet]$ represents the largest singular value of a specified transfer matrix.

It is well known that for a multiple-input multiple-output (MIMO) system, the eigenvalues are a poor representation of the system gain. They don't provide a useful means

of generalizing the single-input single-output (SISO) case. Thus, as a way to quantify the gain of a MIMO system the *singular value decomposition* technique is used.

To give an interpretation for the H_∞ norm, let us consider that $G(s)$ is the transfer function which maps the input, u, on the output, y, thus, $y = G(s)u$. We can define the gain provided by a system for a certain input as the ratio of the L_2 norm of the output signal to L_2 norm of the input signal as:

$$\sup_{||u||_2 \neq 0} \frac{||y||_2}{||u||_2} = \sup_{||u||_2 \neq 0} \frac{||G(s)u||_2}{||u||_2} = ||G(s)||_{gain} \tag{3.2}$$

It turns out that this quantity, $||G(s)||_{gain}$ is actually the H_∞ norm of the system $G(s)$. Thus, it can be said that the H_∞ norm of a system is the largest amplification provided by the system for the energy of an input signal. The H_∞ norm is also called an induced norm.

b. How to compute the H_∞ norm

In the upcoming part some solutions for how to compute the H_∞ norm are presented. At this point it is worth noting that there is no analytic solution to compute the H_∞ norm, in contrast with computing the H_2 norm for which such solutions exist.

The computation of the H_∞ norm is in fact complicated and requires some searching.

Let us consider the $G(s) \in RH_\infty$ and ask to find a solution for computing H_∞ norm defined by equation (3.1). To get an estimation of the wanted norm, we first have to set up a grid of frequency points as described next:

$$freq = [\omega_1, \omega_2, \ldots, \omega_N] \tag{3.3}$$

Then an estimation for $||G(s)||_\infty$ is obtained as:

$$\max_{1 \leq k \leq N} \bar{\sigma}[G(j\omega_k)] \tag{3.4}$$

Clearly, this method is computationally expensive, for each frequency, ω_k, the procedure to compute the singular values decomposition has to be applied.

Fortunately, there is another way to approximate $||G(s)||_\infty$, the so-called *Bisection Method*, which was for the first time described in [BBK89]. The technique uses the state space description of the transfer function $G(s)$.

Before providing the Bisection Algorithm, let us recall the following lemma:

Theorem 5 *Let $\gamma > 0$ and the transfer function*

$$G(s) \quad = \quad C(sI - A)B + D \quad \in \quad RH_\infty \tag{3.5}$$

Then $||G(s)||_\infty < \gamma$ if and only if $\bar{\sigma}(D) < \gamma$ and the Hamiltonian matrix H has no eigenvalues on the imaginary axis where

$$H \quad = \quad \begin{pmatrix} A + BR^{-1}D^TC & BR^{-1}B^T \\ -C^T(I + DR^{-1}D^T)C & -(A + BR^{-1}D^TC)^T \end{pmatrix} \tag{3.6}$$

and $R = \gamma^2 I - D^T D$

where the matrices A, B, C, D are obtained from the state space representation for transfer function $G(s)$.

Based on the Theorem 5 the bisection algorithm to compute $||G(s)||_\infty$ can be delivered:

Step 1: Select an upper bound γ_u and a lower bound γ_l such that $\gamma_l < ||G(s)||_\infty < \gamma_u$

Step 2: If $(\gamma_l + \gamma_u) \setminus 2 \leq \epsilon$, stop; Thus $||G(s)||_\infty \approx (\gamma_l + \gamma_u) \setminus 2$. Otherwise go to the next step

Step 3: Set $\gamma = (\gamma_l + \gamma_u) \setminus 2$

Step 4: Test if $||G(s)||_\infty < \gamma$ by computing the eigenvalues of H for the given γ.

Step 5: If H has an eigenvalue on imaginary axis, set $\gamma_l = \gamma$; otherwise set $\gamma_u = \gamma$; go back to Step 2.

At this point, it is obvious that for computing $||G(s)||_\infty$ a search is required, either over ω or γ.

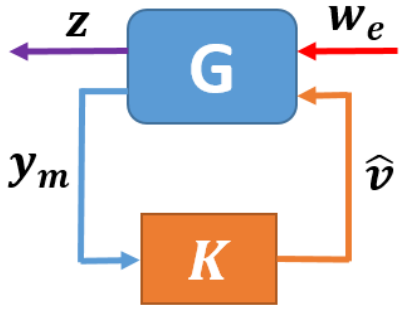

Figure 3.1: Block diagram for H_∞ framework

c. H_∞ Control problem

i. H_∞ framework

Classically, the basic block diagram used to describe the control problem in terms of H_∞ norm is shown in Figure 3.1.

The notations in the H_∞ framework have the following interpretation, G is the so-called generalized plant, it contains the information about the nominal model of the system together with the performance specification of the control problem (more details about this part will be presented later). We consider only finite-dimensional linear time-invariant systems which are in RH_∞. Next, K is the controller which has to be designed such that the control specifications are met.

The signals involved in the connection between the system and the controller have the following signification:

- w_e: *generalized disturbance* and represents the signal that affects the system, but cannot be influenced by the controller;
- $\hat{v}$: *control input* and is the output of the controller;
- z: *controlled variable* and is used to describe if the controller should have some specified properties (they usually have to converge towards zero);
- y_m: *measured outputs* and defines the signal that enters in the controller.

For a better illustration of the H_∞ control problem, a general mathematical description will be given in terms of state space representation and transfer function for the generalized plant G as well as for the controller K.

Let us consider the state space representation for the generalized plant as follows:

$$\begin{aligned} \dot{x} &= \mathcal{A}x + \mathcal{B}_1 w_e + \mathcal{B}_2 \hat{v} \\ z &= C_1 x + \mathcal{D}_{11} w_e + \mathcal{D}_{12} \hat{v} \\ y_m &= C_2 x + \mathcal{D}_{21} w_e + \mathcal{D}_{22} \hat{v} \end{aligned} \tag{3.7}$$

where x is the state of the generalized plant. The other signals have the same signification as presented above.

And in terms of transfer function:

$$G(s) = \left[\begin{array}{c|cc} \mathcal{A} & \mathcal{B}_1 & \mathcal{B}_2 \\ \hline C_1 & \mathcal{D}_{11} & \mathcal{D}_{12} \\ C_2 & \mathcal{D}_{21} & \mathcal{D}_{22} \end{array}\right] = \left[\begin{array}{c|c} \mathcal{A} & \mathcal{B} \\ \hline C & \mathcal{D} \end{array}\right] = C(sI - \mathcal{A})\mathcal{B} + \mathcal{D} \tag{3.8}$$

As for the controller description we have:

$$\begin{aligned} \dot{x}_K &= \mathcal{A}_\mathcal{K} x_K + \mathcal{B}_\mathcal{K} y_m \\ \hat{v} &= C_\mathcal{K} x_K + \mathcal{D}_\mathcal{K} y_m \end{aligned} \tag{3.9}$$

where x_K is the state of the controller. It can be noticed that the controller has its own dynamics.

And in terms of transfer function:

$$K(s) = \left[\begin{array}{c|c} \mathcal{A}_\mathcal{K} & \mathcal{B}_\mathcal{K} \\ \hline C_\mathcal{K} & \mathcal{D}_\mathcal{K} \end{array}\right] = C_\mathcal{K}(sI - \mathcal{A}_\mathcal{K})\mathcal{B}_\mathcal{K} + \mathcal{D}_\mathcal{K} \tag{3.10}$$

ii. Performance specification

Another reason to design a feedback control, besides to stabilize the system, is to achieve some desired performances. In order to do that, we have to find a way to link the indicated specifications with the feedback system performances.

It turns out that the performance specifications can be formulated in terms of desired closed loop sensitivity functions and considered together with the nominal model of the process into the so-called generalized plant. Afterwards, a controller can be obtained using the generalized plant model so that finally the desired performances are met.

To justify the statement above, let us consider the nominal transfer function of the system (no performance specifications defined) as :

$$\begin{bmatrix} \tilde{z} \\ y \end{bmatrix} = \tilde{G}(s) \begin{bmatrix} \tilde{w}_e \\ \hat{v} \end{bmatrix} \tag{3.11}$$

Often, performance specifications arise by specifying how signals have to be attenuated in the closed loop interconnection. For instance, we can design some weighting functions to shape the behavior of the controlled variable, $\tilde{z}$ and yet the one of external signals, $\tilde{w}_e$. This leads to the following equations:

$$z = W_z(s)\tilde{z} \quad and \quad \tilde{w}_e = W_w(s)w_e \tag{3.12}$$

where $W_z(s)$ and $W_w(s)$ are the weighting functions designed on the basis of the performance specifications.

Now, based on the new variables introduced by equation (3.12) the Figure 3.1 is modified as shown in Figure 3.2 describing the weighted interconnection.

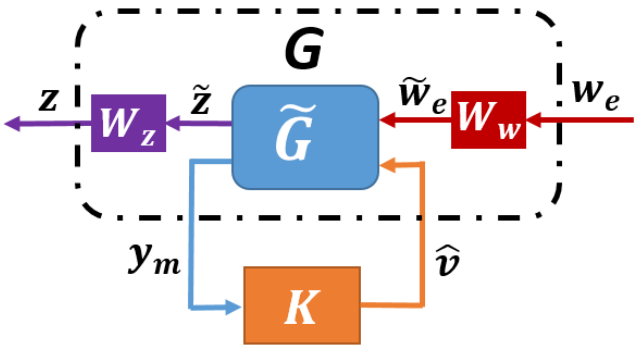

Figure 3.2: Block diagram for weighted interconnection

Furthermore, we can write the closed loop system equations in terms of weighting functions as:

$$||T_{\tilde{z}\tilde{w}_e}(j\omega)|| \leq \frac{1}{|W_z(j\omega)||W_w(j\omega)|}, \text{ for all } \omega \tag{3.13}$$

where $T_{\tilde{z}\tilde{w}_e}(s)$ is the closed loop transfer function between $\tilde{w}_e$ and $\tilde{z}$.

It can be noticed that the generalized plant, $G(s)$, is a mix between the nominal model system, $\tilde{G}(s)$ and the performance specifications, $W_z(s)$ and $W_w(s)$. This approach is

also known as *the four-block problem for H_∞ design* and a more detailed description can be found in [ES90].

Finally, one can design a controller K, for the generalized plant G such that the condition of stability and the desired performance specifications are satisfied (of course assuming that the constrains are not incompatible with the problem we try to solve).

iii. H_∞ error feedback regulation problem

Let us consider the system interconnection shown in Figure 3.1, where, as before, we assume that both, the generalized plant, G and the controller, K, are real rational and proper (belong to RH_∞). Moreover, the realization of transfer matrix G can be simplified. Thus, it can be taken to be of the form:

$$G(s) = \left[\begin{array}{c|cc} \mathcal{A} & \mathcal{B}_1 & \mathcal{B}_2 \\ \hline C_1 & 0 & \mathcal{D}_{12} \\ C_2 & \mathcal{D}_{21} & 0 \end{array}\right] \tag{3.14}$$

In particular, if $\mathcal{D}_{11}$ is zero, it means that no external signals, w_e (like state or measurement noises), are considered being part of the cost function. The matrix $\mathcal{D}_{22}$ is considered zero for the sake of simplicity. The extension for the case where $\mathcal{D}_{22} \neq 0$ can be found in [GD88].

Also, later in this section it will be seen that this simplified problem formulation is enough to find a robust H_∞ controller for the control-based observer.

Some additional assumptions have to be made concerning simplified generalizing plant $G(s)$, which are listed next:

A1. The pair $(\mathcal{A}, \mathcal{B}_1)$ is controllable and the pair $(\mathcal{A}, C_1)$ is observable.

A2. The pair $(\mathcal{A}, \mathcal{B}_2)$ is stabilizable and the pair $(\mathcal{A}, C_2)$ is detectable.

A3. $\mathcal{D}_{12}^T \begin{bmatrix} C_1 & \mathcal{D}_{12} \end{bmatrix} = \begin{bmatrix} 0 & I \end{bmatrix}$

A4. $\begin{bmatrix} \mathcal{B}_1 \\ \mathcal{D}_{21} \end{bmatrix} \mathcal{D}_{21}^T = \begin{bmatrix} 0 \\ I \end{bmatrix}$

In the field of robust controllers design, it is well known that finding an optimal H_∞ controller is usually both theoretically and numerically difficult, as shown in [GD60]. Thus, in practice, it is preferred to obtain an *suboptimal controller*.

Let us formulate the suboptimal H_∞ control problem:

Problem formulation: *Given an attenuation $\gamma > 0$, find an controller K, if there is one, such that*

$$||T_{zw_e}(s)||_\infty \quad < \quad \gamma \tag{3.15}$$

where $T_{zw_e}(s)$ is the closed loop function between w_e and z concerning the transfer function described by equation (3.14).

iv. H_∞ output feedback controller solution

So far, we defined the H_∞ system norm, we described an algorithm for how to compute such a system norm and we formulated the control problem in terms of H_∞ framework. Finally, we can provide the solution for H_∞ control problem.

But before that, we have to mention that the solution for suboptimal controller K involves solving two Riccati equations. Let us, then, define the corresponding Riccati equations.

The first one is written in terms of $\mathcal{X}_\infty$:

$$\mathcal{X}_\infty\mathcal{A} + \mathcal{A}^T\mathcal{X}_\infty + \mathcal{X}_\infty(\tfrac{1}{\gamma^2}\mathcal{B}_1\mathcal{B}_1^T - \mathcal{B}_2\mathcal{B}_2^T)\mathcal{X}_\infty + C_1^TC_1 \quad = \quad 0 \tag{3.16}$$

While the second one is written in terms of $\mathcal{Y}_\infty$:

$$\mathcal{A}\mathcal{Y}_\infty + \mathcal{Y}_\infty\mathcal{A}^T + \mathcal{Y}_\infty(\tfrac{1}{\gamma^2}C_1^TC_1 - C_2^TC_2)\mathcal{Y}_\infty + \mathcal{B}_1\mathcal{B}_1^T \quad = \quad 0 \tag{3.17}$$

The controller is given by the following theorem:

Theorem 6 *There exist a controller K such that $||T_{zw_e}(s)||_\infty < \gamma$ if and only if the conditions hold:*

1. *There exists a stabilizing solution $\mathcal{X}_\infty > 0$ for equation (3.16).*

2. *There exists a stabilizing solution $\mathcal{Y}_\infty > 0$ for equation (3.17).*

3. *$\rho(\mathcal{X}_\infty \mathcal{Y}_\infty) < \gamma^2$, where $\rho(\bullet)$ is the spectral radius of a certain matrix.*

Moreover, when these conditions hold, one such controller is:

$$K(s) = \left[\begin{array}{c|c} \mathcal{A}_\infty & -\mathcal{Z}_\infty \mathcal{L}_\infty \\ \hline \mathcal{F}_\infty & 0 \end{array}\right] \tag{3.18}$$

where the controller matrices are defined as

- $\mathcal{A}_\infty = \mathcal{A} + \gamma^{-2}\mathcal{B}_1\mathcal{B}_1^T\mathcal{X}_\infty + \mathcal{B}_2\mathcal{F}_\infty + \mathcal{Z}_\infty\mathcal{L}_\infty\mathcal{C}_2$
- $\mathcal{F}_\infty = -\mathcal{B}_2^T\mathcal{X}_\infty$
- $\mathcal{L}_\infty = -\mathcal{Y}_\infty\mathcal{C}_2^T$
- $\mathcal{Z}_\infty = (\mathcal{I} - \gamma^{-2}\mathcal{Y}_\infty\mathcal{X}_\infty)^{-1}$

Moreover, it is interesting to write the state space representation of the solution to highlight a special structure of the controller.

Thus, the controller can be written as

$$\begin{aligned} \dot{x}_K &= \mathcal{A}x_K + \mathcal{B}_1\hat{w}_{worst} + \mathcal{B}_2 u + \mathcal{Z}_\infty\mathcal{L}_\infty(\mathcal{C}_2 x_K - y_m) \\ \hat{v} &= \mathcal{F}_\infty x_K \\ \hat{w}_{worst} &= \gamma^{-2}\mathcal{B}_1^T\mathcal{X}_\infty x_K \end{aligned} \tag{3.19}$$

One can notice that equation (3.19) has the structure of an observer-based compensator, as it is suggested in [Doy+89]. In the same article it is also mentioned that the controller exhibits the so-called separation property. The formulas can be interpreted as $\hat{w}_{worst}$ represents, in some sense, the worst case of the external inputs. In addition, $\mathcal{Z}_\infty\mathcal{L}_\infty$ is the optimal filter gain to estimate $\hat{v}$, which can also be seen as the optimal input control, in the presence of the worst-case external input, $\hat{w}_{worst}$.

v. H_∞ full information regulation problem

Next, let us consider the case of full information. The realization of transfer matrix G for this formulation cam be described as bellow:

$$G(s) = \left[\begin{array}{c|cc} \mathcal{A} & \mathcal{B}_1 & \mathcal{B}_2 \\ \hline C_1 & \mathcal{D}_{11} & \mathcal{D}_{12} \\ \begin{bmatrix} I \\ 0 \end{bmatrix} & \begin{bmatrix} 0 \\ I \end{bmatrix} & \begin{bmatrix} 0 \\ 0 \end{bmatrix} \end{array}\right] \tag{3.20}$$

Where, in particular $y_m(t) = \begin{bmatrix} x(t) \\ w_e(t) \end{bmatrix}$. In this case it is assumed that the full state $x(t)$ is known at any time, as well as the external signals $w_e(t)$.

Some additional assumptions have to be made concerning the generalized plant $G(s)$, for the full information problem formulation, as listed bellow:

A1. The pair $(\mathcal{A}, \mathcal{B}_1)$ is stabilizable and the pair $(\mathcal{A}, C_1)$ is detectable.

A2. The pair $(\mathcal{A}, \mathcal{B}_2)$ is stabilizable.

A3. $\mathcal{D}_{12}^T \begin{bmatrix} C_1 & \mathcal{D}_{12} \end{bmatrix} = \begin{bmatrix} 0 & I \end{bmatrix}$

Let us formulate the suboptimal H_∞ control problem:

Problem formulation: *Given an attenuation $\gamma > 0$, find an controller K, if there is one, such that*

$$||T_{zw_e}(s)||_\infty < \gamma \tag{3.21}$$

where $T_{zw_e}(s)$ is the closed loop function between w_e and z concerning the transfer function described by equation (3.20).

The solution for H_∞ Full Information problem is given in terms of some Algebraic Riccati Equation solution for which the corresponding Hamiltonian matrix is:

$$\mathcal{H} = \begin{bmatrix} \mathcal{A} & 0 \\ -C_1^T C_1 & -\mathcal{A}^T \end{bmatrix} - \begin{bmatrix} \mathcal{B} \\ -C_1^T \mathcal{D}_{1\bullet} \end{bmatrix} \mathcal{R}^{-1} \begin{bmatrix} \mathcal{D}_{1\bullet}^T C_1 & \mathcal{B} \end{bmatrix} \tag{3.22}$$

where

$$\mathcal{R} = \mathcal{D}_{1\bullet}^T \mathcal{D}_{1\bullet} - \begin{bmatrix} \gamma^2 I & 0 \\ 0 & 0 \end{bmatrix} \quad \mathcal{D}_{1\bullet} = \begin{bmatrix} \mathcal{D}_{11} & \mathcal{D}_{12} \end{bmatrix} \quad \mathcal{B} = \begin{bmatrix} \mathcal{B}_1 & \mathcal{B}_2 \end{bmatrix}$$

The H_∞ full information controller is given by the following theorem:

Theorem 7 *There exists a controller K such that $||T_{zw_e}(s)||_\infty < \gamma$ if and only if the conditions hold:*

1. *$\mathcal{H} \in dom(Ric)$ and $Ric(H) \leq 0$, where $dom(Ric)$ consists of Hamiltonian matrices $\mathcal{H}$ having certain properties (see* **Section 2.1***; [GD60]).*
2. *There exists a stabilizing solution $\mathcal{X}_\infty = \mathcal{X}_2 \mathcal{X}_1^{-1} > 0$ where $\mathcal{X}_1$ and $\mathcal{X}_2$ are computed such that the Im $\begin{bmatrix} \mathcal{X}_1 \\ \mathcal{X}_2 \end{bmatrix}$ is the stabilizing invariant subspace of $\mathcal{H}$.*

Moreover, when these conditions hold, such a controller has the following partition:

$$K = \begin{bmatrix} K_x & K_y \end{bmatrix} \tag{3.23}$$

where the controller matrices are defined as

$$K_x = \begin{bmatrix} \mathcal{T}_2 & I \end{bmatrix} \mathcal{F} \quad K_y = \mathcal{T}_2 \quad \mathcal{T}_2 = \mathcal{D}_{12}^T \mathcal{D}_{11} \tag{3.24}$$

and yet

$$\mathcal{F} = \begin{bmatrix} \mathcal{F}_1 \\ \mathcal{F}_2 \end{bmatrix} = -\mathcal{R}^{-1} \left[\mathcal{D}_{1\bullet}^T \mathcal{C}_1 + \mathcal{B}^T \mathcal{X}_\infty \right] \tag{3.25}$$

3.3 System and model definition

Let us consider the linear case of the control-based paradigm, in particular the equations for the system and the chosen model are provided.

a. Case study: With unknown inputs

As in the previous chapter, let us consider this time the equations , of the *linear system affected by unknown inputs* in addition to the noise as follows:

System:

$$\begin{aligned} \dot{x}(t) &= Ax(t) + B_0u(t) + B_1w(t) + B_2v(t) \\ y(t) &= Cx(t) + D_0u(t) + D_1w(t) + D_2v(t) \end{aligned} \tag{3.26}$$

where again the variables have a similar meaning, namely $x(t) \in \mathbb{R}^n$ is the state vector, $u(t) \in \mathbb{R}^m$ is the known input vector, $v(t) \in \mathbb{R}^q$ is the unknown input vector, $w(t) \in \mathbb{R}^{n+p}$ the vector of noise (state noise $w_x(t) \in \mathbb{R}^n$ and measurement noise $w_y(t) \in \mathbb{R}^p$), thus $w(t) = \begin{bmatrix} w_x(t) \\ w_y(t) \end{bmatrix}$ and finally, $y(t) \in \mathbb{R}^p$ the vector of measured output.

As always, for the linear case, the matrices A, B_0, B_1, B_2, C, D_0, D_1 and D_2, having appropriate dimensions, completely characterize the system.

Once again, for the sake of simplicity, the matrices D_0 and D_2 in equation (3.26) can be considered zero.

At this point, it is clear that the *model* of the system can be chosen as

Model:

$$\begin{aligned} \dot{\hat{x}}(t) &= A\hat{x}(t) + B_0u(t) + B_2\hat{v}(t) \\ \hat{y}(t) &= C\hat{x}(t) \end{aligned} \tag{3.27}$$

A similar remark as before can also be made here, namely the model doesn't take into account the information about the external signals. As it can be expected, the model is driven via $\hat{v}(t)$.

Finally, the error model between the model and the system is described by

Model error:

$$\begin{aligned} \dot{\epsilon}_x(t) &= A\epsilon_x(t) - B_1w(t) - B_2v(t) + B_2\hat{v}(t) \\ \epsilon_y(t) &= C\epsilon_x(t) - D_1w(t) \end{aligned} \tag{3.28}$$

where, as before, $\epsilon_x(t) = \hat{x}(t) - x(t)$ and $\epsilon_y(t) = \hat{y}(t) - y(t)$ and again, one can notice that the error model takes into account the effect of the noise in its description.

3.4 Conditions to obtain a control-based observer

In this section, the conditions that the system and consequently the model (the error model) have to satisfy are provided. In contrast with the previous chapter, for this case the conditions for a control-based observer are not dependent on the control problem chosen to be solved. This is because now we are constrained to control either the chosen model or the error model via the unknown inputs. Just as a reminder, in the previous chapter, for the *error feedback regulator problem* we have solved the full control version of the problem, which basically means that the condition for controllability was always satisfied (since we had access to all states).

Thus, in this case, either if we search to design a controller which is based on the full estimated state, $\hat{x}(t)$, as well as on the system output, $y(t)$ or if we search a controller based on the error, $\epsilon_y(t)$, the conditions will be the same.

The *control law* can be written as

$$\hat{v}(t) = \kappa(\hat{x}(t), y(t), t) \tag{3.29}$$

or respectively

$$\hat{v}(t) = \kappa(\epsilon_y(t), t) \tag{3.30}$$

Where, as before, $\hat{v}(t)$ can either be static controller or it can be generated by a linear, time-invariant, causal, dynamical system defined as:

$$\begin{aligned} \dot{x}_K(t) &= A_K x_K + B_K \begin{bmatrix} \hat{x}(t) \\ y(t) \end{bmatrix} \\ \hat{v}(t) &= C_K x_K + D_K \begin{bmatrix} \hat{x}(t) \\ y(t) \end{bmatrix} \end{aligned} \tag{3.31}$$

or respectively

$$\begin{aligned} \dot{x}_K(t) &= A_K x_K + B_K \epsilon_y(t) \\ \hat{v}(t) &= C_K x_K + D_K \epsilon_y(t) \end{aligned} \tag{3.32}$$

where the controller matrices have the following dimensions: $A_K \in R^{n_K \times n_K}$, $B_K \in R^{n_K \times (n+p)}$, $C_K \in R^{q \times n_K}$ and $D_K \in R^{q \times (n+p)}$.

Again, when the the controller doesn't have its own dynamic the equation (2.13) becomes

$$\hat{v}(t) = K\begin{bmatrix}\hat{x}(t)\\ y(t)\end{bmatrix} = \begin{bmatrix}K_x & K_y\end{bmatrix}\begin{bmatrix}\hat{x}(t)\\ y(t)\end{bmatrix} \tag{3.33}$$

or respectively

$$\hat{v}(t) = K\epsilon_y(t) \tag{3.34}$$

where $K \in R^{q\times(n+p)}$ is a constant matrix (in particular, $K_x \in R^{q\times n}$ and $K_y \in R^{q\times p}$).

The conditions for existence of a control-based observer following the *full information regulation problem* is given in the next theorem:

Theorem 8 *A control-based observer for the system described by equation (3.26) can be obtained by solving the associate full information regulator problem or error feedback regulator problem if*

a. *The pair* (A, C) *is observable.*

b. *The pair* (A, B_2) *is controllable*

c. *The matrix* $\begin{bmatrix}sI - A & B_2\\ C & 0\end{bmatrix}$ *is of rank n+p, for all* $s \in \mathbb{C}$

Remarks:

1. The condition imposed by Theorem 8 ensures the state estimation error can be made less than some $\epsilon > 0$.

2. Notice that, as mentioned in [BM15],the convergence of the state estimation under the conditions of Theorem 8 may depend on the zeros of the transfer between $v(t)$ and $y(t)$.

$$||\hat{x}(t) - x(t)|| \leq \epsilon + \xi V \tag{3.35}$$

where ξ depends on the zeros of the transfer between $y(t)$ and $v(t)$, while V comes from the assumption that $v(t)$ (together with its derivatives) are uniformly bounded by V.

Due to the condition c, which states that there are no invariant zero between $v(t)$ and $y(t)$, $\xi = 0$ in equation (3.35). This means that the state as well as the unknown input can be estimated arbitrarily fast and accurate.

Moreover, the condition c can be relaxed, but this will influence the quality of both the state and the unknown input estimation as indicated by equation (3.35). In particular, the zeros of the mentioned transfer as well as the rate of variation of $v(t)$ have limiting effects on the estimation accuracy and the estimation time.

3. One can notice that the conditions a. and c. of the Theorem 4 can be expressed in terms of *strong observability*. According to [Hau83], a system is *strongly observable* if the triplet $\{A, B_v, C\}$ has no invariant zeros.

   Moreover, in [FLD07] it is shown how to check this property of *strong observability*, based on the concept of the relative degree of a system following [Isi96].

   Let us recall the theorem regarding the result of *strong observability* given in [FLD07]. One might notice that the theorem concerns the relative degree of a system with respect to some unknown inputs $v(t)$.

   Theorem 9 *Strong observability [FLD07]:*

   The system (3.26) is strongly observable if and only if the output, $y(t)$ has the relative degree n with respect to the control input $v(t)$.

   In addition, one can notice that Theorem 9 describes the single-input single-output (SISO) case. The extension for MIMO case is also presented in [FLD07], for which it is assumed that the number of control inputs is equal with the number of outputs ($q = p$)

3.5 H_∞ design methods for control-based observer

For the following part, we focus on designing an H_∞ control strategy in order to build a robust observer using the control-based paradigm. For this design, we will consider the external signals admit some frequency separation property; the unknown inputs, $v(t)$, is considered as a low frequency deterministic signal, while the noise, $w(t)$, is characterized by a non-deterministic Gaussian signal (in particular, high frequency components).

As for the objectives of the optimization problem, we will impose that the observer has to estimate both the state and the unknown inputs.

The reason why we focus on the H_∞ tools to solve this particular problem instead of using for instance Linear Quadratic Gaussian (LQG) solution, is because of robustness issues. If we search for guaranteed margins for LQG regulators, according to [Doy78], 'there are none'.

In this chapter we will look at the two problem formulations mentioned before, namely the *error feedback regulation problem*, respectively the *full information regulation problem*, but now in the H_∞ framework. Thus, the control problem can be formulated as:

1. Compute a control law, $\hat{v}(t)$, as defined in equation (3.30) by solving the H_∞ *error feedback regulator problem* for the *error model* described by equation (3.28), such that $\lim_{t\to\infty} \epsilon_y(t) = 0$
2. Compute a control law, $\hat{v}(t)$, as defined in equation (3.29) by solving the H_∞ *full information regulator problem* for the *model* described by equation (3.27), such that $\lim_{t\to\infty} (\hat{y}(t) - y(t)) = 0$

a. H_∞ error feedback regulation problem

Let us recall the model described by equation (3.28)

Error model:

$$\begin{aligned} \tilde{G}: \quad \dot{\epsilon}_x &= A\epsilon_x - B_1 w - B_2 v + B_2 \hat{v} \\ \epsilon_y &= C\epsilon_x - D_1 w \end{aligned} \tag{3.36}$$

For which a controller as described in equation (3.30) is chosen as

Control law:

$$\hat{v}(t) = \kappa(\epsilon_y(t), t)$$

Problem definition:

Given the model as in equation (3.28) design a H_∞ controller

$$\begin{aligned} \dot{x}_K(t) &= A_K x_K + B_K \epsilon_y(t) \\ \hat{v}(t) &= C_K x_K + D_K \epsilon_y(t) \end{aligned} \tag{3.37}$$

as a solution for error feedback regulator problem, such that $\lim_{t\to\infty} \epsilon_y(t) = 0$.

At this point, we have to formulate the control problem for the control-based observer in terms of the H_∞ framework as described in equation (3.8).

We start with the definition of the generalized plant G, which is a combination between the error model $\tilde{G}$ having the state ϵ_x (see equation (3.28)) and the templates which arise from the performance specifications being described by the state x_{ps} (which will be defined later in this chapter). Let us consider that the generalized plant state for this particular problem is denoted as

$$x_G = \begin{bmatrix} \epsilon_x \\ x_{ps} \end{bmatrix}$$

Moreover, the signification of the signals presented in H_∞ framework is given again, w_e represents the external signals, $\hat{v}$ the control input which will be computed, ϵ_y is the measured output (instead of y_m) and the controlled variable will be characterized by z. The definition of performance specifications leads to multiple cases of this problem. Here we will mention just two of them.

i. Case 1

For this case we design templates to map the performance specifications, in particular, for the output error signal and the control input signal, namely ϵ_y and $\hat{v}$. The block diagram of this configuration is shown in Figure 3.3.

The mathematical equations for this particular case using H_∞ framework is given next:

$$\begin{aligned} \dot{x}_G &= A_G x_G + B_{G1} w_e + B_{G2} \hat{v} \\ z &= C_{G1} x_G + D_{G11} w_e + D_{G12} \hat{v} \\ \epsilon_y &= C_{G2} x_G + D_{G21} w_e + D_{G22} \hat{v} \end{aligned} \tag{3.38}$$

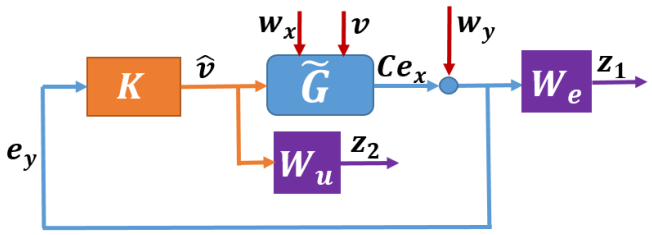

Figure 3.3: Block diagram for case 1

The corresponding vectors for state (x_G), external inputs (w_e), noise (w) and controlled variable (z) are

$$x_G = \begin{bmatrix} \epsilon_x \\ x_{ps} \end{bmatrix} \quad w_e = \begin{bmatrix} w \\ v \end{bmatrix} \quad w = \begin{bmatrix} w_x \\ w_y \end{bmatrix} \quad z = \begin{bmatrix} z_1 \\ z_2 \end{bmatrix} \tag{3.39}$$

Let us consider the matrices B_{1x} and D_{1y} which correspond to state noise respectively to measurement noise.

The matrices which describe equation (3.38) can be expended as

$$A_G = \begin{bmatrix} A & 0 & 0 \\ B_{1ps}C & A_{1ps} & 0 \\ 0 & 0 & A_{2ps} \end{bmatrix} \quad B_{G1} = \begin{bmatrix} -B_{1x} & 0 & -B_2 \\ 0 & B_{1ps} & 0 \\ 0 & 0 & 0 \end{bmatrix} \quad B_{G2} = \begin{bmatrix} B_2 \\ 0 \\ B_{2ps} \end{bmatrix}$$
$$C_{G1} = \begin{bmatrix} D_{1ps}C & C_{1ps} & 0 \\ 0 & 0 & C_{2ps} \end{bmatrix} \quad D_{G11} = \begin{bmatrix} 0 & -D_{1ps}D_{1y} & 0 \\ 0 & 0 & 0 \end{bmatrix} \quad D_{G12} = \begin{bmatrix} 0 \\ D_{2ps} \end{bmatrix}$$
$$C_{G2} = \begin{bmatrix} C & 0 & 0 \end{bmatrix} \quad D_{G21} = \begin{bmatrix} -D_{1y} & 0 \end{bmatrix} \quad D_{G22} = 0$$

Furthermore, to ensure the performance objectives related to sensitivity closed-loop functions such as: tracking errors (the template $W_e(s)$ will shape the sensitivity closed loop function $S(s)$):

$$\bar{\sigma}(S(j\omega)) = \frac{1}{|W_e(j\omega)|}, \text{ for all } \omega \tag{3.40}$$

where the inverse of $W_e(s)$ can be chosen as a high pass filter as below:

$$\frac{1}{W_e(s)} = \frac{s + \omega_e \epsilon_e}{s/M_e + \omega_e} \tag{3.41}$$

In addition, to ensure the performance objectives related to sensitivity closed-loop functions such as: control input saturation (the template $W_u(s)$ will shape the sensitivity closed loop function $KS(s)$):

$$\bar{\sigma}(KS(j\omega)) = \frac{1}{|W_u(j\omega)|}, \text{ for all } \omega \tag{3.42}$$

where the inverse of $W_u(s)$ can be chosen under the form:

$$\frac{1}{W_u(s)} = \frac{\epsilon_u s + \omega_u}{s + \omega_u / M_u} \tag{3.43}$$

Thus, we can express the performance specification in terms of matrix transfer as

$$\begin{bmatrix} z_1 \\ z_2 \end{bmatrix} = \begin{bmatrix} W_e(s) & 0 \\ 0 & W_u(s) \end{bmatrix} \begin{bmatrix} \epsilon_y \\ \hat{v} \end{bmatrix} \tag{3.44}$$

Next, based on $W_e(s)$ and $W_u(s)$ we can obtain the matrix representation for A_{1ps}, A_{2ps}, B_{1ps}, B_{2ps}, C_{1ps}, C_{2ps} and D_{2ps} knowing that

$$W_e(s) = \left[\begin{array}{c|c} A_{1ps} & B_{1ps} \\ \hline C_{1ps} & D_{1ps} \end{array}\right] \tag{3.45}$$

and

$$W_u(s) = \left[\begin{array}{c|c} A_{2ps} & B_{2ps} \\ \hline C_{2ps} & D_{2ps} \end{array}\right] \tag{3.46}$$

Thus, equation (3.38) is now fully described.

Finally, the H_∞ control problem can be formulated as:

Given the model described by (3.38) under the observability-controlability assumptions design an output feedback H_∞ controller such that

$$||T_{zw_e}(s)||_\infty < \gamma \tag{3.47}$$

where $\gamma > 0$ and $T_{zw_e}(s)$ is the closed loop transfer function between w_e and z.

Remarks:

1. It can be noticed that D_{G11} is not zero, which violates the assumption made in Theorem 6. This, in fact, doesn't pose any problem for computing a H_∞ controller, as that assumption was made for the sake of simplicity. Without it, the formulas describing the controller become very complicated. A full description of H_∞ controller can be found in [GD88], for the case when D_{G11} is not zero.

2. One can also suggest that the information about the external inputs, such as the state noise, the measurement noise and the unknown inputs are not taken into account for H_∞ controller design. This remark will lead to the second case.

ii. Case 2

As it was mentioned above, the second formulation includes the detail that the noise and the unknown inputs belong to different frequency bands. The block diagram for this case can be seen in Figure 3.4.

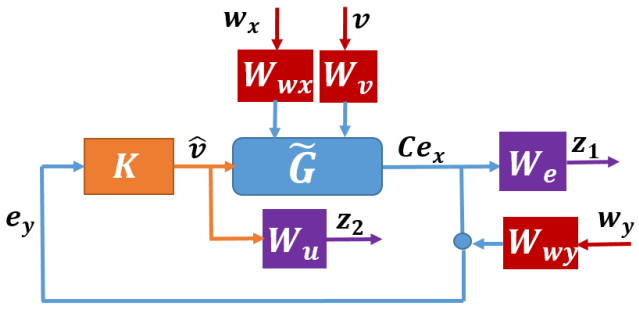

Figure 3.4: Block diagram for case 2

It might seem redundant, but let us present again all the steps to formulate the H_∞ control problem, as some of the matrices will be different and more performance specifications will be taken into account.

The mathematical formulation of H_∞ problem is

$$\begin{aligned} \dot{x}_G &= A_G x_G + B_{G1} w_e + B_{G2} \hat{v} \\ z &= C_{G1} x_G + D_{G11} w_e + D_{G12} \hat{v} \\ \epsilon_y &= C_{G2} x_G + D_{G21} w_e + D_{G22} \hat{v} \end{aligned} \tag{3.48}$$

The corresponding vectors for state (x_G), external inputs (w_e), noise (w) and controlled variable (z) are

$$x_G = \begin{bmatrix} \epsilon_x \\ x_{ps} \end{bmatrix} \quad w_e = \begin{bmatrix} w \\ v \end{bmatrix} \quad w = \begin{bmatrix} w_x \\ w_y \end{bmatrix} \quad z = \begin{bmatrix} z_1 \\ z_2 \end{bmatrix} \tag{3.49}$$

As before, we consider the matrices B_{1x} and D_{1y} related to state and measurement noises.

The matrices which describe equation (3.48) can be expended as

$$A_G = \begin{bmatrix} A & 0 & 0 & 0 & 0 & 0 \\ 0 & A_x & 0 & 0 & 0 & 0 \\ 0 & 0 & A_y & 0 & 0 & 0 \\ 0 & 0 & 0 & A_v & 0 & 0 \\ B_{1ps}C & 0 & 0 & 0 & A_{1ps} & 0 \\ 0 & 0 & 0 & 0 & 0 & A_{2ps} \end{bmatrix} \quad B_{G1} = \begin{bmatrix} -B_{1x} & 0 & -B_2 \\ B_x & 0 & 0 \\ 0 & B_y & 0 \\ 0 & 0 & B_v \\ 0 & 0 & 0 \\ 0 & 0 & 0 \end{bmatrix} \quad B_{G2} = \begin{bmatrix} B_2 \\ 0 \\ 0 \\ 0 \\ 0 \\ B_{2ps} \end{bmatrix}$$

$$C_{G1} = \begin{bmatrix} D_{1ps}C & 0 & 0 & 0 & C_{1ps} & 0 \\ 0 & 0 & 0 & 0 & 0 & C_{2ps} \end{bmatrix} \quad D_{G11} = \begin{bmatrix} 0 & 0 & 0 \\ 0 & 0 & 0 \end{bmatrix} \quad D_{G12} = \begin{bmatrix} 0 \\ D_{2ps} \end{bmatrix}$$

$$C_{G2} = \begin{bmatrix} C & 0 & 0 & C_y & 0 & 0 \end{bmatrix} \quad D_{G21} = \begin{bmatrix} 0 & D_y & 0 \end{bmatrix} \quad D_{G22} = 0$$

Again, we define the performance specification for our H_∞ control problem similar to the previous case.

The inverse of $W_e(s)$ is a high pass filter

$$\frac{1}{W_e(s)} = \frac{s + \omega_e \epsilon_e}{s/M_e + \omega_e} \tag{3.50}$$

having the state space representation

$$W_e(s) = \left[\begin{array}{c|c} A_{1ps} & B_{1ps} \\ \hline C_{1ps} & D_{1ps} \end{array}\right] \tag{3.51}$$

The inverse of $W_u(s)$ is a low pass filter

$$\frac{1}{W_u(s)} = \frac{\epsilon_u s + \omega_u}{s + \omega_u/M_u} \tag{3.52}$$

with the corresponding state space representation

$$W_u(s) \quad = \quad \left[\begin{array}{c|c} A_{2ps} & B_{2ps} \\ \hline C_{2ps} & D_{2ps} \end{array}\right] \tag{3.53}$$

In addition to the previous case, we define the templates for the external signals. In particular, the ones corresponding to the state and measurement noises are modeled as high pass filters:

$$W_{wx}(s) = \frac{s + \omega_{wx}\epsilon_{wx}}{s/M_{wx} + \omega_{wx}} \, , \, W_{wy}(s) = \frac{s + \omega_{wy}\epsilon_{wy}}{s/M_{wy} + \omega_{wy}} \tag{3.54}$$

having the state space representation

$$W_{we}(s) = \left[\begin{array}{c|c} A_x & B_x \\ \hline C_x & D_x \end{array}\right] \quad W_{wy}(s) = \left[\begin{array}{c|c} A_y & B_y \\ \hline C_y & D_y \end{array}\right] \tag{3.55}$$

while the unknown inputs can be modeled by a low pass filter

$$W_v(s) = \frac{\epsilon_v s + \omega_v}{s + \omega_v/M_v} \tag{3.56}$$

with the corresponding state space representation

$$W_v(s) \quad = \quad \left[\begin{array}{c|c} A_v & B_v \\ \hline C_v & D_v \end{array}\right] \tag{3.57}$$

Finally, the H_∞ control problem can be formulated as:

Given the model described by (3.38) under the observability-controlability assumptions design an output feedback H_∞ controller such that

$$||T_{zw_e}(s)||_\infty \quad < \quad \gamma \tag{3.58}$$

where $\gamma > 0$ and $T_{zw_e}(s)$ is the closed loop transfer function between w_e and z.

Remarks:

1. As it was mentioned before, the motivation for this second case is to also model the external signals, knowing that the unknown inputs are described by a deterministic low frequency signal, while the noises are characterized by non-deterministic signals having, in particular components in the high frequency range. These properties are captured by the equations (3.54) and (3.56).

2. Both cases are based on the *Output feedback H_∞ controller*, which means that the control law described by equation (3.37) contains a description of the error model together with the performance specification related to each case. This is the reason of the increased complexity of the observer, but as we will see later the quality of the estimation for both state and unknown inputs is quite accurate.

b. H_∞ Full information regulation problem

This time, let us recall the model described by equation (3.27)

Model:

$$\begin{aligned} \tilde{G}: \quad \dot{\hat{x}}(t) &= A\hat{x}(t) + B_0 u(t) + B_2 \hat{v}(t) \\ \hat{y}(t) &= C\hat{x}(t) \end{aligned} \tag{3.59}$$

For which a controller as described in equation (3.29) is chosen as

Control law:

$$\hat{v}(t) = \kappa(\hat{x}(t), y(t), t)$$

Problem definition:

Given the model as in equation (2.5) design an H_∞ controller

$$\hat{v}(t) = K \begin{bmatrix} \hat{x}(t) \\ y(t) \end{bmatrix} = \begin{bmatrix} -K_x & K_y \end{bmatrix} \begin{bmatrix} \hat{x}(t) \\ y(t) \end{bmatrix} \tag{3.60}$$

as a solution for full information regulator problem, such that $\lim_{t\to\infty} \hat{y}((t) - y(t)) = 0.$

An important part in the designing methodology of the H_∞ controller is the performance specification, here described by x_{ps}, which implies to choose some apriori templates for the controlled variables. The state dimension of this equation depends

on the complexity of the chosen templates. Let us consider that the generalized plant state for this particular problem, which combines the model $\tilde{G}$ having the state $\hat{x}$ and the performance specification, denoted as

$$x_G(t) = \begin{bmatrix} \hat{x}(t) \\ x_{ps}(t) \end{bmatrix}$$

Moreover, the signification of the signals presented in H_∞ framework is given again, $w_e(t)$ represents the external signals hereby $y(t)$, $\hat{v}(t)$ the control input which will be computed, the measured output $y_m(t) = \begin{bmatrix} \hat{x}(t) \\ y(t) \end{bmatrix}$ and the controlled variable will be characterized by $z(t)$. The block diagram of the related control problem is shown in Figure 3.5.

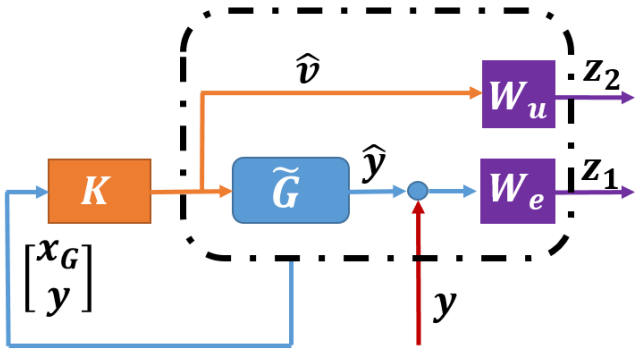

Figure 3.5: Block diagram for H_∞ FI case

The mathematical equations for this particular case using the H_∞ framework is given next:

$$\begin{aligned} \dot{x}_G(t) &= A_G x_G(t) + B_{G1} w_e(t) + B_{G2} \hat{v}(t) \\ z(t) &= C_{G1} x_G(t) + D_{G11} w_e(t) + D_{G12} \hat{v}(t) \\ y_m(t) &= C_{G2} x_G(t) + D_{G21} w_e(t) \end{aligned} \tag{3.61}$$

The corresponding vectors for state (x_G), external inputs (w_e), control input ($\hat{v}$) and controlled variable (z) are

$$x_G = \begin{bmatrix} \hat{x} \\ x_{ps} \end{bmatrix} \quad w_e = y \quad z = \begin{bmatrix} z_1 \\ z_2 \end{bmatrix} \tag{3.62}$$

The matrices which describe equation (3.61) can be expended as

$$A_G = \begin{bmatrix} A & 0 \\ A_{1ps} & A_{2ps} \end{bmatrix} \quad B_{G1} = \begin{bmatrix} 0 \\ B_{1ps} \end{bmatrix} \quad B_{G2} = \begin{bmatrix} B_2 \\ B_{2ps} \end{bmatrix}$$
$$C_{G2} = \begin{bmatrix} I & 0 \\ 0 & 0 \end{bmatrix} \quad D_{G21} = \begin{bmatrix} 0 \\ I \end{bmatrix} \quad D_{G22} = \begin{bmatrix} 0 \\ 0 \end{bmatrix}$$

The information about performance specification is captured by the following state space equation

$$\dot{x}_{ps}(t) = A_{1ps}\hat{x}(t) + A_{2ps}x_{ps}(t) + B_{1ps}y(t) + B_{2ps}\hat{v}(t) \tag{3.63}$$

At this point, the H_∞ full information control problem can be formulated as

Given the model described by (3.61) under the observability-controlability assumptions design an output feedback H_∞ controller such that

$$||T_{zw_e}(s)||_\infty < \gamma \tag{3.64}$$

where $\gamma > 0$ and $T_{zw_e}(s)$ is the closed loop transfer function between w_e and z.

Remarks:

- The complexity of the observer obtained using *full information* H_∞ is lower than in the previous case, but this approach doesn't take into account the information about the state noise, which leads to less accurate results for state and unknown inputs estimation.

3.6 Simulation results

In this section, let us illustrate the performances of the above mentioned control-based observer design in H_∞ framework. For the sake of illustration, a simple case of a 2^{nd} order system including some unknown inputs in addition to state and measurement noise will be considered.

a. System definition

Let us consider the case of a second order linear system as follows:

$$\begin{aligned} \dot{x}_1(t) &= x_2(t) + w_{x1}(t) \\ \dot{x}_2(t) &= -\omega_0^2 x_1(t) - 2\zeta_0\omega_0 x_2(t) + u(t) + w_{x2}(t) + v(t) \\ y(t) &= x_1(t) + w_y(t) \end{aligned} \tag{3.65}$$

where $u(t)$ is the known input, $v(t)$ is some bounded deterministic disturbance (e.g. a sine wave - in a certain low frequency band) and $w_{x1}(t)$, $w_{x2}(t)$, $w_y(t)$ are zero-mean Gaussian noises. We also assume that the frequency band of the deterministic signal doesn't overlap with the frequency band of the noise signal.

b. Numerical values

The system parameters are: $\omega_0 = 10\ rad/sec$, $\zeta_0 = 0.1$, the deterministic unknown signal is in the frequency band of [0.1 - 20] rad/sec and the noise signal contains frequencies which are over $70\ rad/sec$.

c. Simulation scenario

For the first 3 seconds, $v(t)$ (unknown input) and $u(t)$ (known input) are both 0.

After 3 seconds, v (unknown input) - a sinusoidal signal of $1\ rad/sec$ - enters into scenario, u (known input) is still null.

Finally, after 10 seconds, $u(t)$ (known input) - a step signal - is activated, while v (unknown input) remains the same.

d. Results

i. Case 1

For this case, in order to compute the control-based observer, the H_∞ controller design allows us to choose the two templates to meet the performance specification imposed by a particular application.

Hereby, $\frac{1}{W_e(s)}$ is chosen as a high pass filter, while $\frac{1}{W_u(s)}$ is chosen as a low pass filter. Even though these templates are designed to shape, in particular, the sensitivity closed loop function $S(s)$ (transfer function from w_y to ϵ_y) and $KS(s)$ (the transfer function from w_y to $\hat{v}$), it can also be noticed that as a consequence the other transfer functions are shaped based on this choice. For instance, the sensitivity closed loop function $T(s)$ and $\tilde{T}(s)$ (the transfer functions from w_{x2} and w_{x1} to $\hat{v}$) are constrained to follow the template imposed by $\frac{1}{W_u(s)}$, while the sensitivity closed loop function $GS(s)$ and $\tilde{G}S(s)$ (the transfer functions from w_{x2} and w_{x1} to e_y) are constrained to follow the template imposed by $\frac{1}{W_e(s)}$. The shapes of all closed loop transfer functions together with their templates are shown in Figure 3.6 and Figure 3.7.

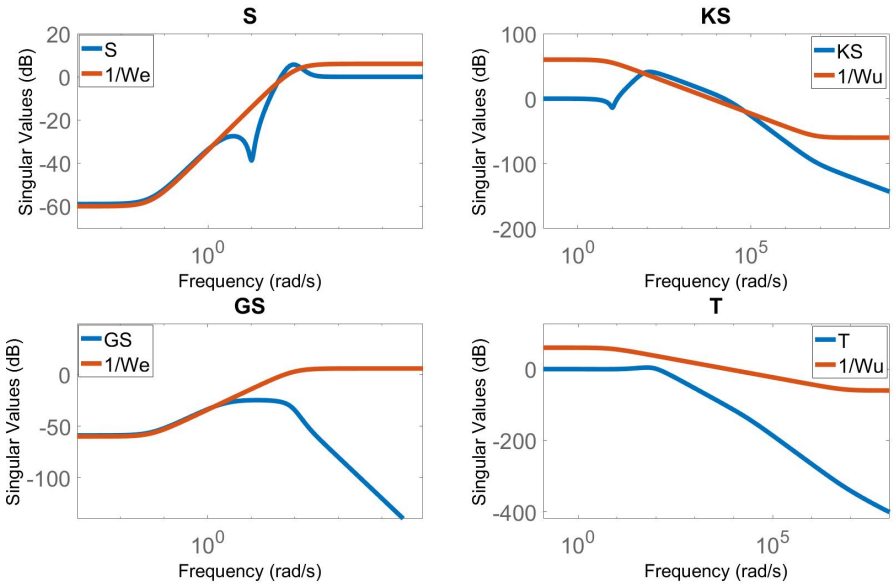

Figure 3.6: Case 1: Transfer functions $S(s)$, $KS(s)$, $GS(s)$ and $T(s)$

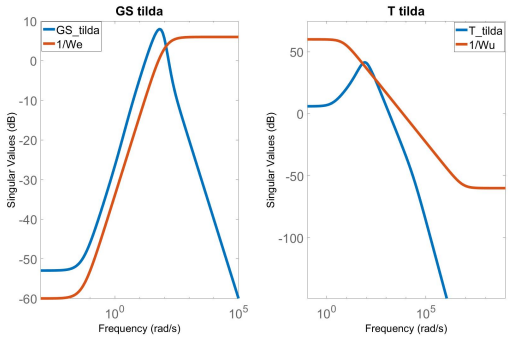

Figure 3.7: Case 1: Transfer functions $\tilde{GS}(s)$ and $\tilde{T}(s)$

Clearly, the constraints imposed by the chosen templates are not satisfied by all the transfer functions, which is translated by the fact that γ will be greater than one.

This can be seen a little conservative and it can lead to some limitations in terms of the performance of the observer, suggesting that we should expect that the estimation of the unknown input, $\hat{v}(t)$, is 'noisy', since the transfer between $w_{x2}(t)$ and $\hat{v}(t)$ is $KS(s)$ (from Figure 3.6 (up right plot) it can be seen that $KS(s)$ is significant in high frequency range and w_{x2} has high frequency components, as specified above). The same remark can be made about the transfer function $\tilde{T}(s)$ (the transfer between w_{x1} and $\hat{v}$, see Figure 3.7 (right plot)).

Basically, for this particular case, the H_∞ framework uses only two templates to shape six sensitivity functions (in fact there are eight sensitivity functions, but the ones from

w_{x2} and v to z_1 respectively z_2 are the same), as shown in Figures 3.6 and 3.7, hence the conservative aspect of this controller.

The results shown in Figure 3.8 illustrate this expected behavior, for instance, we obtain a good estimation for state x_1, while for the state x_2 and the unknown inputs the observer delivers quite noisy estimations.

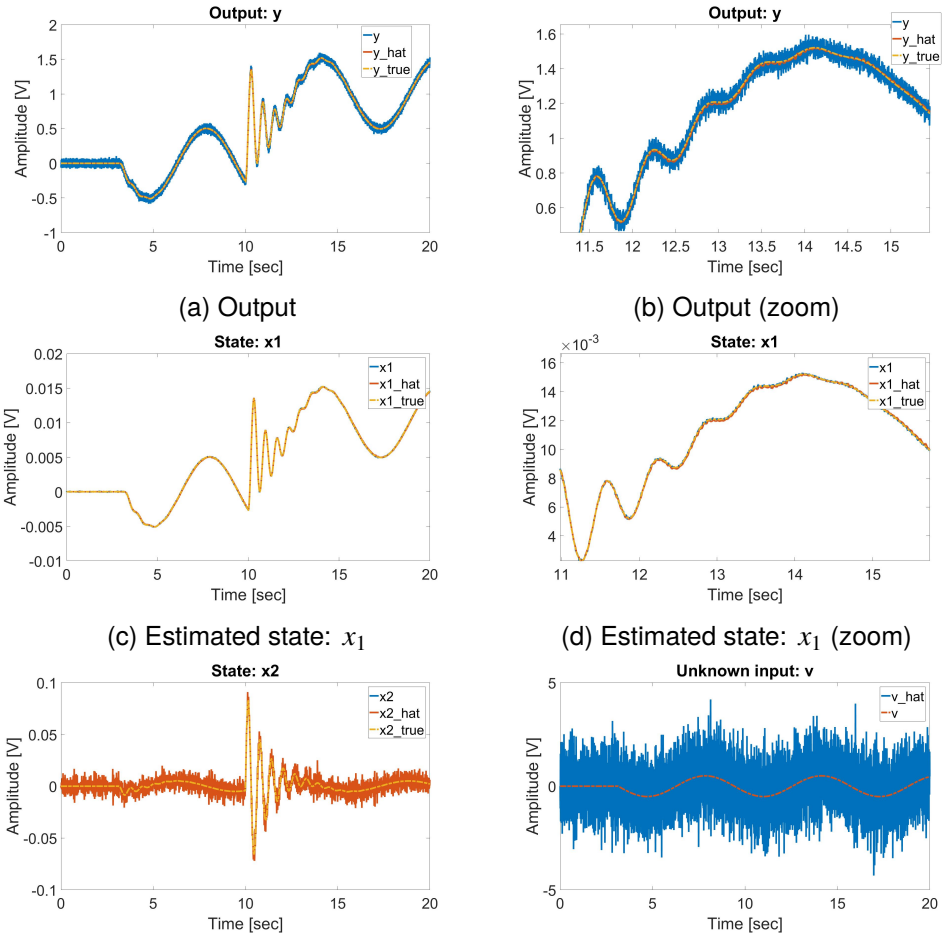

(a) Output

(b) Output (zoom)

(c) Estimated state: x_1

(d) Estimated state: x_1 (zoom)

(e) Estimated state: x_2

(f) Unknown input

Figure 3.8: CbO - Control strategy H_∞ - case 1

ii. Case 2

As for case 2, in order to compute the control-based observer, the H_∞ controller design allows us to choose no more than six templates to meet the performance specification imposed by a particular application. This, of course, increases the degree of freedom to shape the closed loop sensitivity functions in a more precise way.

In particular, $\frac{1}{W_e(s)}$, $W_{wx}(s)$ and $W_{wy}(s)$ are chosen as a high pass filter, while $\frac{1}{W_u(s)}$ and $W_v(s)$ are chosen as a low pass filter.

Clearly in this case we have more flexibility to define and meet some very particular performance specifications which will lead to better results in terms of both state and unknown input estimation.

Let us show the closed loop sensitivity functions together with the templates which are supposed to be met by the design of the H_∞ controller in Figure 3.9 and Figure 3.10

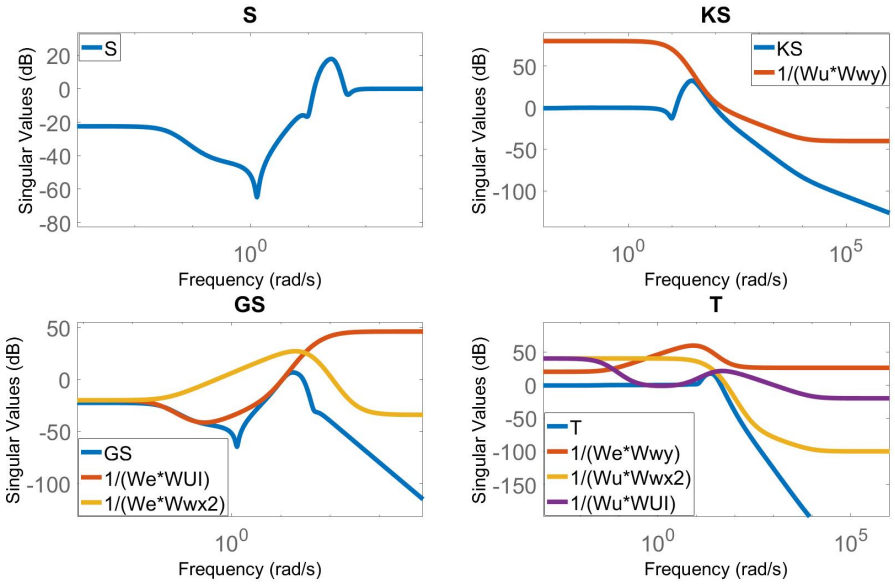

Figure 3.9: Case 2: Transfer functions $S(s)$, $KS(s)$, $GS(s)$ and $T(s)$

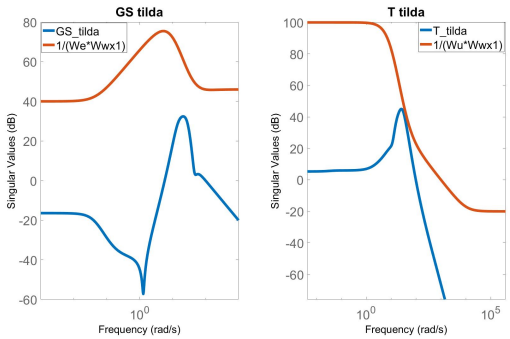

Figure 3.10: Case 2: Transfer functions $\tilde{GS}(s)$ and $\tilde{T}(s)$

One can notice that for this case, the eight templates allow us to shape the closed loop sensitivity functions in a more precise manner. See, for instance, the $GS(s)$ and

$T(s)$ shown in Figure 3.9. Because the information about the external signals is also taken into account when the H_∞ control problem is defined, the obtained observer gives better results in terms of state estimation and unknown input estimation, see for example Figure 3.11.

As always, there is a price to pay if one wants to obtain better estimations, here it is payed in terms of the complexity of the observer.

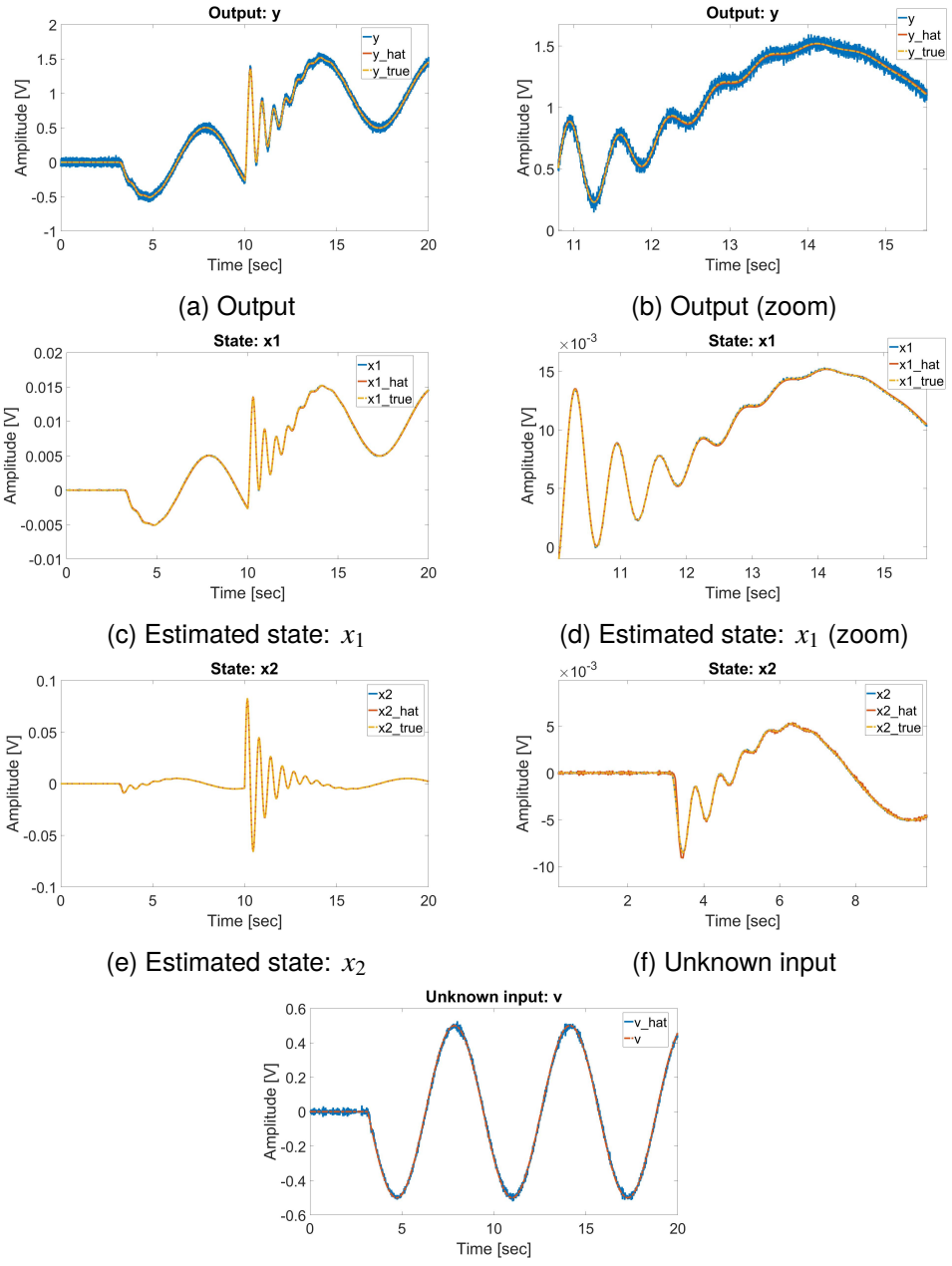

(a) Output

(b) Output (zoom)

(c) Estimated state: x_1

(d) Estimated state: x_1 (zoom)

(e) Estimated state: x_2

(f) Unknown input

(g) Unknown input

Figure 3.11: CbO - Control strategy H_∞ - case 2

In Table 3.1 a measurement of the means square error between the real values and the estimated ones is given, so as to illustrate the performances of the proposed control-based observer (***CbO***). In particular, we have the controller ***O**utput **F**eedback* H_∞ ***-** case **1*** (entry two CbO: OF H_∞ - 1) and the controller ***O**utput **F**eedback* H_∞ ***-** case **2*** (entry three CbO: OF H_∞ - 2). Also, the results are compared with the solution provided by the control-based observer solving H_∞ **F**ull **I**nformation regulation problem (entry four CbO: H_∞ FI).

As for the first entry in Table 3.1 (entry one H_∞ **obs**erver), a classical H_∞ observer design for the extended system having the new extended state $x_E(t) = \begin{bmatrix} x(t) \\ v(t) \end{bmatrix}$, for which the unknown inputs, $v(t)$ are considered slowly varying i.e. $\dot{v}(t) = 0$. The reader is kindly advised to check [PBV18a] for the design procedure for such an observer.

Table 3.1: Mean Square Error (MSE) - Estimation results

Method	MSE(y, $\hat{y}$)	MSE(x_1, $\hat{x}_1$)	MSE(x_1, $\hat{x}_1$)	MSE(v, $\hat{v}$)
H_∞ obs	$1.13 \cdot 10^{-2}$	$1.13 \cdot 10^{-6}$	$5.70 \cdot 10^{-3}$	$8.67 \cdot 10^{-2}$
CbO: OF H_∞ - 1	$6.42 \cdot 10^{-5}$	$6.42 \cdot 10^{-9}$	$2.98 \cdot 10^{-5}$	$9.37 \cdot 10^{-1}$
CbO: OF H_∞ - 2	$4.36 \cdot 10^{-5}$	$4.36 \cdot 10^{-9}$	$8.81 \cdot 10^{-8}$	$5.72 \cdot 10^{-5}$
CbO: FI H_∞	$1.1 \cdot 10^{-3}$	$1.07 \cdot 10^{-7}$	$1.5 \cdot 10^{-5}$	$1.16 \cdot 10^{-1}$

Combining the qualitative results presented in Figures 3.8 and Figures 3.11 with the numerical values in Table 3.1, we can easily notice that the solution for the control-based observer in terms of output feedback H_∞ controller presented as the case 2, exhibits the best results for both state and unknown inputs estimation, but one can also notice that the complexity of the obtained observer is elevated. A potential solution for the complexity problem can be found in terms of controller reduction, a topic already studied in the case of H_∞ control methods. This approach is left as future perspective to be investigated.

We can also notice that the results for the output feedback H_∞ controller (case 1) and full information H_∞ solution are pretty similar. This is also the reason why the quantitative results for the full information solution were not presented.

3.7 Conclusions

In this chapter a robust method of designing a control-based observer using H_∞ tools has been presented. In particular, the problem of estimating the state and the

unknown inputs for a linear system by solving the *error feedback regulation problem* for the error model as well as the *full information regulation problem* for the chosen model have been investigated.

The H_∞ framework provides us several degrees of freedom to design a control-based observer, depending on the performance specification we want to define. We can group these solutions in two main classes of observers each one depending on the control problem we solve, namely, the first one based on the *output feedback H_∞ controller* and the second one relying on the *full information H_∞ controller*. Clearly, each class of observers will inherit the advantages, but also the disadvantages of the related control solutions.

From the simulation results presented in the current chapter, it is easy to see that if we design an *output feedback H_∞ controller* (case 2) in the context of a control-based observer the estimations obtained for both the state and unknown inputs are quite accurate, showing the robustness capabilities against the state and measurement noises of the proposed approach.

Is it worth noting that, using the control-based paradigm for this particular case of systems, having unknown inputs in conjunction with a PI controller, we obtain an observer quite similar to another classical solution called PI observer [BS88a]. The observers are not identical, one of the main difference is that for the PI observer the "proportional" part of the correction term affects all the states, and the unknown inputs are estimated only by the "integral" part of it. As in the case of a control-based observer using a PI controller, the model is controlled directly via the unknown inputs and their estimation is given by the output of the PI controller, both the "proportional" and "integral" parts.

Moreover, compared with PI observer which assumes that the unknown inputs vary slowly so that its derivative can be considered null, i.e. $\dot{v}(t) \approx 0$, the control-based observer assumes that corresponded unknown inputs are in a certain range of frequency, and the design controller will deliver their approximation. Some optimal (sub-optimal) solutions to find the gain matrix of a PI observer can be found in [GK08] or more recently in [Yam+15].

Finally, to highlight the advantages and disadvantages of the proposed method compared with the classical ones described in the Introduction and also using other control methods to design a control based observer as in Chapter 2, one can check the articles [PBV18a] and [PBV18b].

CHAPTER 4

REAL-TIME EXPERIMENTAL RESULTS: SCANNING TUNNELING MICROSCOPE

This Chapter Answers
1. What is a tunneling current phenomenon?
2. What is a Scanning Tunneling Microscope (STM)?
3. How to model such a device?
4. How to control a STM?
5. How to reconstruct a surface image using a STM?
6. How to apply control-based observers for surface reconstruction?

4.1 Introduction

In this chapter, the first experimental application will be presented, based on a prototype built in the Gipsa-lab, which reproduces the operation of a Scanning Tunneling Microscope. This device (STM in short) was invented in 1986 by Gerd Binnig and Heinrich Rohrer [BR86] , together with its variant called Atomic Force Microscope (AFM) [BQG86].

The field of nanoscience made a huge step forward with those two devices, since they helped in the development of many applications from various research fields and they still underpin many research topics.

Traditionally, STM/AFM microscopes represent a rich source of challenges for the control system field, mainly because one has to guarantee a precise control having nanometric resolution in spite of all the nonlinearities and noise present in the process (see for example [EM11], [Taj+17] and [BSH94]). Even if the physical principles on which these two microscopes are based are different, both of them allow to obtain images at a nanoscale level.

In the present chapter, our attention will be focused on Scanning Tunneling Microscope. In particular, this device is based on a quantum principle called tunneling-current phenomenon, which will be presented in more details in the first section hereafter. Briefly speaking, physics states that if two electrically conductive materials are positioned with a distance lower than one nanometer between them, and set to different potentials, then electrons will appear to move from one of them to the other, creating a current effect, called "tunneling current". If its intensity is kept constant while a sample is scanned, then an image having a nanometer resolution of the surface variation can be obtained. Standard operation thus, needs control, but generally limited to PI for vertical tip motion, and even open loop for horizontal displacements. In this chapter, the first goal is to illustrate how the use of observers, in particular following some of the control-based approaches developed before, can improve this STM operation, and ultimately the obtained surface imaging. But another contribution is a proposal for improving the control methodology itself, relying on the H_∞ framework recalled in the former observer context, and directly applied in a Multi-Input Muti-Output context. Notice that the extension of this second part of the work to the ultimate imaging application is left as a perspective.

This chapter thus includes first recalls on the quantum phenomenon at the core of the microscope, so-called tunneling current, and then presents the experimental set-up

of a Scanning-Tunneling-Microscope that is used for real time experimental manipulation. On this basis, the enhancement of STM operation by using three individual PI's for vertical and horizontal motions, combined with the use of control-based observers, is presented, with illustrations first in control performances, and then in surface estimation. Finally, the control improvement based on MIMO H_∞ approach is introduced, with related illustrative real time experiments.

4.2 Tunneling current principle

As it was mentioned, Scanning Tunneling Microscopy is based on a physical phenomenon called the tunneling current. Due to its essential part in this scanning process, our concern in the present section is to describe how the tunneling current is defined and what are the conditions that should be met, such that this phenomenon occurs. To that end [Lou14] was used as theoretical support to describe the equations of tunneling current phenomenon.

Classical Mechanics states that a particle (an electron in our case) cannot overcome a potential barrier if it doesn't have enough energy. This means that the particle will not be able to pass through that barrier, it will be bounced back. On the other hand, due to the strange behavior of an electron, that can be both a particle and a wave in the same time (wave-particle duality), quantum mechanics claims that it has a non-zero probability that the electron could be found on the other side of the potential barrier. In other words, the electron can 'tunnel' right through the potential barrier.

Let's return to our case, we have two electrical conductive materials, a sample and a sharp tip. In materials, the electrons follow the Pauli exclusion principle which says that two electrons cannot occupy the same quantum state. As a consequence, the electrons will fill up the unoccupied states with the lowest energy. The kinetic energy of the highest state occupied is called the *Fermi level*. Thus, we can say that in metals, the electrons fill the energy levels up to the Fermi level (see Figure 4.1).

The next step is to get the tip and the surface to a certain distance (less then 1 nm). As it can be seen in Figure 4.1, both metals have their Fermi level aligned ($E_{F_s} = E_F$ and $E_{F_t} = E_F$) and they are separated by a vacuum gap (potential barrier). In order for an electron to leave one metal and travel through the barrier right on the other one, it takes an additional amount of energy. This particular amount of energy is called work function (ϕ). Since the Fermi levels of the metals are aligned, nothing can happens because there aren't any empty energy states available for the electrons

to go into.

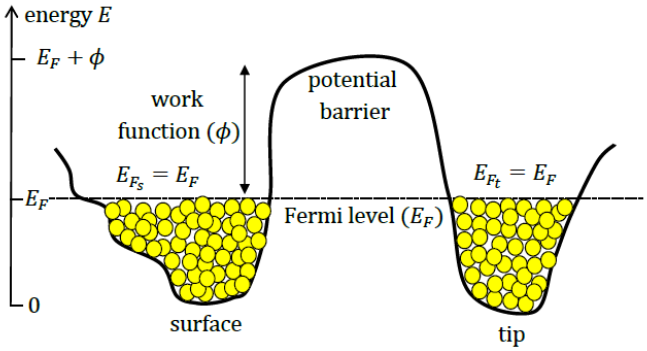

Figure 4.1: Materials Fermi level - unbiased case [Ryb15]

The final step is to apply a voltage bias (V_b) between the tip and the sample as it is illustrated in Figure 4.2. As soon as this voltage bias is applied, the Fermi levels of the metals aren't aligned anymore ($E_{F_s} = E_F$ and $E_{F_t} = E_F - eV_b$). This leads to the creation of empty energy states available which allows the electrons to 'tunnel' the vacuum barrier. This electrons flow is called tunneling current. The direction of the tunneling current depends on the polarity of the voltage bias applied.

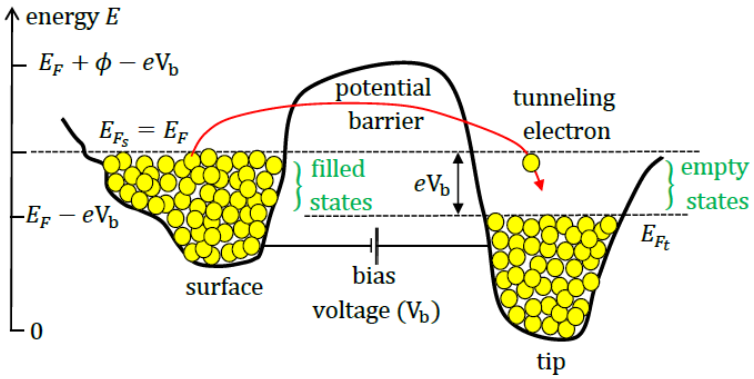

Figure 4.2: Materials Fermi level - biased case [Ryb15]

Mathematically, in classical mechanics, the total energy of an electron is described by the equation:

$$\frac{p^2}{2m} + V(z) = E \tag{4.1}$$

where

m – mass of the electron
p – momentum of the electron
$V(z)$ – potential energy at z position
E – total energy of the electron

Working under the Classical Mechanics assumptions, it can be easily seen that in the case where $E > V(z)$, the electron has a non-zero momentum described by the equation:

$$p = \sqrt{2m(E - V(z))} \tag{4.2}$$

On the contrary, in the case where $E < V(z)$, the electron cannot overcome the potential barrier, it is bounced back.

On the other hand, in the Quantum Mechanics field, due to the wave-particle duality principle, we can consider that the electron behaves as a wave. Under this assumption and knowing that in atoms the orbital's potential is time-invariant, we can use the one-dimensional time-independent Schrödinger equation to describe the electron's behavior:

$$-\frac{\hbar^2}{2m}\frac{\partial^2}{\partial z^2}\psi(z) + V(z)\psi(z) = E\psi(z) \tag{4.3}$$

where

$\hbar$ – reduced Plank constant
$\psi(z)$ – electron's wave function

We can consider that the vacuum gap between the tip and the surface (the potential barrier) can be modeled as follows:

$$V(z) = \begin{cases} V_0 & z \in (0, d) \\ 0 & \text{if not} \end{cases} \tag{4.4}$$

where d will be set to the value of $1\ nm$.

Under these hypothesis the space can be divided into three main regions, each characterized by a one-dimensional time-invariant Schr$\ddot{o}$dinger equation.

The first region lies before z = 0 (outside the potential barrier). It is characterized by the fact that $E > V(z)$. Having in mind the equation (4.4), the corresponding Schrödinger equation is:

$$\frac{\hbar^2}{2m}\frac{\partial^2}{\partial z^2}\psi_1(z) + E\psi_1(z) = 0 \tag{4.5}$$

This differential equation can be solved by switching to s-plane using the Laplace operator, getting:

$$(\frac{\hbar^2}{2m}s^2 + E)\Psi_1(s) = 0 \tag{4.6}$$

Which leads us to the following solution for s:

$$s_{1,2} = \pm i\frac{\sqrt{2mE}}{\hbar} \tag{4.7}$$

Finally, we turn back to the time domain having the differential equation solution corresponding to the first region:

$$\psi_1(z) = C_{11}e^{i\kappa_0 z} + C_{12}e^{-i\kappa_0 z} \tag{4.8}$$

where $\kappa_0 = \frac{\sqrt{2mE}}{\hbar}$.

The third region corresponds to $z > d$ (also outside the potential barrier) which is also characterized by $E > V(z)$ and is described by the next Schrödinger equation:

$$\frac{\hbar^2}{2m}\frac{\partial^2}{\partial z^2}\psi_3(z) + E\psi_3(z) = 0 \tag{4.9}$$

Following the same steps we get the differential equation solution:

$$\psi_3(z) = C_{31}e^{i\kappa_0 z} + C_{32}e^{-i\kappa_0 z} \tag{4.10}$$

Notice that the equations (4.8) and (4.10) correspond to some oscillating waves. This fact is also illustrated in Figure 4.3.

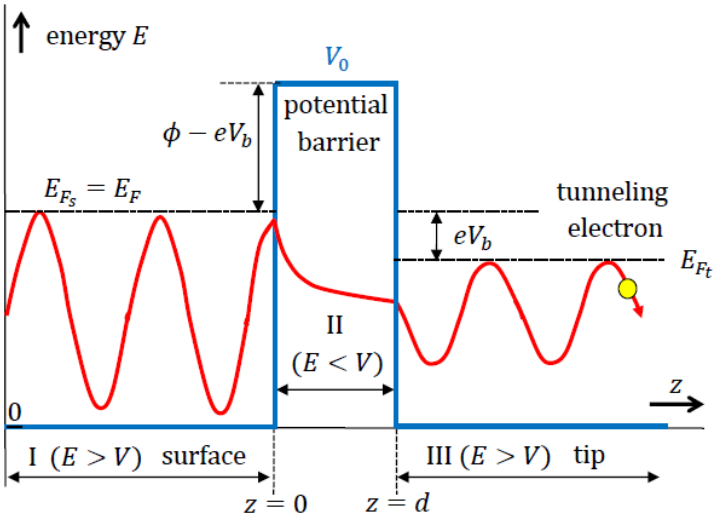

Figure 4.3: Wave function form in different regions [Ahm11]

The second region describes the electron's behavior in the potential barrier ($z \in (0, d)$). This part is characterized by the fact that $E < V(z)$ and from the equation (4.4) results that $V(z) = V_0$. This leads to the following Schrödinger equation:

$$\frac{\hbar^2}{2m}\frac{\partial^2}{\partial z^2}\psi_2(z) + (E - V_0)\psi_2(z) = 0 \tag{4.11}$$

having the following equation in s-plane:

$$(\frac{\hbar^2}{2m}s^2 + E - V_0)\Psi_1(s) = 0 \tag{4.12}$$

From this we get the solution:

$$s_{1,2} = \pm\frac{\sqrt{2m(V_0 - E)}}{\hbar} \tag{4.13}$$

Thus, we obtain the wave function inside the potential barrier:

$$\psi_2(z) = C_{21}e^{\kappa_1 z} + C_{22}e^{-\kappa_1 z} \tag{4.14}$$

where $\kappa_1 = \frac{\sqrt{2m(V_0-E)}}{\hbar}$.

The wave function that characterize the second region is:

$$\psi_2(z) = \psi_2(0)e^{-\kappa_1 z} \tag{4.15}$$

Next, a way to approximate the solution of equation (4.14) is presented.

As we stated before, the Quantum Mechanics claims that it has a non-zero probability for an electron to be found on the other side of the potential barrier. Having the electron's wave function that describes its behavior during the second region (the potential barrier) we can compute the probability of finding an electron behind the barrier, which is proportional to the square of the wave function's absolute value:

$$P(d) \propto |\psi_2(d)|^2 \tag{4.16}$$

This leads to the following expression for the searched probability:

$$P(d) \propto |\psi_2(0)|^2 e^{-2\kappa_1 d} \tag{4.17}$$

As we said above, one of the essential steps of obtaining a tunneling current, besides of the small distance between the tip and the surface, is to apply a voltage bias on the surface with respect to the tip. In this case the difference between the potential barrier and the electron's total energy decreases with the amount of energy corresponding to the voltage bias applied, as it is described in the next equation:

$$\begin{aligned} V_0 - E &= \phi \qquad \text{(unbiased case)} \\ V_0 - E &= \phi - eV_b \quad \text{(biased case)} \end{aligned} \tag{4.18}$$

One can choose the voltage bias applied such that ($\phi >> eV_b$). Also, in the Scanning Tunneling Microscopy application, if the materials for tip and surface differ electrically, the work function (ϕ) can roughly be approximated by the average of the work functions of the tip and surface. Those assumptions help to simplify the form of the exponentially decaying rate:

$$\kappa_1 \approx \frac{\sqrt{2m\phi}}{\hbar} \tag{4.19}$$

On the other hand, when this voltage bias (V_b) is applied, as we mentioned earlier, some empty energy states are created on the tip with respect to the surface (depending on the polarity of the voltage bias applied). Tunneling current can be related to the density of those empty states of the tip (or the density of the filled states of the surface). Thus, a flow of electrons occurs between the tip and the surface. In

fact, increasing the number of these states we increase the intensity of the tunneling current.

The number of those states can be found by subtracting the tip's Fermi level (E_{F_t}) from the surface's Fermi level (E_{F_s}). We already discussed earlier that after we apply the voltage bias (V_b) between the tip and the surface, we can consider that $E_{F_s} = E_F$ and $E_{F_t} = E_F - eV_b$. Now, we can define the tunneling current as being proportional to the sum of the probabilities (4.17), as we defined them above, taken over the energy range formed between the tip and the surface:

$$i_t \propto \sum_{E_F - eV_b}^{E_F} |\psi_2(0)|^2 e^{-2\kappa_1 d} \tag{4.20}$$

Next, let us define the local density of the states (LDoS) near some energy region E in an interval ϵ at the position z as:

$$\rho_{LDoS}(z, E) = \frac{1}{\epsilon} \sum_{E-\epsilon}^{E} |\psi(z)|^2 \tag{4.21}$$

Considering that the wave function's continuity conditions are met, the tunneling current expression (4.20) can be rewritten in terms of (4.21) at the surface location $z = 0$, near the surface's Fermi level $E = E_F$ in the interval $\epsilon = eV_b$ as:

$$i_t \propto eV_b \rho_{LDoS}(0, E_F) e^{-2\kappa_1 d} \tag{4.22}$$

Defining the following constants $g = e\rho_{LDoS}(0, E_F)$ and $k = 2\kappa_1$ (the materials properties are embedded in the last one), we can rewrite the tunneling current equation as follows:

$$i_t = gV_b e^{-kd} \tag{4.23}$$

Finally, a graphical representation of the tunneling current described by equation (4.23) is given in Figure 4.4, with values corresponding to our experiment. This experiment is more precisely described in the next section.

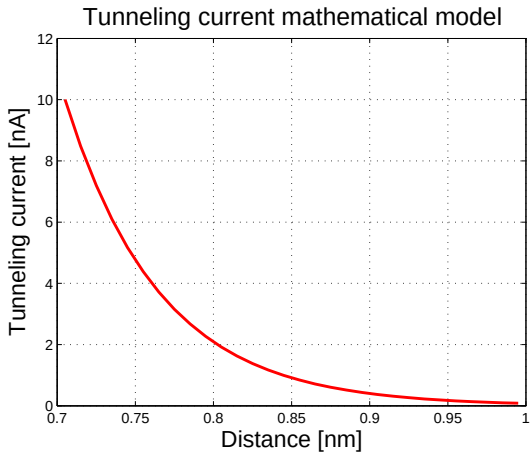

Figure 4.4: Tunneling current mathematical model

4.3 Scanning-Tunneling-Microscope platform description

Experimental setup

Let us introduce here, the experimental device under consideration, based on the quantum phenomenon described before. It is a Scanning Tunneling Microscope-like (STM) device built in the GIPSA-lab, as part of former PhD thesis [Bla10], [Ahm11] and [Ryb15], from now on referred as GIPSA STM throughout this chapter. Figure 4.5 illustrates a set of components that device integrates.

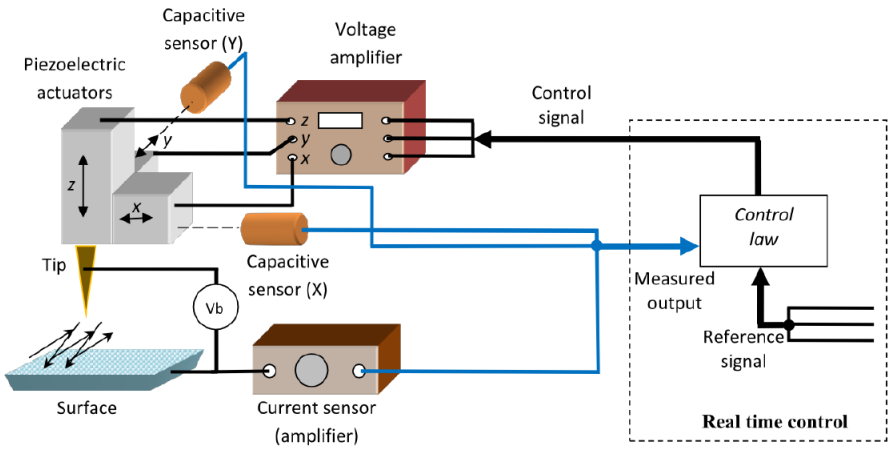

Figure 4.5: Scanning Tunneling Microscope (STM) components

Briefly speaking, a Platinum-Iridium tip is driven over a graphite sample in all dimensional axes (x,y,z) by three piezoelectric actuators. In particular, for the x and y axes the motion is provided by a TRITOR T-402-00 actuator having a gain of $235\ nm/V$ and a bandwidth of $630\ Hz$, while for the z axis a PSt 150 actuator is used having

a smaller gain, only $1.2\ nm/V$, but a much higher bandwidth which can reach 120 kHz to ensure a more precise movement in the vertical axis.

The appropriate control signals (u) are fed by a PC to the piezoelectric actuators, and magnified by a voltage amplifier (v) having a gain of $15\ V/V$ and a bandwidth of 4 kHz.

Moreover, the displacement (p) in x and y directions is provided by two capacitive sensors (y) having a gain of $200\ V/mm$ and a bandwidth of $8.5\ kHz$. On the other hand, for z direction, the information about tip-sample distance (d) is provided by a high gain current sensor having a gain of $10^9\ V/nA$ and a bandwidth of $13\ kHz$ which measures the intensity of the tunneling current (i_t).

The signals acquisition is ensured using an analog-to-digital converter while the numerical control inputs are fed back to the system through a digital-to-analog converter. The integrity of the numerical signals are also guaranteed by anti-aliasing filters having the cut frequency at $10\ kHz$. This allows to choose a sampling frequency up to $20\ kHz$. Finally, the control algorithms are designed using Matlab/Simulink^{TM} and sent to the target PC via ethernet.

Device Modeling

In the present subsection the dynamical behavior of the GIPSA STM is given. For a more detailed model, one can check [Ryb15]. In Figure 4.6 a block diagram of the system under consideration is shown which summarizes the components of the device described above, while in equations (4.27), (4.28) respectively (4.36) given below, a state space representation of the x axis, y axis respectively z axis is considered.

The model captures the particularities of the dynamics which characterize this system such as structural vibration as well as hysteresis, creep (Nonlinearity NL in Figure 4.6), cross-coupling and tunneling current phenomenon.

The three directional movements can be divided into two parts which can be referred to as Scanning Mode (x and y axes displacement) and Tunneling Current Mode (for z axis displacement), as it is also illustrated in Figure 4.6. The first one ensures that the tip moves according to a certain pattern over the surface, while the second one is in charge of maintaining a constant tunneling current during the scanning process.

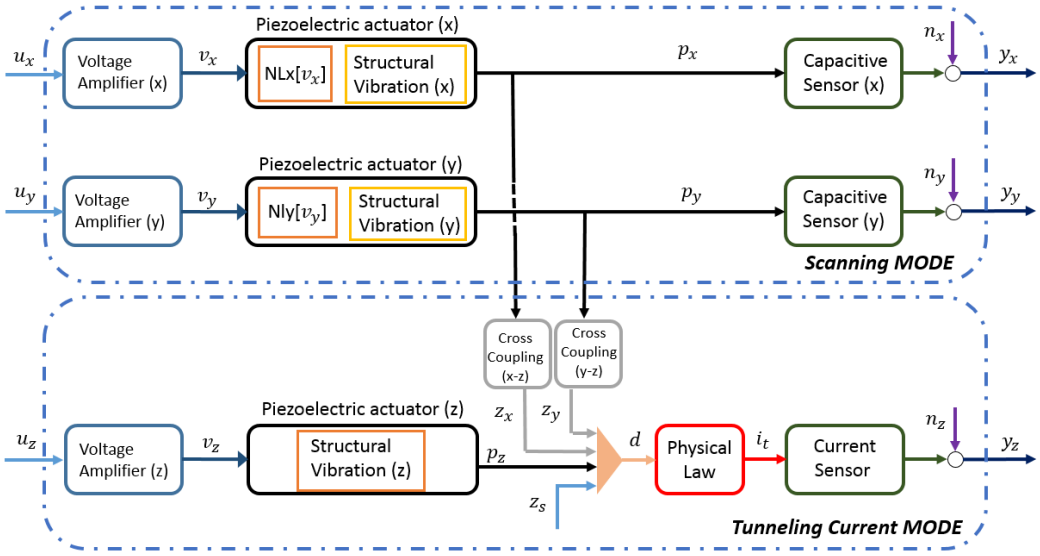

Figure 4.6: STM system description: X-Y-Z axes

X - Y Axes: Scanning Mode

In this subsection the dynamical behavior of GIPSA STM, is explicitly given for horizontal (x and y) axes, (for more information see [Ryb15]). This model describes the dynamics of the above mentioned components by referring to some well-known behaviors for an STM device such as hysteresis, creep, structural vibration, cross-coupling and tunneling current phenomenon. It basically gathers all the information in terms of gains and bandwidths into linear and nonlinear models.

In particular, for x and y directions, voltage amplifier can be easily represented as first order transfer function as in equation below (for x):

$$\begin{aligned} \dot{x}_{vx}(t) &= -\omega_{vx} x_{vx}(t) + u_x(t) \\ v_x(t) &= G_{vx}\omega_{vx} x_{vx}(t) \end{aligned} \tag{4.24}$$

where $u_x(t)$ is the control input for x axis, $x_{vx}(t)$ is the state and $v_x(t)$ the output of the voltage amplifier, while G_{vx} and ω_{vx} stand for the static gain and the bandwidth of the amplifier.

Next, the model for piezoelectric actuators contains two parts, the linear part (which corresponds to the structural vibrations of piezo actuators) and the static nonlinear part (which describes basically the hysteresis of piezo actuators). The behavior of

piezoelectric actuators is captured by the following equation (for x again):

$$\begin{aligned} \dot{x}_{1px}(t) &= x_{2px}(t) \\ \dot{x}_{2px}(t) &= -\omega_{px}^2 x_{1px}(t) - 2\zeta_{px}\omega_{pz} x_{2px}(t) + NL[v_x(t)] \\ p_x(t) &= \omega_{px}^2 x_{1px}(t) \end{aligned} \tag{4.25}$$

where $NL[v_x(t)]$ represents the static nonlinearities of piezoelectric actuator, $x_{1px}(t)$, $x_{2px}(t)$ are the states and $p_x(t)$ is the output of the piezoelectric actuator. Again G_{px}, ω_{px} and ζ_{px} are the static gain, bandwidth and damping of the piezoelectric actuator.

Finally, the displacement for x and y directions is measured, as said before, by a capacitive sensor which can be as well modeled as a first order transfer function:

$$\begin{aligned} \dot{x}_{capx}(t) &= -\omega_{capx} x_{capx}(t) + p_x(t) \\ y_x(t) &= G_{capx}\omega_{capx} x_{capx}(t) + n_x(t) \end{aligned} \tag{4.26}$$

where n_x stands for the measurement noise for x axis, $x_{capx}(t)$ is the state of capacitive actuator and y_x is the output of x direction, while G_{capx} and ω_{capx} refer to static gain and bandwidth of the capacitive sensor, respectively.

It is worth noting that the equations to describe y axis can be easily written by replacing in equations (4.24), (4.25) and (4.26) the index 'x' of state and parameters variables by 'y'.

Let us summarize the equations in a compact way as follows:

- For x axis:

$$\begin{aligned} \dot{x}_{vx}(t) &= -\omega_{vx} x_{vx}(t) + u_x(t) \\ \dot{x}_{1px}(t) &= x_{2px}(t) \\ \dot{x}_{2px}(t) &= -\omega_{px}^2 x_{1px}(t) - 2\zeta_{px}\omega_{px} x_{2px}(t) \\ &\quad + NL[G_{vx}\omega_{vx} x_{vx}(t)] \\ \dot{x}_{capx}(t) &= -\omega_{capx} x_{capx}(t) + p_x(t) \\ y_x(t) &= G_{capx}\omega_{capx} x_{capx}(t) + n_x(t) \end{aligned} \tag{4.27}$$

- For y axis:

$$\begin{aligned}
\dot{x}_{vy}(t) &= -\omega_{vy}x_{vy}(t) + u_y(t) \\
\dot{x}_{1py}(t) &= x_{2py}(t) \\
\dot{x}_{2py}(t) &= -\omega_{py}^2 x_{1py}(t) - 2\zeta_{py}\omega_{py}x_{2py}(t) \\
&\quad +NL[G_{vy}\omega_{vy}x_{vy}(t)] \\
\dot{x}_{capy}(t) &= -\omega_{capy}x_{capy}(t) + p_y(t) \\
y_y(t) &= G_{capy}\omega_{capy}x_{capy}(t) + n_y(t)
\end{aligned} \tag{4.28}$$

The numerical values of the parameters which describe the equations (4.27) and (4.28) can be found in Table 4.1 at the the end of this section.

Z Axis - Tunneling Current Mode

Moving on to the z axis description, the mathematical model can be obtained in a similar manner.

For the voltage amplifier the same model is given:

$$\begin{aligned}
\dot{x}_{vz}(t) &= -\omega_{vz}x_{vz}(t) + u_z(t) \\
v_z(t) &= G_{vz}\omega_{vz}x_{vz}(t)
\end{aligned} \tag{4.29}$$

with gain G_{vz} and bandwidth ω_{vz}, while for piezoelectric actuator the static nonlinearity, represented by hysteresis, can be omitted since the displacement in the z axis is of nanometers only:

$$\begin{aligned}
\dot{x}_{1pz}(t) &= x_{2pz}(t) \\
\dot{x}_{2pz}(t) &= -\omega_{pz}^2 x_{1pz}(t) - 2\zeta_{pz}\omega_{pz}x_{2pz}(t) + v_z(t) \\
p_z(t) &= -G_{pz}\omega_{pz}^2 x_{1pz}(t)
\end{aligned} \tag{4.30}$$

including here the parameters for bandwidth ω_{pz}, damping coefficient ζ_{pz} and gain G_{pz}

Next, tunneling current $i_t(t)$ is described, which is the core of such a device, and the source of nonlinearity for z axis. This term is exponentially dependent on the distance between the tip and the scanned surface, relation which can be described by the equation:

$$i_t(t) = gV_b e^{-kd(t)} \tag{4.31}$$

In equation (4.31), g and k are some constants which are computed based on the materials of which the tip and the sample are made and V_b is the voltage bias applied between the surface and the tip (one of the conditions needed for obtaining the tunneling current).

The distance, $d(t)$, the between tip and the surface is given by the following equation:

$$d(t) = d_0 + p_z(t) + z_x(t) + z_y(t) - z_s(t) \tag{4.32}$$

where d_0 is the initial distance between the tip and the surface, $p_z(t)$ is the piezo actuator position for the z axis, $z_s(t)$ is the surface variation, $z_x(t)$ and $z_y(t)$ are cross-coupling effects between the z axis and the x axis, respectively the z axis and the y axis.

Cross-coupling between the axis for such a device can be modeling according to [Wu+09] as a high pass filter transfer function as follows:

$$\begin{aligned} \dot{x}_{zx}(t) &= -\omega_{zx} x_{zx}(t) + p_x(t) \\ z_x(t) &= -G_{zx}\omega_{zx} x_{zx}(t) + G_{zx} p_x(t) \end{aligned} \tag{4.33}$$

and

$$\begin{aligned} \dot{x}_{zy}(t) &= -\omega_{zy} x_{zy}(t) + p_y(t) \\ z_y(t) &= -G_{zy}\omega_{zy} x_{zy}(t) + G_{zy} p_y(t) \end{aligned} \tag{4.34}$$

where G_{zx} and G_{zy} are the gains and ω_{zx} and ω_{zy} are the bandwidths of the cross-coupling state space representation.

Next, the tunneling current is measured by a high gain current sensor simply described by a first order transfer function, with gain G_i and bandwidth ω_i:

$$\begin{aligned} \dot{x}_i(t) &= -\omega_i x_i(t) + i_t(t) \\ y_z(t) &= G_i \omega_i x_i(t) + n_z(t) \end{aligned} \tag{4.35}$$

The z axis can be finally described in a similar compact manner as

$$\begin{aligned}
\dot{x}_{vz}(t) &= -\omega_{vz}x_{vz}(t) + u_z(t) \\
\dot{x}_{1pz}(t) &= x_{2pz}(t) \\
\dot{x}_{2pz}(t) &= -\omega_{pz}^2 x_{1pz}(t) - 2\zeta_{pz}\omega_{pz}x_{2pz}(t) + G_{vz}\omega_{vz}x_{vz}(t) \\
\dot{x}_{zx}(t) &= -\omega_{zx}x_{zx}(t) + \omega_{px}^2 x_{1px}(t) \\
\dot{x}_{zy}(t) &= -\omega_{zy}x_{zy}(t) + \omega_{py}^2 x_{1py}(t) \\
\dot{x}_i(t) &= -\omega_i x_i(t) + i_t(t) \\
y_z(t) &= G_i\omega_i x_i(t) + n_z(t)
\end{aligned} \tag{4.36}$$

4.4 Experimental protocol

This section deals with the experimental protocol in real time in order to test the 3D control method that we will consider here, as well as to obtain images of surface reconstruction.

Experimental device - numerical values

The control algorithms are validated using the GIPSA STM, which was presented in Figure 4.6. The parameters of the device are summarized in Table 4.1.

Table 4.1: GIPSA STM Parameters

Parameters	Value	Unit	Signification	Axis
G_{vx}, G_{vy}, G_{vz}	15	V/V	Voltage amplifier gain	x, y, z
$\omega_{vx}, \omega_{vy}, \omega_{vz}$	4	kHz	Voltage ampl. bandwidth	x, y, z
G_{px}, G_{py}	235	nm/V	Piezo actuator gain	x, y
G_{pz}	1.2	nm/V	Piezo actuator gain	z
ω_{px}, ω_{py}	0.63	kHz	Piezo actuator bandwidth	x y
ω_{pz}	120	kHz	Piezo actuator bandwidth	z
ζ_{px}, ζ_{py}	0.5	-	Piezo actuator damping	x y
ζ_{pz}	0.7	-	Piezo actuator damping	z
G_{capx}, G_{capy}	200	V/mm	Capacitive sensor gain	x, y
G_i	10^9	V/nA	Current sensor gain	z
$\omega_{capx}, \omega_{capy}$	8.5	kHz	Capacitive sensor bandwidth	x y
ω_i	13	kHz	Current sensor bandwidth	z
g	0.0011	-	Tunneling current constant	z
V_b	1.025	v	Voltage bias	z
k	16.5	nm^{-1}	Material constant	z

Scanning mode

One of the most used scanning strategy for the x and y directions is the so called raster method shown in Figure 4.7.

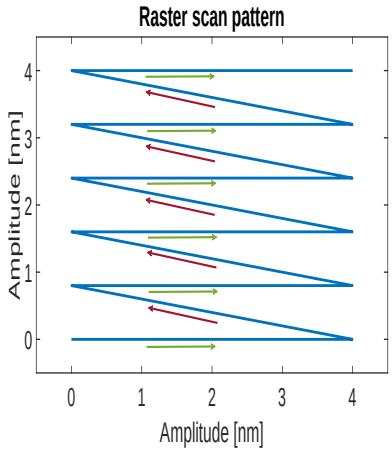

Figure 4.7: Raster scan pattern

To obtain the raster pattern, one has to combine two particular reference signals, namely a triangular signal for one of the axis (classically called fast axis) and a pseudo-ramp signal for the other axis (classically called slow axis), see, for example, Figures 4.8a and 4.8b.

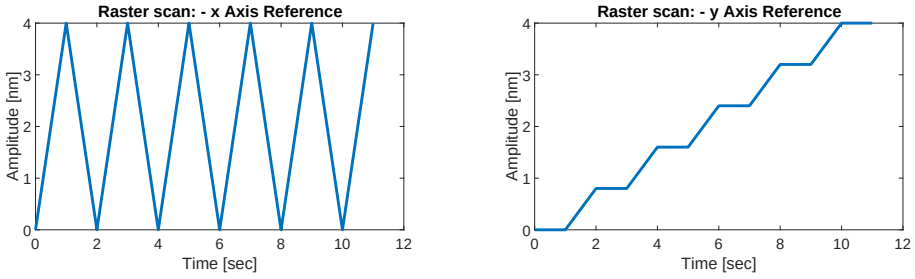

(a) x axis reference signal (fast axis) (b) y axis reference signal (slow axis)

Figure 4.8: Raster scan

Moreover, because of the chosen operation mode for the STM-device, namely constant current mode, the reference signal for z axis is set to a constant.

The reference signals for all the three directions are summarized in Table 4.2.

Table 4.2: Reference signals for the all three axes

	Reference signal
x Axis	Triangular signal - Figure 4.8a
y Axis	Pseudo - ramp signal - Figure 4.8b
z Axis	Step signal

Graphite surface

The sample used as a reference during the real time experiments to validate the proposed control and imaging approaches is a graphite surface [Hem+03]. This is a usual choice for the calibration of such a microscope, in particular because of the well-known structure of the carbon atoms, which is displayed in Figure 4.9.

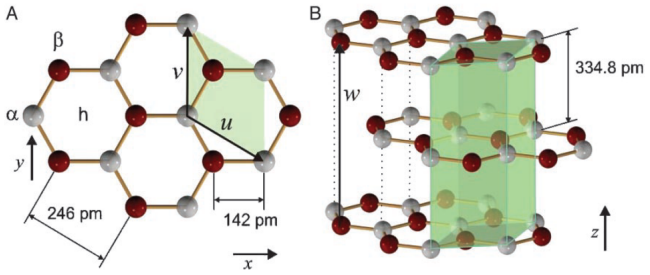

Figure 4.9: Carbon atoms in graphite crystal structure [Hem+03]

Moreover, allow us to provide an image of a graphite surface obtained with a commercial Scanning-Tunneling-Microscope, namely *Easyscan 2 STM* produced by Nanosurf. The experiments were conducted in the research lab CIME Nanotech, Grenoble, France.

On the left side of Figure 4.10 one can notice a surface of $2.5 \times 2.5\ nm$ which shows how the carbon atoms are distributed on a graphite probe. On the other hand, on the right side of the same figure the profile of the tunneling current for a particular line is displayed.

The control as well as the image reconstruction algorithms are validated using the GIPSA STM. The parameters of the device are summarized in Table 4.1. In the following sections the real time experiments are presented.

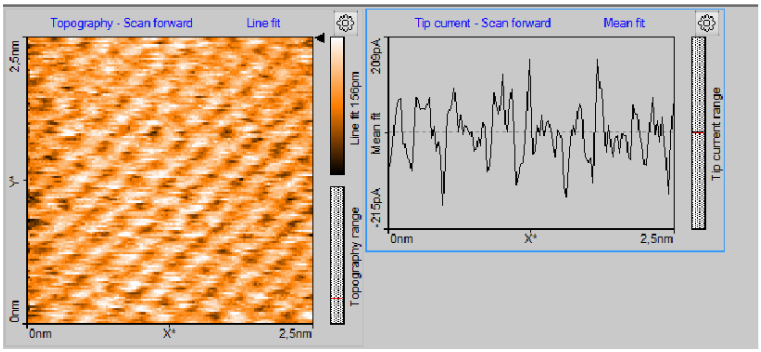

Figure 4.10: Carbon atoms in graphite crystal structure: Standard STM

4.5 Control-based observer application to control and image reconstruction using a Scanning-Tunneling-Microscope

In this section the proposed control-based observer paradigm will be used to improve the control and to enhance the image reconstruction of a graphite surface using the Scanning-Tunneling-Microscope described above.

The solution chosen to control a commercial STM is often limited to a PI controller (or maybe PID controller) for the vertical axis, to ensure that the atomic resolution is achieved, while for the horizontal axes, a simple operation in open loop is deployed. This is mainly due to the simplicity of the solution - easy to understand - and the reduced number of parameters which have to be fixed. One of the disadvantage of the method is the level of noise and the cross-coupling between the axes which can still affect the quality of the control, as well as the quality of the image reconstruction.

To overcome these drawbacks, we propose to use on top of a set of feedforward techniques for horizontal axes, a set of three individual PI controllers, whose capabilities are enhanced by a control-based observer, to ensure a filtering effect, which will allow us to increase the bandwidth of the controllers and to deliver a less noisy image of the scanned surface. This strategy will be generically called single-input single-output (SISO) approach, since individual control strategies are deployed for each axis. The method is detailed next.

4.5.1 Control strategy

Let us consider the control strategy for the Scanning-Tunneling-Microscope described above, which combines:

i. Feedforward controller

ii. Feedback controller

iii. Observer techniques

Nonetheless, the main focus is on the observer part, which highlights the capabilities of the control-based observer paradigm, presented in the methodological part of the present thesis, to enhance the performances of a PI controller, as well as to improve the quality of topographic imaging of a graphite sample.

a. Scanning mode

The Scanning mode control strategy combines a feedforward controller, based on the Modified Prandtl-Ishlinskii approach [RVB15] with a feedback controller, hereby a PI controller, which is enhanced by an observer. Figure 4.11 presents the proposed control strategy for the x and y directions.

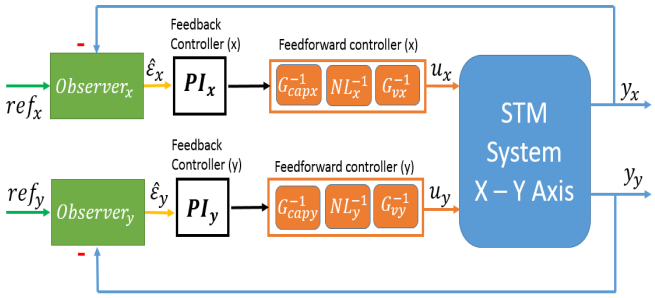

Figure 4.11: Scanning mode: Control Strategy for STM system (X-Y axes)

i. Feedforward controller

The aim of this pre-compensation is to deal with the static nonlinearity of piezoelectric actuator and, more precisely, to compensate the hysteresis effect of such an actuator.

The method used for this particular task is a Modified Prandtl-Ishlinki approach. One of the advantages of this method is that it captures the asymmetric loops of the hysteresis model. In order to do that, the approach uses two elementary operators, namely the backlash operator and the one-side dead-zone operator. The obtained model contains a combination of a certain number of these two elementary operators (chosen as a trade-off between the complexity of the model and computational time).

The model is calibrated in three steps:

Stage 1: Initialization

At this step, the parameters corresponding to the threshold of the model are initialized depending of the range of input $v(t)$ and output $p(t)$ of the piezoelectric actuator.

Stage 2: Identification

Next, the weights of the model are computed using the least-square minimization of the error between the wanted model and the real hysteresis of the actuator. At this point, a model of the hysteresis is provided.

State 3: Inversion

Finally, the model identified in the previous step is inverted and consequently the parameters of NL_x^{-1} and NL_y^{-1} are provided, which will be used to correct the hysteresis effect of the piezoelectric actuator as shown in Figure 4.11.

Readers who are interested in a more detailed description of Modified Prandtl-Ishlinkii method can refer to [AKR07].

ii. Feedback controller

Notice that in the feedforward approach, if a method to correct the hysteresis was provided, the solution is just an approximation of the real actuator hysteresis, thus some subsequent errors are expected to appear. Moreover, piezoelectric actuators also exhibit another type of nonlinearity known as creep, which can also alter the wanted behavior of the STM-device.

As a remedy it is proposed a feedback controller, here represented by a classical PI control strategy, to correct for the aforementioned errors.

To design the PI controller, we consider only the linear part of the piezoelectric actuator, represented here by the structural vibration model (see Figure 4.6). This choice is motivated by the fact that the bandwidths of the Voltage Amplifier and the Capacitive Sensor are much larger than the bandwidth of the piezoelectric actuator and so they can be characterized only by their corresponding static gains.

Based on the models described by equation (4.27), respectively by equation (4.28), reduced until they capture only the structural vibration of the piezoelectric actuators, the gains Kp_x and Ki_x, respectively Kp_y and Ki_y, have been computed using a pole placement method so that to ensure a desired closed loop behavior.

iii. Observer design

The purpose of designing an observer for this particular application is to get a filtered estimation for tip position p_x respectively p_y. The reason why it is needed to get this estimation, arises from the fact that the tip has to move just several nanometers in the x and y directions and at this level any noise can deteriorate the performances of control algorithms. The measurement noise introduced by the capacitive sensor is quite high (this is shown in section 4.5 dedicated to experimental results).

This is the perfect setup to test the capabilities of a control-based observer presented in the previous chapters. For this case, a PI controller is chosen to drive the model of the capacitive sensor so that its output follows the measured output. One of the main goals is to obtain some noiseless estimation of the tip positions on the horizontal axes. Thus, to do that, we consider the corresponding tip positions, $p_x(t)$ and $p_y(t)$ as unknown inputs, and use the proposed control-based observer to estimate them, in particular $\hat{p}_x(t)$ and $\hat{p}_x(t)$. The setup of the observer is shown in Figure 4.12, in particular for the x axis:

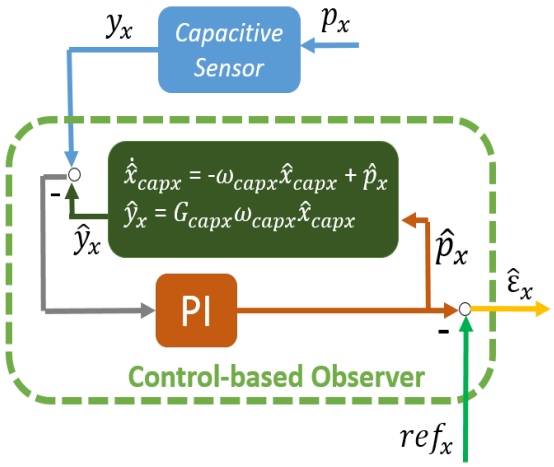

Figure 4.12: Control-based Observer: Tip position estimation (x axis)

Next, let us briefly retrace the steps to design a control-based observer using a proportional-integral control strategy based on the error between the estimated output and the real output. In particular, we search to solve an error feedback regulation problem to finally get the estimation of the unknown inputs, $\hat{p}_x(t)$ and $\hat{p}_y(t)$.

First, we consider the model of the observer as:

$$\begin{aligned} \dot{\hat{x}}_{capx}(t) &= -\omega_{capx}\hat{x}_{capx}(t) + \hat{p}_x(t) \\ \hat{y}_x(t) &= G_{capx}\omega_{capx}\hat{x}_{capx}(t) \end{aligned} \tag{4.37}$$

having the driving variable represented by $\hat{p}_x$.

In the attempt to keep the observer design simple, as it was already mentioned, a PI control law is proposed to solve the internal control problem of the observer, which gives the following estimation of the tip position for the x axis:

$$\hat{p}_x(t) = Kobs_{px}[y_x(t) - \hat{y}_x(t)] + Kobs_{ix}\int_0^t [y_x(\tau) - \hat{y}_x(\tau)]d\tau \tag{4.38}$$

It is clear that the conditions to design the control-based observer are fulfilled, namely, the system is strongly observable and the model is controllable under the control variable $p_x(t)$.

The selection of $Kobs_{px}$ and $Kobs_{ix}$ is made based on the pole placement method. The choice of the desired poles is made as a trade-off between the observer convergence speed and the quality of the estimation in terms of noise.

A similar design procedure is conducted also for the y axis which will lead to find the estimation of the tip position for the y axis, in particular $\hat{p}_y$ is computed.

b. Tunneling current mode

For the vertical axis, the hysteresis effect of the piezoelectric actuator can be ignored since the tip displacement is subnanometric, thus the control strategy will combine only a feedback controller and an observer to control and estimate tunneling current, $i_t(t)$. The control strategy is summarized in Figure 4.13.

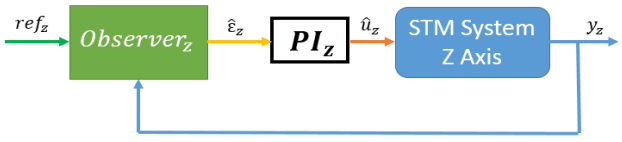

Figure 4.13: Tunneling Current mode: Control Strategy for STM system (z axis)

i. Feedback controller

Since the vertical axis is nonlinear due to the tunneling current expression, let us first linearize it around an equilibrium point, (d_0, i_0).

Using Taylor expansion to linearize equation (4.31) around the equilibrium (d_0, i_0), we get:

$$i_t(t) - i_0 = -ki_0(d(t) - d_0) \tag{4.39}$$

Finally, considering $\Delta i_t(t) = i_t(t) - i_0$ and $\Delta d(t) = (d(t) - d_0)$, we get that:

$$\Delta i_t(t) = -ki_0\Delta d(t) \tag{4.40}$$

Let us consider the transfer function of the vertical axis between $u_z(t)$ and $y_z(t)$ considering the linearized model of the tunneling current:

$$H_z(s) = \frac{Y_z(s)}{U_z(s)} = \frac{G_{vz}\omega_{vz}}{s + \omega_{vz}} \frac{G_{pz}\omega_{pz}^2}{s^2 + 2\zeta_{pz}\omega_{pz}s + \omega_{pz}^2} ki_0 \frac{G_i\omega_i}{s + \omega_i} \tag{4.41}$$

In the equation above, one can notice that the bandwidth of the current sensor, as well as the one of the piezoelectric actuator are much faster than the bandwidth of the voltage amplifier, for this particular case; thus the open loop transfer function for vertical axis can be simplified to a first order transfer function:

$$H_{z_{red}}(s) = G_{pz}ki_0G_i \frac{G_{vz}\omega_{vz}}{s + \omega_{vz}} \tag{4.42}$$

Next, to design PI controller for the z axis, we consider the simplified mathematical model described by equation (4.42) based on which the gains of the controller, Kp_z and Ki_z are computed using the pole placement technique.

ii. Observer design

Similarly to the previous subsection, a control-based observer is also designed to obtain an estimation of the tunneling current, i_t. To that end, the model of the current sensor is considered driven by a PI controller as well such that the output of the model will follow the real output of the vertical axis, as presented in Figure 4.14:

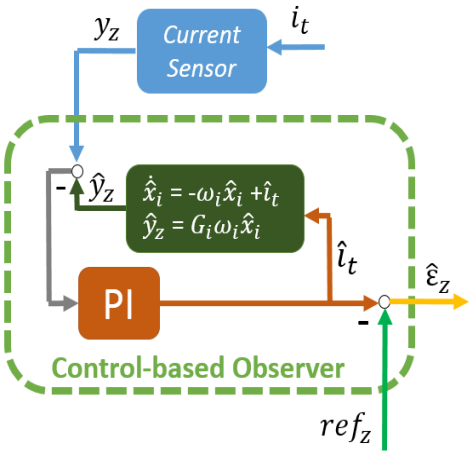

Figure 4.14: Control-based Observer: Tunneling current estimation (Z Axis)

This time, the model of the observer is given by the next equations:

$$\begin{aligned} \dot{\hat{x}}_i(t) &= -\omega_i \hat{x}_i(t) + \hat{i}_t(t) \\ \hat{y}_z(t) &= G_i \omega_i \hat{x}_i(t) \end{aligned} \tag{4.43}$$

having the driving variable represented by $\hat{i}_t(t)$.

Again, a PI control law is proposed to solve the internal control problem of the observer, which gives the following estimation of the tunneling current:

$$\hat{i}_t(t) = Kobs_{pz}[y_z(t) - \hat{y}_z(t)] + Kobs_{iz} \int_0^t [y_z(\tau) - \hat{y}_z(\tau)] d\tau \tag{4.44}$$

Assuming the tracking condition is met, $\hat{i}_t$ can be seen as an estimation of the tunneling current, $i_t(t)$. As for the conditions for which such an observer can be designed, it is clear that the system is strongly observable (considering $i_t(t)$ as the unknown input), while the chosen model is controllable using the driving variable $\hat{i}_t(t)$.

The selection of $Kobs_{pz}$ and $Kobs_{iz}$ is again based on the pole placement method considering a trade-off between the convergence speed and the quality of estimation.

c. Experimental results SISO approach - 3D scan

The goal of this subsection is to present the results of 3D control algorithms. First, the results of the Feedforward controller are presented, secondly, the capabilities of

the enhanced PI controllers using the Control-based Observer are illustrated. Finally an analysis of the Signal-to-Noise Ratio (SNR) is conducted for the method using the observer, as well as for the one when the observer is not used.

i. Modified Prandtl-Ishlinkii (MPI) method

In Figure 4.15, it can be seen that the feedforward approach has good results for both the x and y axes. It can also be spotted that it is not an exact approximation, and also that a phenomenon of creep is additionally present, hence a feedback controller needed.

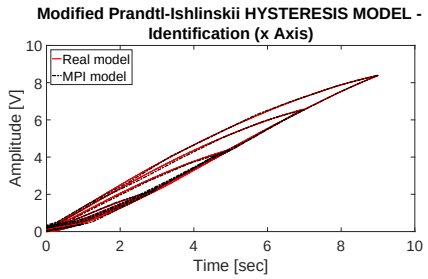

(a) Hysteresis model - x Axis

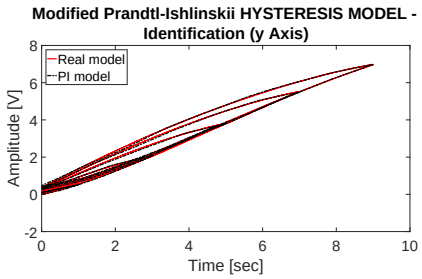

(b) Hysteresis model - y Axis

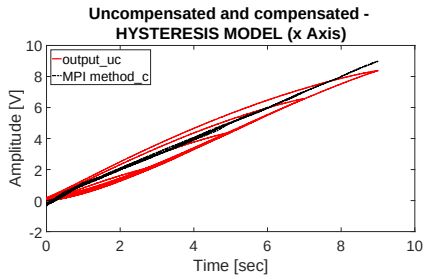

(c) Linearized model - x axis

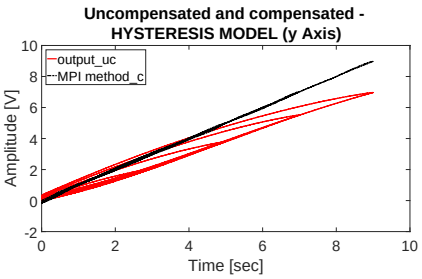

(d) Linearized model - y axis

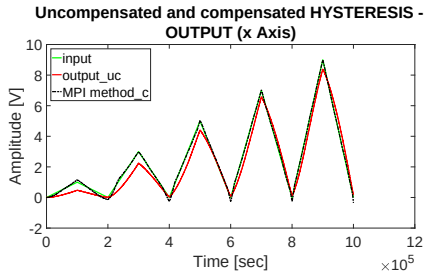

(e) Hysteresis compensation - x axis

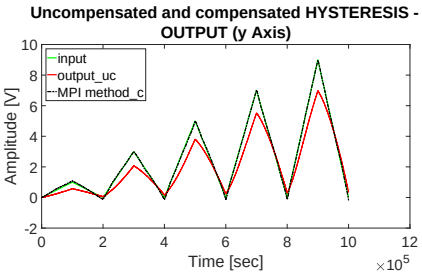

(f) Hysteresis compensation - x axis

Figure 4.15: Feedforward controller based on the MPI method

ii. Feedback controller: PI + Observer

The purpose of the feedback controller in this application, for the x and y axis, is to compensate the residual error inherited after the pre-compensation of hysteresis using the MPI method, as well as to correct the error introduced by the creep effect. As for the z axis, the purpose is to maintain a certain distance between the tip and the sample (less than 1 nm) during the scanning procedure.

As for the aim of the observer, it is supposed to reduce the measurement noise by providing better estimations of the tunneling current, $i_t(t)$, the tip position, $p_x(t)$ respectively $p_y(t)$, which can be used to improve the performances of the proposed algorithms.

On the one hand, in Figures 4.16a, 4.16c and 4.16e are shown the results for the tip position for the x axis, tip position for the y axis and the intensity of the tunneling current for the case when the observer is not used, meaning that the PI controllers use the noisy measurements.

On the other hand, Figures 4.16b, 4.16d and 4.16f show the results for the tip position for the x axis, the tip position for the y axis and the intensity of the tunneling current for the case when the observer is used, thus with PI controllers using the estimated variables which are much less noisy.

By comparing those two sets of figures, the improvement with the observer is obvious.

d. SNR analysis

Table 4.3 shows the Signal-to-Noise Ratio for the case when the observer is not used, and for the case when the Control-based Observer is used to reduce the measurement noise. This obviously confirms the conclusion of figure comparison.

Table 4.3: Signal-to-Noise Ratio Analysis

	Observer OFF	Observer ON
x Axis	62.2227 $[dB]$	82.1337 $[dB]$
y Axis	62.4148 $[dB]$	94.9612 $[dB]$
z Axis	1.9599 $[dB]$	6.7994 $[dB]$

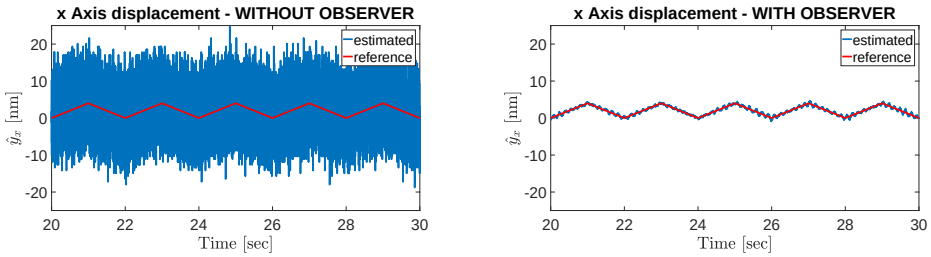

(a) x Axis displacement: Without Obs

(b) x Axis displacement: With Obs

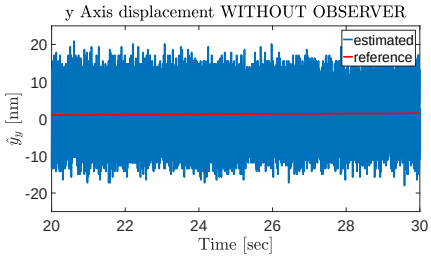

(c) y Axis displacement: Without Obs

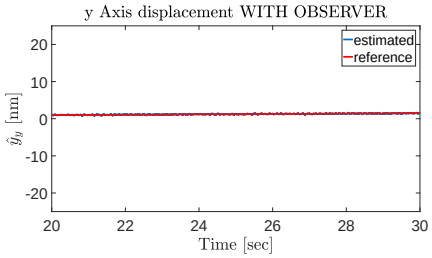

(d) y Axis displacement: With Obs

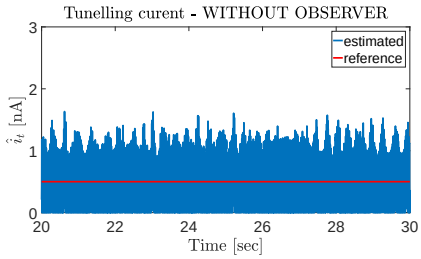

(e) z Axis displacement: Without Obs

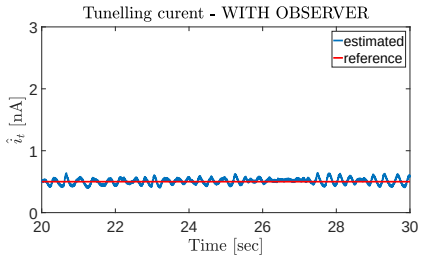

(f) z Axis displacement: With Obs

Figure 4.16: STM Experimental results for all the three axes

4.5.2 Image reconstruction for graphite sample

As it was specified, one of the applications for which the Scanning Tunneling Microscope is used concerns topographic imaging having nanometric resolution for specific electric conductive materials. Basically, the device provides images of how the atoms are arranged on the scanned surface.

Over time, two approaches for the STM surface reconstruction application have been used. For the first one, it is supposed to fix the height of the tip at a certain level and the surface variation can be found using the variation of the tunneling current intensity while scanning a certain surface. The main disadvantage of this approach is that if the topography of the surface is sharp the tip and/or the surface can be damaged.

In this thesis, we are concerned with the second approach, the so called constant current mode, which, as the name suggests, implies to keep constant tunneling current intensity between the tip and the surface while scanning, and, in the end, the

surface variation can be retrieved from the control input used to maintain the wanted tunneling current value.

In order to derive the equation for surface reconstruction, let us consider the block diagram for the vertical axis (Tunneling Current Mode) as shown in Figure 4.17:

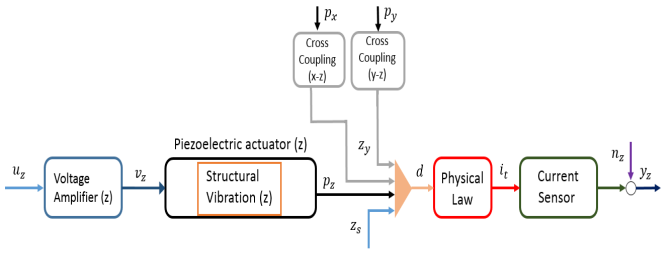

Figure 4.17: Vertical Z axis model - block diagram

One of the simplest ways of finding the surface variation equation is to consider the inverse of equation (4.31) and ignoring the cross-coupling presented in equation (4.32) as well as all the dynamics of the components, namely the voltage amplifier, the piezoelectric actuator and the current sensor. This leads to the following simplified equation for surface reconstruction:

$$\tilde{z}_s(t) = \frac{1}{k} ln \frac{y_z(t)}{G_i g V_b} - G_{vz} G_{pz} u_z(t) \tag{4.45}$$

Of course, to improve surface reconstruction, one can also consider the cross-coupling between the x and z axis as well as the one between the y and z. Thus a more accurate surface estimation can be delivered using the equation:

$$\bar{z}_s(t) = \frac{1}{k} ln \frac{y_z(t)}{G_i g V_b} - G_{vz} G_{pz} u_z(t) + z_x(t) + z_y(t) \tag{4.46}$$

At this point, it is clear that $\bar{z}_s$ is computed based on the control input for the vertical axis, $u_z(t)$, and on the outputs for all three directions, $y_z(t)$, $y_x(t)$ respectively $y_y(t)$, which are all corrupted by measurement noise, as Figure 4.6 illustrates. The last two noisy outputs are used to compute cross-coupling $z_x(t)$ and $z_y(t)$.

It is worth noting that, because of the proposed control strategy, which uses an observer to enhance the capabilities of the PI controllers, one can directly use the estimated variables for tunneling current, $\hat{i}_t(t)$, tip position for the x axis, $\hat{p_x}(t)$ as well

as for the y axis, $\hat{p_y}(t)$. This ultimately leads to the following equation for surface reconstruction:

$$\hat{z}_s(t) = \frac{1}{k} ln \frac{\hat{i}_t(t)}{gV_b} - G_{vz}G_{pz}u_z(t) + \hat{z}_x(t) + \hat{z}_y(t) \tag{4.47}$$

a. Surface reconstruction results

In this subsection the results for surface reconstruction are presented. In order to illustrate the capabilities of the proposed method, three cases are considered. For the first one, the observer is not used and the feedback control strategy is only based on the noisy measurements. Next, for the second case, the proposed observer is used online only for the scanning mode, namely the x and y directions. Finally, the third case presents the method where the Control-based Observer is used online, for all three directional axes.

CASE 1: NO Observers used

Figure 4.18a shows how the reconstructed surface is buried deep into noise if the observers are not used to enhance the feedback controllers. No discernible pattern can be seen to identify the carbon atoms for the scanned graphite surface.

CASE 2: Online Observer used for the x and y axis, but NO Observers used for the vertical axis

if the observer correction is used only for the scanning mode, namely for the x and y axis control, the proposed method indicates some improvements for surface reconstruction. In Figure 4.18b one can spot some discernible shapes which can correspond to carbon atoms displayed in the scanned graphite sample. Still a significant amount of noise blurs the clarity of the image.

CASE 3: Online Observers used all three axes

a surface of graphite sample is scanned while the full 3D control strategy proposed is used where the performance of the feedback controllers (here PI controllers) is

improved with online Control-based Observers. In Figure 4.18c, one can clearly see the carbon atoms. This illustrates the performances of the proposed method.

Further, some details about the numerical values for the reference signals parameters are given. The fast axis has an amplitude of $4\ nm$ and it takes one second for each line to scan the sample. The value of the tunneling current has been set to $0.5\ nA$. The acquisition time for each reconstructed image is 30 seconds.

It is worth noting that all the measurements concerning the GIPSA STM are conducted in air and no control over the temperature, humidity or atmospheric pressure is ensured.

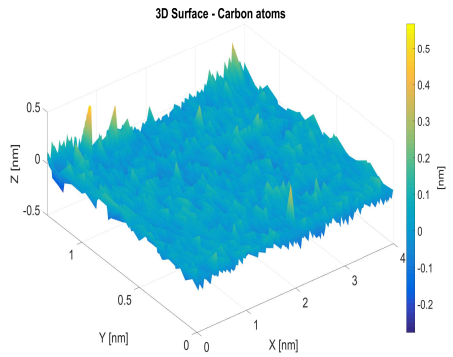

(a) Without Observer for xyz axis

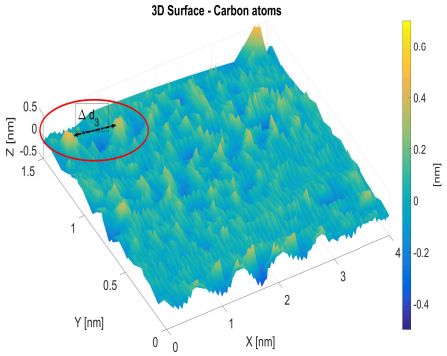

(b) With Observer for xy axis and Without Observer for z axis

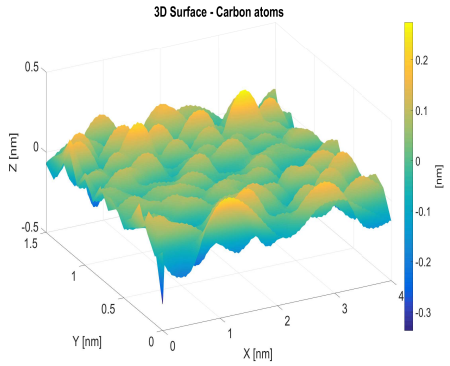

(c) With Observer for xyz axis

Figure 4.18: Surface reconstruction for graphite sample

b. SNR analysis for image reconstruction

In order to quantify the robustness against noise of the proposed method for the surface reconstruction application, a signal-to-noise (SNR) analysis is conducted.

This task is not trivial, since the reference signal for scanned surface is not available. Nonetheless, one can notice that based on the information provided in [Hem+03] and summarized in Figure 4.9 some hypothesis about the signal bandwidth to extract useful features can be made. Moreover, in [Bla10] some information on how to characterize the noise for GIPSA STM is given.

Based on those assumptions a rough approximation of SNR for reconstructed surfaces shown in Figures 4.18a, 4.18b and 4.18c is computed and presented in Table 4.4.

This way a quantitative characterization of the robustness against noise for surface reconstruction purpose of the presented method can be delivered, confirming again the gain of performance with the use of the observer.

Table 4.4: Signal-To-Noise Ratio Analysis for Surface Reconstruction Signal

	SNR
CASE 1	$-2.9800\ [dB]$
CASE 2	$1.6366\ [dB]$
CASE 3	$21.9898\ [dB]$

4.6 Multiple-Input Multiple-Output approach (H_∞ controller)

In this section, we propose to improve the control methodology itself by designing a multiple-input multiple-output (MIMO) controller, relying on robust techniques in terms of H_∞ tools to ensure the control in real-time for all three directions of this experimental STM device. These methods have been recalled when we presented the robust version of the control-based observer.

This work comes as an extension of the proposed solution in [AVB17], where the MIMO case was treated just in simulation.

For this proposed control strategy, we augment the system description presented in Figure 4.6 by also taking into consideration the cross-coupling between the horizontal axes. A block diagram of the augmented system is given in Figure 4.19

Next the H_∞ control problem for an STM device is described.

a. Nominal model

In this section the nominal model of the experimental STM device is given taking advantage of the mathematical description provided in the former section.

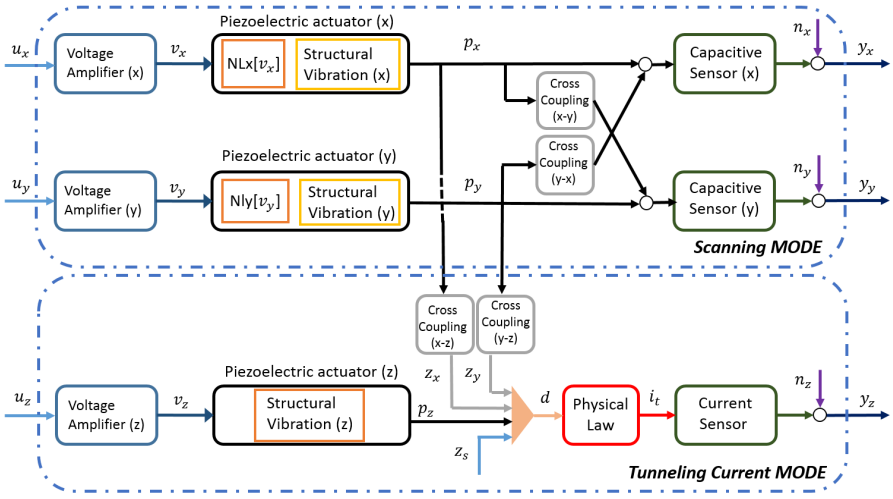

Figure 4.19: Experimental STM block diagram (augmented system)

Considering the system input u, having the components u_x, u_y and u_z, respectively the system output y, with the components y_x, y_y and y_z, the MIMO representation of the experimental STM device in terms of transfer functions can be written as follows:

$$\begin{bmatrix} y_x \\ y_y \\ y_z \end{bmatrix} = \begin{bmatrix} H_{xx}(s) & H_{yx}(s) & 0 \\ H_{xy}(s) & H_{yy}(s) & 0 \\ H_{xz}(s) & H_{yz}(s) & H_{zz}(s) \end{bmatrix} \begin{bmatrix} u_x \\ u_y \\ u_z \end{bmatrix} \tag{4.48}$$

where the transfer functions which describe equation (4.48) are obtained as:

$$\begin{aligned} Hxx(s) &= H_{VAx}(s)H_{Piezox}(s)H_{CSx}(s) \\ Hyx(s) &= H_{VAy}(s)H_{Piezoy}(s)H_{CCyx}(s)H_{CSx}(s) \\ Hxy(s) &= H_{VAx}(s)H_{Piezox}(s)H_{CCxy}(s)H_{CSy}(s) \\ Hyy(s) &= H_{VAy}(s)H_{Piezoy}(s)H_{CSy}(s) \\ Hxz(s) &= -H_{VAx}(s)H_{Piezox}(s)H_{CCxz}(s)ki_0H_{CSz}(s) \\ Hyz(s) &= -H_{VAy}(s)H_{Piezoy}(s)H_{CCyz}(s)ki_0H_{CSz}(s) \\ Hzz(s) &= -H_{VAz}(s)H_{Piezoz}(s)ki_0H_{CSz}(s) \end{aligned} \tag{4.49}$$

One can notice that the nonlinear part of the piezoelectric actuator for the x and y axes has been omitted. It will be considered as a disturbance for the linear model described by equation (4.48).

All the transfer functions in equation (4.49) represent the Laplace transformation of state space representation for the STM components described earlier in this chapter.

Moreover, compared with the model shown in Figure 4.6, it can be spotted the cross-coupling effect for horizontal axes, described in particular using the transfer functions $H_{yx}(s)$ and $H_{xy}(s)$.

b. Performance specification

Considering again as a potential application the one of obtaining an image having nanometric resolution using such an experimental STM in constant current mode, one has to ensure certain control performances in terms of system stability, tracking errors, actuators saturation and robustness against model uncertainties and noise (as we have already seen in the previous section). It is well-known that these performance specifications can be described in terms of closed-loop sensitivity functions [ES90].

In particular for our case, one can be interested to design template functions for the closed-loop sensitivity functions corresponding to *Output sensitivity function* (S_O), *Control sensitivity function* (KS_O) and *Complementary sensitivity function* (T_O).

Due to the fact that the H_∞ controller design is for a MIMO system, the performance specifications are formulated in terms of singular values, σ.

Next, some classical templates for the closed-loop sensitivity functions which the controller has to satisfy are recalled.

i. Output Sensitivity Function (S_O)

The performance objectives related to closed-loop stability, steady-state errors and bandwidth can be expressed as:

$$\max(\sigma(S_o(j\omega))) \leq \frac{1}{|W_e(j\omega)|}, \text{ for all } \omega \tag{4.50}$$

where the inverse of $W_e(s)$ is a high pass filter as:

$$\frac{1}{W_e(s)} = \frac{s + \omega_S \epsilon_S}{s/M_S + \omega_S} \tag{4.51}$$

ii. Output Control Sensitivity Function (KS_O)

The performance objectives related to actuators constraints is given by:

$$\max(\sigma(KS_o(j\omega))) \leq \frac{1}{|W_u(j\omega)|}, \text{ for all } \omega \tag{4.52}$$

where the inverse of $W_u(s)$ is a low pass filter as:

$$\frac{1}{W_u(s)} = \frac{\epsilon_{KS}s + \omega_{KS}}{s + \omega_{KS}/M_u} \tag{4.53}$$

iii. Output Complementary Sensitivity Function (T_O)

The performance objectives related to tracking errors and overshoot recalls:

$$\max(\sigma(T_o(j\omega))) \leq \frac{1}{|W_t(j\omega)|}, \text{ for all } \omega \tag{4.54}$$

where the inverse of $W_t(s)$ is a low pass filter as:

$$\frac{1}{W_t(s)} = \frac{\epsilon_T s + \omega_T}{s + \omega_T/M_T} \tag{4.55}$$

d. 3D H_∞ controller design

i. Generalized plant

Considering the nominal model defined by equation (4.48) together with the performance specification described above, one can obtain the generalized plant that links the external signals (reference signals (r) and surface variation (z_s - see Figure 4.19)) and control signal (u) with controlled signals (z_1, z_2, z_3) and measured outputs (ϵ, hereby defined as the difference between reference (r) and system output (y)) as shown in Figure 4.20.

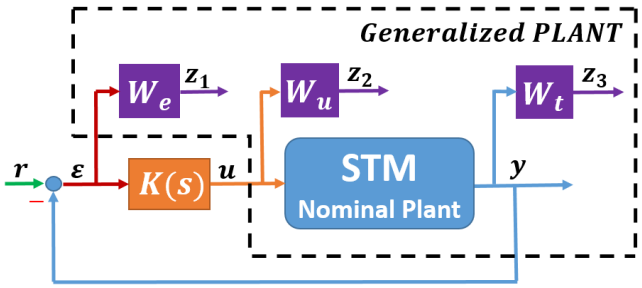

Figure 4.20: Control strategy: Generalized plant

This can be also described in terms of equation (4.56) where $H_{Gen}(s)$ is the transfer function of the generalized plant.

$$\begin{bmatrix} z_1 \\ z_2 \\ z_3 \\ \epsilon \end{bmatrix} = H_{Gen}(s) \begin{bmatrix} r \\ z_s \\ u \end{bmatrix} \tag{4.56}$$

ii. H_∞ controller design

Finally, a controller $K(s)$ is computed such that, given an attenuation γ, the following optimization problem is solved

$$\left\| T_{zw}(s) \right\|_\infty < \gamma \tag{4.57}$$

where $T_{zw}(s)$ is the closed-loop function between external signals and controlled ones via the controller $K(s)$.

It is worth noticing that z_1, z_2, z_3, r, u and y are vectors having three components each one corresponding to the three spatial dimensions.

Moreover, the performance specifications defined above, $We(s)$, $Wu(s)$ and $Wt(s)$ are diagonal matrices belonging to RH_∞^{3x3}. Clearly, one can define different templates for each channel depending on the application objectives.

e. System identification

This subsection is dedicated to system identification which will provide the nominal model for H_∞ controller design.

Scanning MODE:

For this mode, x and y directions, the goal is to identify the direct transfers between system inputs and outputs, as well as the cross-coupling between them.

As stated before, for this mode nonlinearities, like hysteresis, and disturbances, like creep, are present because of piezoelectric actuators. This behavior can cause problems when one wants to conduct an identification procedure. To handle that, a set of Disturbance observers are designed, based on the models suggested in section II, to compensate this behavior [RVB15]. Using this technique a linear model for direct and cross-coupling for horizontal axes can be delivered.

As for the signals used for identification, a set of chirp signals are designed having an amplitude of 0.5V and a frequency variation between 0.1 Hz and 1000 Hz. This particular range has been chosen due to the fact that the data sheet of the piezoelectric actuators suggests that the resonance frequency of the actuators is 630Hz for the x axis, respectively 685Hz for the y axis.

The corresponding signals which reflect the direct and cross-coupling interaction between the x and y axes are shown in Figures 4.21a, 4.21b, 4.21c and 4.21d.

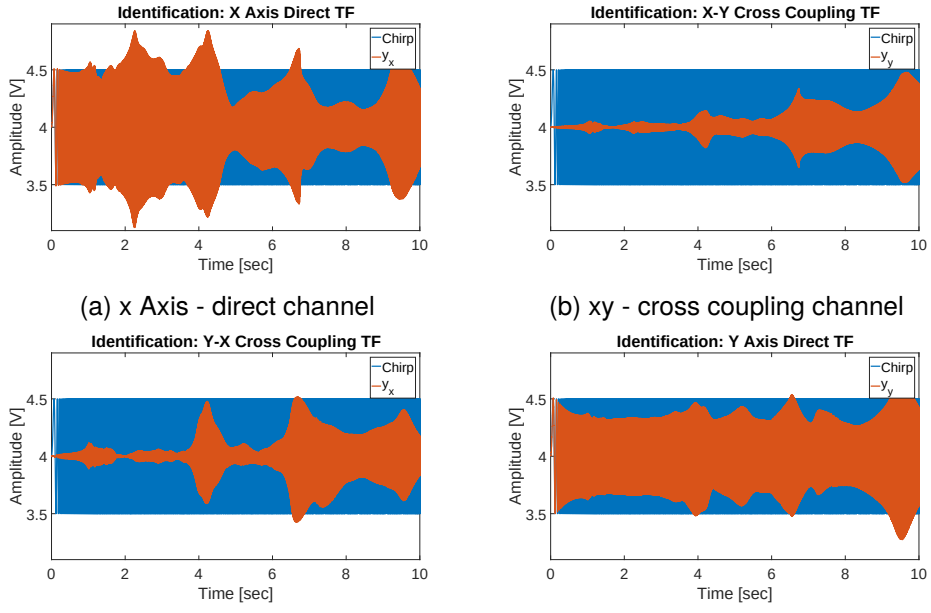

(a) x Axis - direct channel

(b) xy - cross coupling channel

(c) yx - cross coupling channel

(d) y Axis - direct channel

Figure 4.21: Scanning MODE transfer function identification

Finally, using the Matlab^{TM} toolbox 'systemIdentification', the four transfer functions describing direct and cross-coupling of horizontal axes are obtained, with frequency

responses shown in Figure 4.22. In particular, for direct channels corresponding to the x and y axes a second order transfer function has been obtained, while for the cross-coupling channels transfer functions having two poles and one zero has been found.

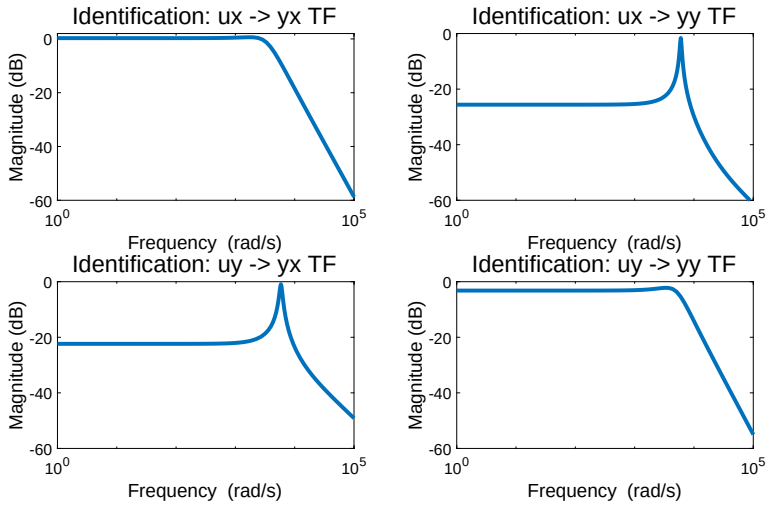

Figure 4.22: Scanning MODE identification: Transfer functions

Tunneling Current MODE:

For the vertical axis, different problems arise during the identification procedure. Due to the nonlinearity and sensibility of the tunneling current, again a closed loop identification technique is required. In this case, a PI controller is chosen to ensure a certain intensity of the tunneling current (the equilibrium one - 0.5nA) and then an excitation signal in terms of a pseudo-random binary sequence (PRBS) is designed.

The corresponding signals used for vertical axes identification are shown in Figure 4.23.

Finally, using the Matlab^{TM} toolbox 'systemIdentification', the transfer function describing the vertical axis model is computed and shown in Figure 4.22. The cross-coupling between the xz and yz axes is modeled as a first order high pass filter as shown in Figure 4.24.

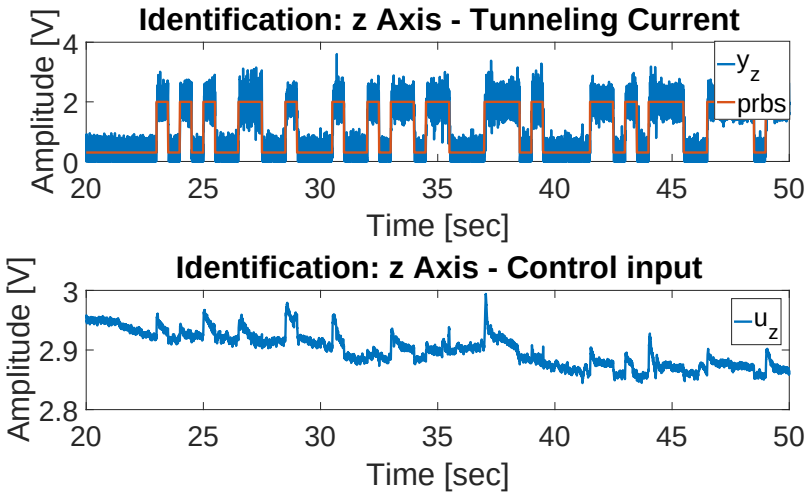

Figure 4.23: Tunneling current mode: identification signals

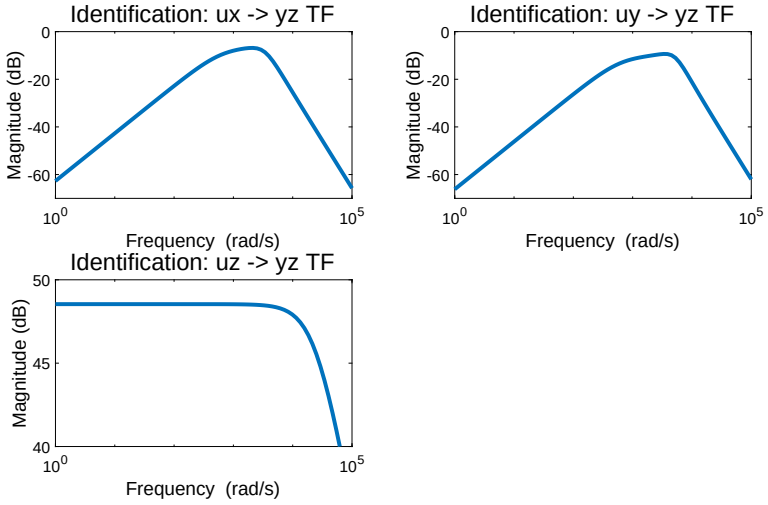

Figure 4.24: Tunneling current mode: transfer function identification

f. 3D H_∞ controller results

i. Performance specification for H_∞ controller

In this section the particular performance specifications in terms of templates for sensitivity functions are given in Table 4.5.

Scanning MODE and Tunneling Current MODE:

The numerical values which describe the templates are expressed in [dB] for amplitude and [rad/sec] for bandwidth.

Table 4.5: Performance Specification

	S_o	T_o	KS_o
Fast axis:	$M_S = 6$ $\epsilon = -60$ $\omega_S = 565.5$	$M_T = 0$ $\epsilon = -60$ $\omega_T = 565.5$	$M_{KS} = 20$ $\epsilon_{KS} = -60$ $\omega_{KS} = 2,513.5$
Slow axis:	$M_S = 6$ $\epsilon = -60$ $\omega_S = 63$	$M_T = 0$ $\epsilon = -60$ $\omega_T = 63$	$M_{KS} = 20$ $\epsilon_{KS} = -60$ $\omega_{KS} = 628.5$
z axis:	$M_S = 6$ $\epsilon = -60$ $\omega_S = 628.5$	-	$M_{KS} = 0$ $\epsilon_{KS} = 60$ $\omega_{KS} = 3,141$

Table 4.6: Quantitative comparison: Mean square error

	x Axis	y Axis	z Axis	
H_∞	1.0362 10^{-6}	7.7107 10^{-7}	0.1526	0.5Hz
PI	6.4464 10^{-6}	8.5832 10^{-7}	0.1660	0.5Hz
H_∞	6.8311 10^{-6}	8.5680 10^{-7}	0.1795	2Hz
PI	90.425 10^{-6}	11.402 10^{-7}	0.3629	2Hz

ii. Experimental results MIMO approach - 3D scan

Finally, real-time experiments results for the proposed 3D H_∞ controller are provided in Figures 4.25a - 4.25f, together with a comparison using a PI controller for each axis (a frequent choice as control strategy for commercial STM devices). The gains of PI controller have been computed using a pole place method.

As scanning parameters, a surface of $1\mu m^2$ and a constant value of $0.5nA$ for tunneling current have been chosen.

The advantage of the proposed controller over the classical SISO solution of using three PI controllers is given by the fact that the robust design of the H_∞ controller allows to increase the bandwidth of the controller so that a faster scanning signal can be used, while for the vertical axis a more accurate control is delivered since the cross-coupling between the horizontal and vertical axis is taken into account.

A quantitative comparison between the results obtained with the H_∞ controller and the SISO approach composed by three PI controllers in terms of mean square error (MSE) is given in Table 4.6.

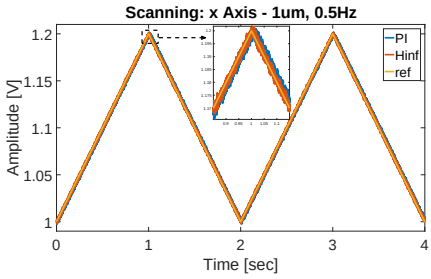

(a) Fast axis - range: $4\mu m$, freq: $0.5Hz$

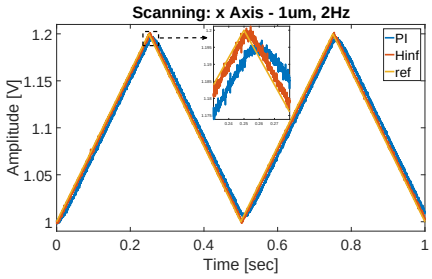

(b) Fast axis - range: $4\mu m$, freq: $2Hz$

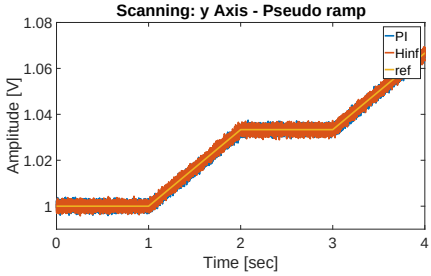

(c) Slow axis - range: $4\mu m$

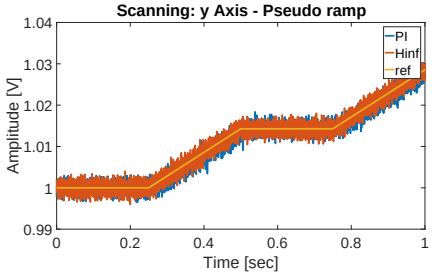

(d) Slow axis - range: $4\mu m$

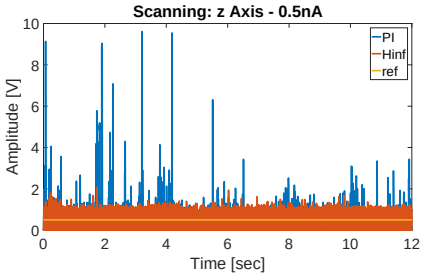

(e) Vertical axis - constant tunneling current

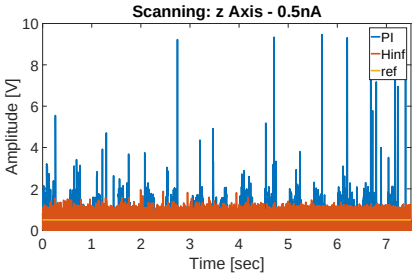

(f) Vertical axis - constant tunneling current

Figure 4.25: 3D Scanning results for H_∞ controller

4.7 Conclusions

In this chapter the concept of tunneling current and how it can be used in order to obtain nanometric resolution images using a Scanning Tunneling Microscope have been presented. In addition, the components of such a device, as well as the mathematical description have been given.

Moreover, two solutions to control in 3D a Scanning Tunneling Microscope have been developed and presented, namely a Single Input Single Output approach based on three independent PI controllers enhanced using a control-based observer, on top of a set of feedforward controllers for horizontal axes. Moreover, using the same technique the topographic image of a graphite sample has been improved, pointing out capabilities of such a technique for unknown input reconstruction. The results of

this work already led to one article published in American Control Conference (2018) [Pop+18].

On the other hand, the second method proposed to enhance the control of the STM device presented is a Multiple Input Multiple Output solution using a H_∞ tools to obtain a robust controller. As the previous solution, these results were also published in a conference, namely in Control and Decision Conference (2019) [Pop+19].

Finally, the image reconstruction for the second method is left as a perspective for future work.

CHAPTER 5

REAL-TIME EXPERIMENTAL RESULTS: MAGNETIC LEVITATION SYSTEM

This Chapter Answers
1. What is a magnetic levitation process?
2. How to model such a device?
3. How to control a magnetic levitation process?
4. How to reconstruct the input disturbance?

5.1 Introduction

In this chapter, the second example of application for control-based observer approaches is presented. It is here based on a pedagogical magnetic levitation process as proposed by Feedback Instruments Ltd, called Maglev, and the idea is to illustrate a different control based observer technique, for a different type of use: the problem that we consider here is indeed that of input disturbance estimation, and the methodology that will be chosen is a Linear Quadratic Integrator controller to drive the observer.

The method will be shown to be very effective for this estimation problem, with results both in simulation and in real time.

The chapter starts with a description of the process and its operation, before presenting the proposed observer for the considered input disturbance estimation problem. It finally shows the obtained results, both in simulation and through real time experiments.

5.2 Magnetic levitation process description

a. Maglev device

The magnetic levitation device considered in the present article is Maglev unit 33-942S manufactured by Feedback Instruments Ltd [Bib]. This device is made of a coil, which is used to generate an appropriate magnetic field, and an infra-red sensor which measures the position of an iron ball. The goal of the experiment is to maintain the iron ball at a given position by using the magnetic field variation. The components of the device can be seen in Figure 5.1.

On the other hand, the control algorithms used to achieve the positioning goal, are developed in $Matlab/Simulink^{TM}$ based on the measured signals which are received via an Analog-to-Digital Converter and the appropriate control inputs are sent via a Digital-to-Analog Converter back to the process.

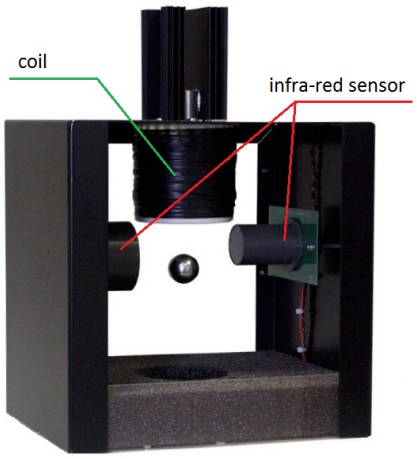

Figure 5.1: Maglev device

b. Maglev model

One of the simplest ways to model the magnetic levitation process is by using the Newton's second law of motion:

$$m\ddot{x} = mg - F_m \tag{5.1}$$

where x is the iron ball position (which means that the second derivative of x is the ball acceleration) considered downwards with respect to the coil, m is the mass of the iron ball, g is the gravitational acceleration constant and finally, F_m is the electromagnetic force which is a nonlinear function of the current, i, passing through the coil and the ball position, x, described by the following equation:

$$F_m = k\left(\frac{i}{x}\right)^2 \tag{5.2}$$

In the above equation, k is a constant depending on the coil parameters.

According to equations (5.1) and (5.2), we get the nonlinear model for the maglev process:

$$m\ddot{x} = mg - k\left(\frac{i}{x}\right)^2 \tag{5.3}$$

Here current i can be considered as the control input and it can be easily seen from Figure 5.2, where $i = 0$, that the process is unstable. This means that the process needs a control to be stabilized.

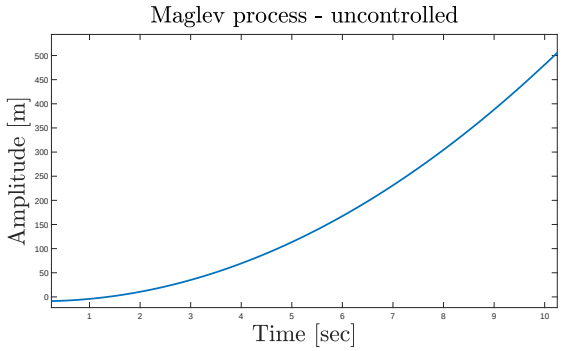

Figure 5.2: Uncontrolled Maglev process

c. Maglev control

Some advanced control strategies have already been studied for this type of system, such as a high-order sliding mode control [GS16], a robust control design [BM16] and a control based on a nonlinear state estimator [NS16].

In the present work, where the ball control is not our main interest, let us stick to the simple, but efficent enough, PID controller. The first step in order to design the controller is to linearize the system model around an equilibrium point, let's say (i_0, x_0).

Applying the Taylor approximation for equation (5.3) and neglecting the high order derivative terms, we get:

$$m\ddot{x} = (mg - k\frac{i^2}{x^2}) - 2k\frac{i}{x^2}\Big|_{(i_0,x_0)}\Delta i + 2k\frac{i^2}{x^3}\Big|_{(i_0,x_0)}\Delta x \tag{5.4}$$

Furthermore, considering that the steady state is $mg = k\frac{i_0^2}{x_0^2}$ and dividing equation (5.4) by m, we obtain:

$$\ddot{x} = -2\frac{g}{i_0}\Delta i + 2\frac{g}{x_0}\Delta x \tag{5.5}$$

Finally, using the Laplace transform, the linearized Maglev transfer function is obtained as:

$$\frac{\Delta x}{\Delta i} = \frac{-G_i}{s^2 - G_x} \tag{5.6}$$

where $G_i = 2\frac{g}{i_0}$ and $G_x = 2\frac{g}{x_0}$.

The second step for designing the PID controller is to choose the desired dynamics for the closed-loop system. In this case the desired polynomial is set as the product of three different first order transfer functions namely:

$$P_D(s) = (s + \omega_1)(s + \omega_2)(s + \omega_3) \tag{5.7}$$

This directly leads to the following expressions for the PID controller gains:

$$K_p = -\frac{G_x + \omega_1\omega_2 + \omega_1\omega_3 + \omega_2\omega_3}{G_i} \tag{5.8}$$

$$K_i = -\frac{\omega_1\omega_2\omega_3}{G_i} \tag{5.9}$$

$$K_d = -\frac{\omega_1 + \omega_2 + \omega_3}{G_i} \tag{5.10}$$

In order to illustrate the stability of the closed loop system, a pole-zero map of both linearized and closed-loop maglev system is shown in Figure 5.3.

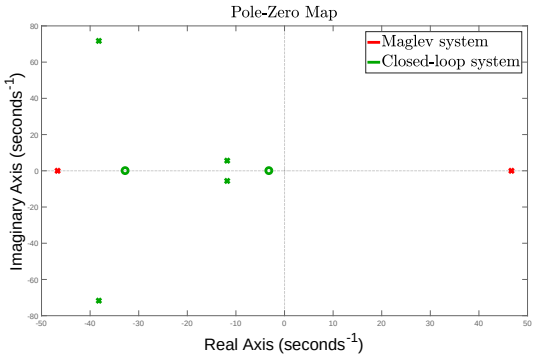

Figure 5.3: Pole-zero map: maglev linearized system (red) and closed-loop system (green)

5.3 Unknown input disturbance estimation

Considering that the Maglev system is stabilized as it was presented in section 5.2, our main point here is to show how using a control-based observer can be used to further solve the problem of estimating input disturbances.

The control strategy chosen for designing the Control-based Observer, in this case, is a Linear Quadratic Integrator (LQI) controller. As it is known, this approach has arisen

by adapting the Linear Quadratic Regulator (LQR) method for the tracking problem, in order to ensure that the output of a system tracks some reference signal. This can be easily done by considering the classical LQR feedback for the augmented system which includes the integrated tracking error as a state of the system. This solution was already presented in Chapter 2 as a design procedure to obtain a control-based observer by solving the *full information regulation problem*.

Let us recall the nonlinear model of the magnetic levitation process:

$$\ddot{x} = g - \frac{k}{m}\left(\frac{u}{x}\right)^2 \tag{5.11}$$

where i has been replaced by u which is a potentially disturbed input described by the equation:

$$u = u_c + d_u \tag{5.12}$$

with u_c being the output of the PID controller designed in Section 5.2 and d_u some additive disturbance. Figure 5.4 shows the block diagram of the process described by equations (5.11) and (5.12), under PID control.

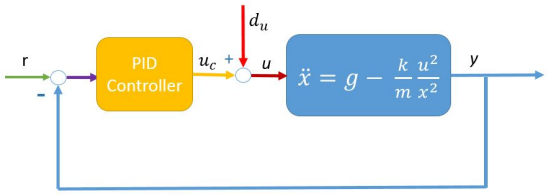

Figure 5.4: Maglev controlled system block diagram

Next, we consider the state-space representation of the Maglev process as described in equation (5.11):

$$\begin{aligned} \dot{x}_1 &= x_2 \\ \dot{x}_2 &= g - \frac{k}{m}\frac{(u_c + d_u)^2}{x_1^2} \\ y &= x_1 \end{aligned} \tag{5.13}$$

Now, we choose a simplified model of the process for our Control-based Observer described by the equations:

$$\begin{aligned} \dot{\hat{x}}_1 &= \hat{x}_2 \\ \dot{\hat{x}}_2 &= -\hat{v} \\ \hat{y} &= \hat{x}_1 \end{aligned} \tag{5.14}$$

Furthermore, the integrated error is considered as in the following equation:

$$x_i(t) = \int_0^t \Big[\hat{y}(\tau) - y(\tau)\Big] d\tau \tag{5.15}$$

Both, equation (5.14) and equation (5.15) lead to the augmented system:

$$\dot{\hat{x}}_e = A_e \hat{x}_e + B_e \hat{v} + D_c y \tag{5.16}$$

where the augmented system's state is $\hat{x}_e = [x_i, \hat{x}]^T$ and the system's matrices are:

$$A_e = \begin{bmatrix} 0 & C \\ 0 & A \end{bmatrix} \quad B_e = \begin{bmatrix} 0 \\ B \end{bmatrix} \quad D_e = \begin{bmatrix} 1 \\ 0 \end{bmatrix} \tag{5.17}$$

The control input law, $\hat{v}$, has the following form:

$$\hat{v} = -K\hat{x}_e \tag{5.18}$$

The control law is obtained by minimizing the cost function:

$$J(\hat{v}(t)) = \int_0^\infty \Big[\hat{x}_e^T(t) Q \hat{x}_e(t) + \hat{v}^T(t) R \hat{v}(t)\Big] dt \tag{5.19}$$

where Q and R are positive semi-definite and definite weighting matrices for the augmented system state, $\hat{x}_e(t)$ and for the control input $\hat{v}(t)$.

Thus, the control input feedback matrix is given by the equation $K = R^{-1} B_e^T P$, where P is the solution of the Algebraic Riccati Equation:

$$A_e^T P + P A_e - K^T R K + Q = 0 \tag{5.20}$$

Finally, as soon as $\hat{v}$ is available, $\hat{d}_u$ can be obtained from:

$$\frac{k}{m}\frac{(u_c + d_u)^2}{x_1^2} - g = \hat{v}$$

Considering that in the nominal case (when $d_u = 0$), the control current u_c is positive, it is expected to remain so for small enough disturbances, which means that an estimate for d_u is given by:

$$\hat{d}_u = \sqrt{\frac{m}{k}(g + \hat{v})y^2} - u_c \tag{5.21}$$

.

This will be illustrated in the next section.

5.4 Simulation and real time results

In this section, the performances of the Control-based Observer for unknown input disturbances are presented. To better illustrate these performances, four different types of disturbances have been used: a step signal, a sinusoidal signal, a rectangular signal and a triangular signal. Both simulation and real time results are shown next.

a. Simulation Results

First, the values of the parameters used to simulate the nonlinear Maglev process are presented in Table 5.1.

Table 5.1: Parameters description

Parameter	Value	Unit	Description
m	0.02	$[kg]$	ball mass
g	9.81	$[N/kg]$	gravitation acc constant
k	2.483 10^{-5}	$[Nm^2/A^2]$	electromagnetic constant
i_0	0.8	$[A]$	coil current equilibrum
x_0	0.009	$[m]$	ball position equilibrum

Secondly, we design a control-based observer as it is described in section 5.3, here choosing $Q = \begin{bmatrix} 10^9 & 0 & 0 \\ 0 & 1 & 0 \\ 0 & 0 & 1 \end{bmatrix}$ and $R = 10^{-4}$.

Figure 5.5 shows that the estimated output of the observer, indeed tracks the real output of the system.

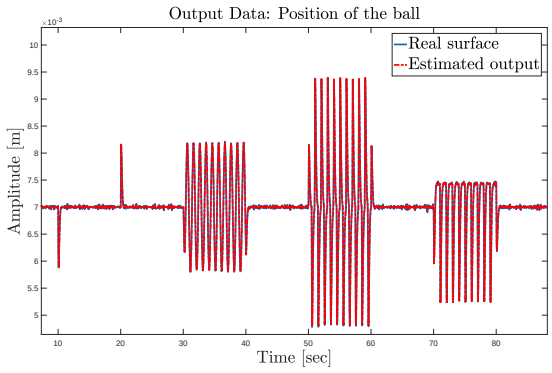

Figure 5.5: Simulation: real output (solid) and estimated output (dash)

Finally, using equation (5.21), the input disturbance is estimated in all four cases, as illustrated in Figures 5.6, 5.7, 5.8, 5.9, for each respective disturbance .

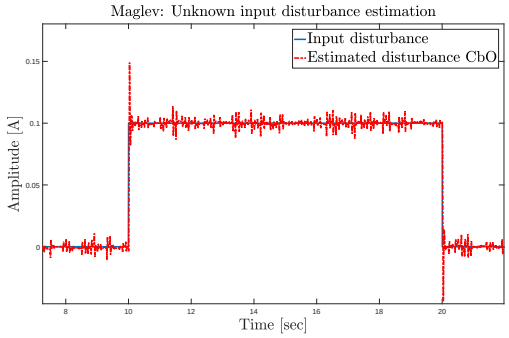

Figure 5.6: Simulation: step input disturbance estimation

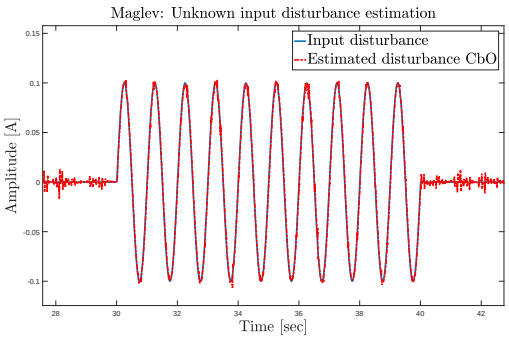

Figure 5.7: Simulation: sinusoidal input disturbance estimation

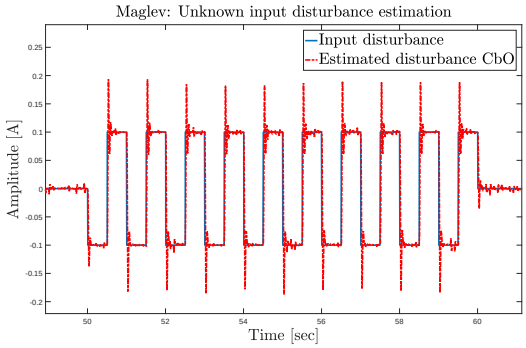

Figure 5.8: Simulation: rectangular input disturbance estimation

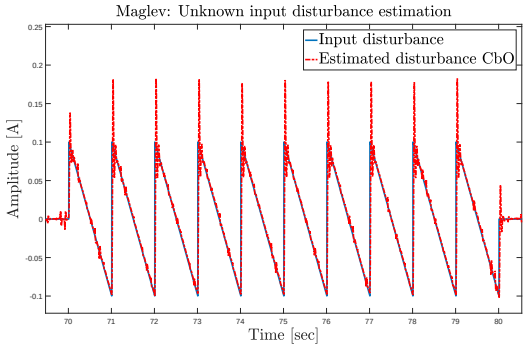

Figure 5.9: Simulation: triangular input disturbance estimation

b. Real-time results

The real-time results have been obtained using the Maglev device manufactured by Feedback Instruments Ltd. For real time experiments, we also try to estimate all the four types of disturbances mentioned above, which are added to the control input in the experiments.

First, the output of the observer's model and the output of real system are shown in Figure 5.10. As in the simulation results, we can see again that the estimated output tracks the real system's output.

Finally, the four estimated disturbances are shown in Figures 5.11, 5.12, 5.13 and 5.14 in comparison with the actually applied one. Notice that for those real-time results the control input, u_c, used in equation (5.21) has been filtered before computing $\hat{d}_u$. In all four cases, the disturbances are very well estimated with the proposed approach. These results indeed show the efficiency of the proposed method.

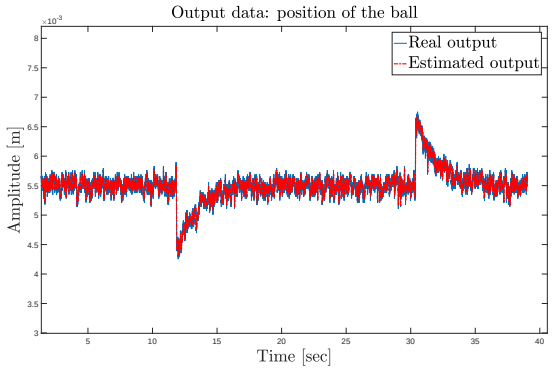

Figure 5.10: Reat-time: real output (solid) and estimated output (dash)

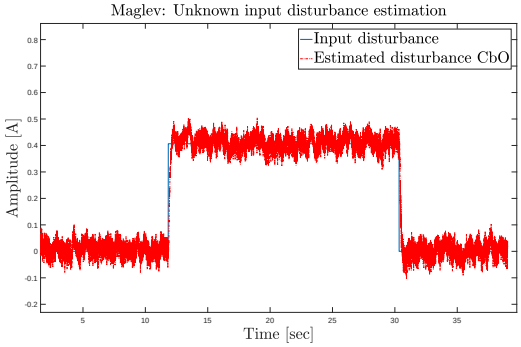

Figure 5.11: Real-time: step input disturbance estimation

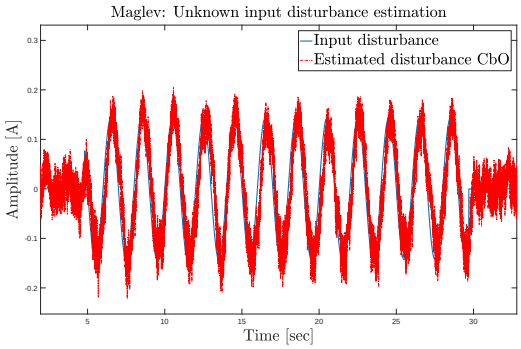

Figure 5.12: Real-time: sinusoidal input disturbance estimation

5.5 Conclusion

In this chapter, a control-based observer approach has been proposed for the unknown input disturbance estimation in the Maglev device. It has been shown to be easily tuned, relying on a well-adapted LQI method (as a control strategy for designing the control-based observer), and to give rise to very efficient results for different types of (unknown) profiles of the disturbance.

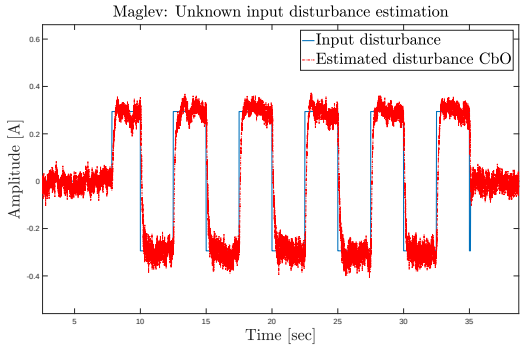

Figure 5.13: Real-time: rectangular input disturbance estimation

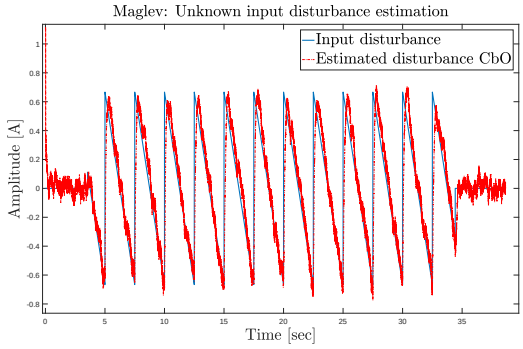

Figure 5.14: Real-time: triangular input disturbance estimation

The work of this section has given rise to publication [PBV17].

CHAPTER 6
CONCLUSIONS AND PERSPECTIVES

6.1 Conclusions

In this thesis the control-based paradigm has been presented, discussed, and applied. The main idea is to convert the observer problem into a control one, and consequently to take advantage of well known control methods to improve the quality of the estimations.

Two system cases have been considered: systems without unknown inputs, and systems with unknown inputs. In the first context some non-optimal solutions like P and PI controllers, together with some optimal ones like LQR and LQI controllers have been listed. It has also been shown how, using this paradigm, some classical observers can be obtained if one carefully chooses the appropriate control strategy (like Luenberger observer, PI observer, Kalman observer and H_∞ observer).

For the case where unknown inputs are present, the control-based paradigm provides a direct way to also estimate the unknown inputs. In this case, the use of H_∞ techniques to provide solutions has been studied.

The conditions that the system and the chosen model have to fulfill have also been presented. In particular, the system has to be observable, while the chosen model has to exhibit some controllability properties in order for the method to be applied. It turns out that, for the case of a system with unknown inputs, the observability conditions extend also to the unknown inputs, while the controllability condition of the model becomes a bit conservative.

About the design itself, two ways to formulate the control problem in order to obtain a control-based observer have been presented. The first one in terms of an error model, while the second one, in terms of driving a copy of the system. Also, depending on the information fed to the controller, two more solutions can be depicted, namely, the output feedback one and the full information one.

Among all these possibilities, it is worth mentioning that depending on the complexity of the chosen control law, the quality of the estimations can increase, but also the complexity of the observer. In particular, if the information about the external signals is taken into account, both the estimation quality and the observer complexity increase: this has been clearly illustrated in the problem of the state and input estimation, for instance.

In a second part of the thesis, two experiment-based applications have been presented. Firstly an example of the Scanning Tunneling Microscope has been considered, for which the of use of control-based observers has been shown to improve control operation, but also the final goal of surface imaging. An improved control approach taking advantage of H_∞ tools has also been proposed towards direct 3D operation. All these methods have been experimentally tested and validated. Secondly, a magnetic levitation process has been handled, for which a control-based observer has been shown to be efficient in solving a different problem of input disturbance estimation. Again, successful experimental results have been provided.

6.2 Perspectives

Even though we covered a large number of methods to design an observer using the control-based observer paradigm and we showed that we can reconstruct the state and the unknown inputs of a system being robust against noise and model uncertainties, still a lot of work can be done to develop this paradigm.

On the one hand, we can use as inspiration the design methods for PI observer [YM95] and sliding mode observers [FDL11], and consider that the correction term, $\hat{v}(t)$ can have two components, i.e. $\hat{v}(t) = \hat{v}_1(t) + \hat{v}_2(t)$, where $\hat{v}_1(t)$ will be designed based on the error between the chosen model output and the system output , i.e. $\hat{v}_1(t) = K_1(\hat{y}(t) - y(t))$ and $\hat{v}_2(t)$ as the output of a controller which has to ensure that $\lim_{t\to\infty}(\hat{y}(t) - y(t)) = 0$.

On the other hand, another perspective is to design an observer which is robust against the parametric uncertainties of the model. Some work has already been done to design robust observers against this kind of uncertainties as in [FSX92], [PM91], [XS94] and [SSF95]. One idea is to explore the capabilities of the H_∞ controller for this type of uncertainties.

Also, a potential perspective, left for further investigation, is the problem of the observer complexity in the case of the Output Feedback H_∞ controller, designed for the

control-based observer. A possible solution for this drawback can be found not far from the controller reduction methods [Zho99], a topic already studied in the case of H_∞ control theory.

Another way to further develop the method is to apply the concepts for the nonlinear case. All the discussion in this manuscript was under the assumption that the systems are linear, but the concept can be useful also in the nonlinear context, as already illustrated in the original article when the paradigm was introduced [BM15].

About applications, the area of nanosciences and operation of related devices also offers a broad range of further challenging cases. We have already thought of possible extensions to AFM problems, for instance. Combining the observer based control with more sophisticated closed loop control, like the H_∞ one, may also be part of future development.

CHAPTER 7

BIBLIOGRAPHY

[AKR07] W T Ang, P K Khosla, and C N Riviere. “Feedforward Controller With Inverse Rate-Dependent Model for Piezoelectric Actuators in Trajectory-Tracking Applications”. In: *IEEE Transactions on Mechatronics* 12 (2007), pp. 134–142.

[AVB17] I Ahmad, A Voda, and G Besançon. “Experimental Validation of H_∞ SISO Control for High Performance Tunneling Current Measurement System and MIMO Extension”. In: *American Control Conference, Seattle, USA* (2017).

[Ahm11] I Ahmad. “Analyse et commande d’un système de mesure à courant tunnel”. PhD thesis. Universite Grenoble Alpes, 2011.

[Ast14] A Astolfi. *Encyclopedia of Systems and control - Chapter: Tracking and regulation in linear systems*. Springer-Verlag, 2014.

[Ast70] K J Astrom. *Introduction to Stochastic Control Theory*. Academic Press, 1970.

[BBK89] S Boyd, V Balakrishnan, and P Kabamba. “A bisection method for computing the H_∞ norm of a transfer matrix and related problems”. In: *Mathematics of Control, Signals, and System (Springer-Verlag New York Inc)* 2 (1989), pp. 207–219.

[BM15] G Besancon and I Munteanu. “Control strategy for state and input observer design”. In: *System & Control Letters* 85 (2015), pp. 118–122.

[BM16] J I Baig and A Mahmood. “Robust control design of a magnetic levitation system”. In: *19th International Multi-Topic Conference, Pakistan*. 2016.

[BM69] G Basile and G Marro. “On the observability of linear, time-invariant systems with unknown inputs”. In: *Journal of optimization theory and applications* 3 (1969), pp. 410–415.

[BQG86] G Binnig, C F Quate, and Ch Gerber. “Atomic Force Microscope”. In: *Physical Review Letters* 56 (1986), pp. 930–933.

[BR86] G Binnig and H Rohrer. “Scanning Tunneling Microscopy”. In: *IBM Journal of Research and Development* 30 (1986), pp. 355–369.

[BS88a] S R Beale and B Shafai. “Robust control system design with the proportional integral observer”. In: *Procedings of the 27th Conference on Decision and Control, Austin, Texas* (1988), pp. 554–557.

[BS88b] S R Beale and B Shafai. “Robust control system design with the proportional integral observers”. In: *Proceedings of 27th Conference on Decision and Control, Texas, USA* (1988), pp. 554–557.

[BSH94] R Banning, P M L O Scholte, and A E Holman. “On the Control of Scanning Tunnelling Microscopes”. In: *Proceedings of IEEE International Conference on Control and Applications, Glasgow, UK, United Kingdom* (1994).

[Bes07] G Besancon. *Nonlinear Observers and applications*. Springer, 2007.

[Bha78] S P Bhattacharyya. “Observer Design for Linear Systems with Unknown Inputs”. In: *IEEE Transactions on Automatic Control* 23 (1978), pp. 483–484.

[Bib] “Magnetic Levitation Control Experiments 33-942S”. In: *Feedback Instruments Ltd. (Manual - Data sheet)* ().

[Bla10] S Blanvillain. “Controle nanoscopique du mouvement par courant tunnel: étude et réalisation”. PhD thesis. Universite Grenoble Alpes, 2010.

[Bob+18] A A Bobtsovabc et al. “A state observer for sensorless control of magnetic levitation systems”. In: *Automatica* 97 (2018), pp. 263–270.

[DFP06] J Davila, L Fridman, and A Poznyak. “Observation and identification of mechanical systems via second order sliding modes”. In: *Iternational journal of control* 79 (2006), pp. 1251–1262.

[DU95] S Drakunov and V Utkin. “Sliding mode observers. Tutorial”. In: *Proceedings of 34th Conference on Decision and Control, New Orleans, LA* (1995), pp. 118–122.

[Doy+89] J C Doyle et al. “State-Space Solution to Standard H_2 and H_∞ Control Problems”. In: *IEEE Trans. on Control Systems* 34 (1989), pp. 831–847.

[Doy78] J C Doyle. “Guaranteed Margins for LQG Regulators”. In: *IEEE Transactions on Automatic Control* 23 (1978), pp. 756–757.

[EM11] E Eleftheriou and S O R Moheimani. *Control technologies for emerging micro and nanoscale systems*. Springer, 2011.

[ES90] M J Englehart and M C Smith. “A four-block problem for H_∞ design: properties and applications”. In: *Proceedings of the 29th Conference on Decision and Control, Honolulu, Hawai* (1990), pp. 2401–2406.

[FB06] T Floquet and J P Barbot. “An observability form for linear systems with unknown inputs”. In: *International journal of control* 79.2 (2006), pp. 132–139.

[FB07] T Floquet and J-P Barbot. “Super twisting algorithm based step-by-step sliding mode observers for nonlinear systems with unknown inputs”. In: *International Journal of Systems Science, Taylor & Francis* (2007).

[FDL11] L Fridman, Jorge Davila, and Arie Levant. “High-order sliding-mode observation for linear systems with unknown inputs”. In: *Nonlinear Analysis: Hybrid Systems* (2011).

[FES07] T Floquet, C Edwards, and S Spurgeon. “On sliding mode observers for systems with unknown inputs”. In: *International Journal of Adaptive Control and Signal Processing* 21.8-9 (2007), pp. 638–656.

[FLD07] L Fridman, Arie Levant, and Jorge Davila. “Observation of linear systems with unknown inputs via high-order sliding-modes”. In: *International journal of Systems Science* 38 (2007), pp. 773–791.

[FSX92] M Fu, C E d Souza, and L Xie. “H_∞ estimation for uncertain systems”. In: *International journal of robust and nonlinear control* 2 (1992), pp. 87–105.

[GD60] K Glover and J C Doyle. “A state space approach to H_∞ optimal control”. In: *Boletin de la Sociedad Mathematica Mexicana* 5 (1960), pp. 102–119.

[GD88] K Glover and J C Doyle. “State-space formulae for all stabilizing controllers that satisfy an H_∞-norm bound and relations to risk sensitivity”. In: *System and Control Letters 11 North-Holland* (1988), pp. 167–172.

[GHO92] J P Gauthier, H Hammouri, and S Othman. “A simple observer for nonlinear systems applications to bioreactors”. In: *IEEE Transactions on Automatic Control* 37 (1992), pp. 875–880.

[GK08] Vincent Gassmann and Dominique Knittel. “H_∞ based PI-observers for web tension estimations in industrial unwinding-winding systems”. In: *Proceedings of 17th World Congress The International Federation of Automatic Control, Seoul, Korea* (2008), pp. 1018–1023.

[GS16] A Goel and A Swarup. “A novel high-order sliding mode control of magnetic levitation system”. In: *IEEE 59th International Midwest Symposium on Circuits and Systems, Abu Dabi, UAE*. 2016.

[GS91] Y Guan and M Saif. “A novel approach to the design of unknown input observers”. In: *IEEE Transactions on Automatic Control* 36.5 (1991), pp. 632–635.

[HM73] G H Hostetter and J S Meditch. “On the generalization of observers to systems with unmeasurable, unknown inputs”. In: *Automatica* 9 (1973), pp. 721–724.

[HM92] M Hou and P C Muller. “Design of observers for linear systems with unknown inputs”. In: *IEEE Transactions on Automatic Control* 37.6 (1992), pp. 871–874.

[Hau83] M L J Hautus. “Strong Detectability and Observers”. In: *Linear algebra and its applications* 50 (1983), pp. 353–368.

[Hem+03] S Hembacher et al. “Revealing the hidden atom in graphite by low-temperature atomic force microscopy”. In: *Proceedings of the National Academy of Science of the United States of America* 100.22 (2003), pp. 12539–12542.

[Isi96] A Isidori. *Nonlinear control systems*. Springer-Verlag, 1996.

[Joh75] C D Johnson. “On observers for systems eith unknown and inaccessible inputs”. In: *Int. J. Control* 21.5 (1975), pp. 825–831.

[KN82] N Kobayashi and T Nakamizo. “An observer design for linear systems with unknown inputs”. In: *Int. J. Control* 35.4 (1982), pp. 605–619.

[KRL12] S Khadraoui, M Rakotondrabe, and P Lutz. “Interval Modeling and Robust Control of Piezoelectric Microactuators”. In: *IEEE Transactions on Control Systems Technology* 20.2 (2012), pp. 486–494.

[KVR80] P Kudva, N Viswanadham, and A Ramakrishna. “Observers for Linear Systems with Unknown Inputs”. In: *IEEE Transanctions on Automatic Control* 25.1 (1980), pp. 113–115.

[Kac79] V T Kaczorek. “Proportional-integral observers for linear multivariable tine-varying systems”. In: *Regelungstechnik* (1979).

[Kal+10] K Kalsi et al. “Sliding-mode observers for systems with unknown inputs: A high-gain approach”. In: *Automatica* 46 (2010), pp. 347–353.

[Kal60a] R E Kalman. “A New Approach to Linear Filtering and Prediction Problems”. In: *Transactions of the ASME Journal of Basic Engineering* 82 (1960), pp. 35–45.

[Kal60b] R E Kalman. “Contributions to the Theory of Optimal Control”. In: *Boletin de la Sociedad Mathematica Mexicana* 5 (1960), pp. 102–119.

[Kur82] J E Kurek. “The State Vector Reconstruction for Linear Systems with Unknown Inputs”. In: *IEEE Transactions on Automatic Control* 28.12 (1982), pp. 1120–1122.

[LA70] W Levine and M Athans. “On the determination of the optimal constant output feedback gains for linear multivariable systems”. In: *IEEE Trans. on Control Systems* 15 (1970), pp. 44–48.

[Lou14] S Lounis. “Theory of Scanning Tunneling Microscopy”. In: *Lecture Notes of the 45th IFF Spring School ’Computing Solids - Models, ab initio methods and supercomputing’*. 2014.

[Lue64] D C Luenberger. “Observing the state of a linear system”. In: *Military Electronics, IEEE Transactions on* 8 (1964), pp. 74–80.

[MMP10] T Menard, E Moulay, and W Perruquetti. “A global high-gain finite-time observer”. In: *IEEE Trans. Automatic Control* 55 (2010), pp. 1500–1506.

[Mor04] J Moreno. “Observer design for nonlinear systems: A dissipative approach”. In: *Proc. IFAC Conference on System Struct. and Control, Oaxaca, Mexico* (2004).

[NK91] K M Nagpal and P P Khargonekar. “Filtering and Smoothing in an H^∞ Setting”. In: *Automatic Control, IEEE Transactions on* 36 (1991), pp. 152–166.

[NS16] A Nayak and B Subudhi. “Discrete backstepping control of magnetic levitation system with a nonlinear state estimator”. In: *IEEE Annual India Conference*. 2016.

[PBV17] A Popescu, G Besançon, and A Voda. “Control-based Observer for unknown input disturbance estimation in magnetic levitation process”. In: *21st International Conference on System Theory, Control and Computing, Sinaia, Romania*. 2017.

[PBV18a] A Popescu, G Besançon, and A Voda. “A new robust observer approach for unknown input and state estimation”. In: *16th European Control Conferenc, Limassol, Cyprus*. 2018.

[PBV18b] A Popescu, G Besançon, and A Voda. “Comparison between different control strategies for estimation purposes using Control-based Observer paradigm”. In: *22st International Conference on System Theory, Control and Computing, Sinaia, Romania*. 2018.

[PM91] I R Petersen and D C McFarlane. “Robust state estimation for uncertain systems”. In: *30th Conference on Decision and Control, Brighton, England* (1991), pp. 2630–2631.

[Pop+18] A Popescu et al. “Control-observer technique for surface imaging with an experimental platform of Scanning-Tunneling-Microscope type”. In: *American Control Conference, Milwaukee, USA* (2018).

[Pop+19] A Popescu et al. “3D H_∞ controller design for an experimental Scanning Tunneling Microscope device”. In: *58th IEEE Conference on Decision and Control, Nice, France*. 2019.

[RVB15] L Ryba, A Voda, and G Besançon. “Experimental comparison of disturbance observer and inverse-basedhysteresis compensation in 3D nanopositioning piezoactuation”. In: *Sensors and Actuators A: Physical* 236 (2015), 190–205.

[Ryb15] L Ryba. “Nanopositionnement 3D à base de mesure à courant tunnel et piezo-actionnement”. PhD thesis. Universite Grenoble Alpes, 2015.

[SC85] B Shafai and R L Carroll. “Design of proportional-integral observer for linear time-varying multivariable systems”. In: *Proceedings of 24th Conference on Decision and Control, Florida, USA* (1985).

[SHM87] J J E Slotine, J K Hedrick, and E A Misawa. “On Sliding Observers for Nonlinear Systems”. In: *Journal Dyn. Sys. Meas. Control* 109 (1987), pp. 245–252.

[SSF95] C E d Souza, U Shaked, and M Fu. “Robust H_∞ filtering for continuous time varying uncertain systems with deterministic input signals”. In: *IEEE Transaction on Signal Processing* 43 (1995), pp. 709–719.

[Sal+11] I Salgado et al. “Generalized Super-Twinsting Observer for Nonlinear Systems”. In: *18th IFAC World Congres, Milano, Italy* (2011).

[Sim06] Dan Simon. *Optimal state estimation*. Wiley, 2006.

[Son98] E Sontag. *Mathematical Control Theory: Deterministic Finite Dimensional Systems. Second Edition*. Springer, 1998.

[Taj+17] F Tajaddodianfar et al. “Stability Analysis of A Scanning Tunneling Microscope Control System”. In: *American Control Conference, Seattle, USA* (2017).

[WD78] S-H Wang and E J Davison. “Observing partial states for Systems with unmeasurable disturbances”. In: *IEEE Transactions on automatic control* 23 (1978), pp. 481–483.

[WZ87] B Walcott and S H Żak. “State observation of nonlinear uncertain dynamical systems”. In: *IEEE Transactions on Automatic Control* 32 (1987), pp. 166–170.

[Woj78] B Wojciechowski. *Analysis and synthesis of proportional-integral observers for single-input-output time invariant continuous systems*. PhD dissertation. Technical University of Gliwice, Poland, 1978.

[Wu+09] Y Wu et al. “A control approach to cross-coupling compensation of piezotube scanners in tapping mode atomic force microscope imaging”. In: *Review of Scientific Instruments* 80 (2009), pp. 043709–1 –043709–10.

[XS94] L Xie and Y C Soh. “Robust Kalman filtering for uncertain systems”. In: *Systems and Control letters* 22 (1994), pp. 123–129.

[YA18] M H A Yaseena and H J Abdb. “Modeling and control for a magnetic levitation system based on SIMLAB platform in real time”. In: *Results in Physics* 8 (2018), pp. 153–159.

[YM95] D Söffker T J Yu and P C Müller. “State estimation of dynamical systems with nonlinearities by using proportional-integral observer”. In: *Journal of Systems Science* 26 (1995), pp. 1571–1582.

[YW72] P C Young and J C Willems. “An approach to the linear multivariable servomechanism problem”. In: *International Journal of Control* 15 (1972), pp. 961–979.

[Yam+15] K Yamamoto et al. “Driver torque estimation in Electric Power Steering system using an H_∞/H_2 Proportional Integral Observer”. In: *Proceedings of 54th IEEE Annual Conference on Decision and Control, Osaka, Japan* (2015), pp. 843–848.

[Zho99] K Zhou. *Essentials of Robust Control*. Prentice Hall, 1999.

ISBN: 978-2-11-129263-5